

# **LYSYL OXIDASE REGULATES TRANSFORMING GROWTH FACTOR- $\beta$ 1 FUNCTION IN BONE**

Phimon Atsawasuwan

A dissertation submitted to the faculty of the University of North Carolina at  
Chapel Hill in partial fulfillment of the requirements for the degree of Doctor of  
Philosophy in the curriculum of School of Dentistry (Oral Biology)

Chapel Hill

2008

Approved by:

Professor	Mitsuo Yamauchi
Professor	Phillip Trackman
Professor	Timothy Wright
Assistant Professor	Yuji Mishina
Assistant Professor	Yoshiyuki Mochida

©2008

Phimon Atsawasuwan

ALL RIGHTS RESERVED

## **ABSTRACT**

**PHIMON ATSAWASUWAN: Lysyl Oxidase Regulates Transforming Growth Factor- $\beta$ 1  
Function in Bone**  
(under the direction of Mitsuo Yamauchi)

Lysyl oxidase (LOX), an amine oxidase critical for the initiation of collagen and elastin cross-linking, has recently been shown to regulate cellular activities possibly by modulating growth factor activity. In this study, we discovered that osteoblastic (MC3T3-E1) cell-derived clones expressing higher (S) levels of LOX exhibited smaller collagen fibrils and lower collagen production than controls (MC, EV) while the clones expressing lower (AS) levels of LOX exhibited larger collagen fibrils and higher amount of collagen leading to subsequent defective mineralization. In order to elucidate the mechanisms by which collagen synthesis is controlled through LOX, we investigated the potential role of LOX in regulating growth factors. We further investigated the interaction of LOX with TGF- $\beta$ 1, a potent growth factor abundant in bone, and evaluated the effect of this interaction. The specific binding between LOX and TGF- $\beta$ 1 was demonstrated both by immunoprecipitation and glutathione-S-transferase pull down assay. Both molecules were co-localized in the extracellular matrix in culture and the binding complex was identified in the mineral-associated fraction of bone matrix. Furthermore, LOX suppressed TGF- $\beta$ 1 induced Smad3 phosphorylation and collagen (I/V) expression but the effects were nullified by  $\beta$ -aminopropionitrile. The suppression of Smad3 phosphorylation was not affected by the presence of catalase. The data indicate that LOX may bind to mature TGF- $\beta$ 1 and regulate its signaling via its amine oxidase activity in bone, thus, may play an important role in bone remodeling and mineralization.

## **ACKNOWLEDGEMENTS**

I would like to express my gratitude to all those who gave me the opportunity to complete this dissertation. To graduate PhD study at UNC-Chapel hill is the most prestigious experience. I am so grateful and thankful for every help I received throughout my study.

I am deeply indebted to my mentor Prof. Dr. Mitsuo Yamauchi whose help, stimulating suggestions and encouragement helped me in all the time of research and writing of this dissertation. He is a major key person for my doctoral student life from the beginning to the end. He has given me his precious time, guidance and constructive comments. His mentorship was paramount in providing a well-rounded experience consistent with my long-term career goals. He encouraged me to grow not only as a researcher but also as an independent thinker. I am not sure that many graduate students are given the opportunity to develop their own individuality and self-sufficiency by being allowed to work with such independence. He also provided me a financial support throughout my study. I would like to express my sincere gratitude and appreciation to him for giving me this honorable privilege to work in his laboratory and finish my research project.

I would like to thank the Ph.D. program in Oral Biology at University of North Carolina at Chapel Hill for giving me a chance to pursue a doctoral degree and Professor Patrick Flood, an Oral Biology Program director, who gave me this chance.

I would like to thank all members of my doctoral dissertation committee, Professor Timothy Wright, Professor Phillip Trackman, Assistant Professor Yuji Mishina and Assistant Professor Yoshiyuki Mochida for their input, valuable discussion and accessibility. In particular, Dr. Mochida who always gives me invaluable advices, intriguing analogy, and edutainment quizzes.

I would like to thank my colleagues in collagen biochemistry laboratory in the past and present, Drs. Parisuthiman, Katafuchi, Pornprasertsuk, Sricholpech, Kaku, Nagaoka, Tokutomi, Kitamura, and Shiiba for their encouragement and friendship. In addition, I would like to express my appreciation to Mrs. Chandlers who passed away many years ago but her friendship is always around.

I would like to gratefully and sincerely thank Dr. Si-urai for his guidance, suggestion and encouragement during the down-time in my graduate study at University of North Carolina at Chapel Hill, Dr. and Mrs. Maixner who always offer helps when I need and a group of Thai students at UNC-Chapel hill who accompany me to stay healthy in the badminton courts.

Finally, and most importantly, I would like to thank my parents and family in Thailand. Their constant support, love, encouragement, quiet patience and faith in me allow me to be as ambitious as I want and pursue my goal.

## TABLE OF CONTENTS

	Page
LIST OF TABLES.....	vii
LIST OF FIGURES.....	viii
LIST OF ABBREVIATIONS AND SYMBOLS.....	x
 Chapter	
I. Introduction.....	1
II. Hypothesis .....	36
III. Study I: Lysyl oxidase regulates collagen quality and quantity in osteoblasts.....	37
Abstract.....	38
Introduction.....	39
Experimental procedures.....	41
Results.....	46
Discussion.....	55
IV. Study II: Lysyl oxidase regulates transforming growth factor- $\beta$ 1 function in bone via its amine oxidase activity.....	58
Abstract.....	59
Introduction.....	60
Experimental procedures.....	63
Results.....	74
Discussion.....	92
V. Concluding remarks.....	96
BIBLIOGRAPHY.....	99

## LIST OF TABLES

Table

<b>Table 1.1</b>	The various regulators and effects on LOX mRNA and enzymatic activity.....	17
<b>Table 1.2</b>	The comparison of LOX family member.....	21
<b>Table 2.1</b>	The amount of total aldehydes and reducible and, non-reducible cross-links in each clone are expressed as mean $\pm$ S.D.....	49
<b>Table 2.2</b>	The fibril density (number fibrils per square micron)..... from each clone are expressed as mean $\pm$ S.D.....	49
<b>Table 3.1</b>	Primers list of constructs used in the study.....	73

## LIST OF FIGURES

Figure

<b>Figure 1.1</b>	Schematic for the biosynthesis of type I collagen. ....	6
<b>Figure 1.2</b>	The sites and reaction of LOX on collagen molecules.....	7
<b>Figure 1.3</b>	Major cross-linking pathways in type I collagen.....	9
<b>Figure 1.4</b>	Pathway for LOX biosynthesis.....	14
<b>Figure 2.1</b>	The level of LOX protein expression in stable clones and controls.....	50
<b>Figure 2.2</b>	Cell proliferation rate of S and AS clones.....	50
<b>Figure 2.3</b>	Amounts of collagen cross-links and their precursor expressed in moles/ mole of collagen at 2 weeks of cultures.....	51
<b>Figure 2.4</b>	Total collagen content from culture matrix and medium at day 3 and 7 of the cultures.....	51
<b>Figure 2.5</b>	Cross-section of the collagen fibrils in the ECM at 3 weeks of cultures observed under TEM and their diameter.....	52
<b>Figure 2.6</b>	Distribution of the collagen fibril diameter in the ECM at ..... 3 weeks of cultures observed under TEM and their diameter distribution... based on total numbers of 500 fibrils.....	53
<b>Figure 2.7</b>	<i>In vitro</i> mineralization assay. ....	54
<b>Figure 3.1</b>	Binding of LOX to TGF- $\beta$ 1/BMPs.....	80
<b>Figure 3.2</b>	LOX constructs and their binding to TGF- $\beta$ 1 by IP-WB.....	81
<b>Figure 3.3</b>	Purity and activity of LOX-V5/His protein.....	82
<b>Figure 3.4</b>	Direct binding of LOX to TGF- $\beta$ 1.....	83
<b>Figure 3.5</b>	Co-localization of LOX and TGF- $\beta$ 1 in a MC cell culture system.....	84
<b>Figure 3.6</b>	Binding of LOX and TGF- $\beta$ 1 in bone extracellular matrix.....	85
<b>Figure 3.7</b>	Effect of LOX overexpression on TGF- $\beta$ signaling in osteoblasts .....	86
<b>Figure 3.8</b>	Effect of over/underexpression of LOX on TGF- $\beta$ signaling in MC3T3-E1 cells.....	87

<b>Figure 3.9</b> Effect of LOX overexpression on BMP signaling in osteoblasts .....	88
<b>Figure 3.10</b> Effect of exogenous LOX protein on TGF- $\beta$ signaling in osteoblasts .....	89
<b>Figure 3.11</b> Effect of LOX on TGF- $\beta$ induced type I and type V collagen expression in osteoblasts.....	90
<b>Figure 3.12</b> Effects of LOX suppression on TGF- $\beta$ signaling by RNA interference.....	91

## LIST OF ABBREVIATIONS AND SYMBOLS

ACP	aldol condensation product
ALP	alkaline phosphatase
AS clone	MC3T3-E1 cells derived clones expressing lower level of LOX
Asp	aspartic acid
Asn	asparagine
ATTC	American type culture collection
bFGF	basic fibroblast growth factor
Bip	binding proteins
BMP	bone morphogenetic protein
bp	basepair(s)
C-	carboxy-
cDNA	complimentary deoxyribonucleic acid
COLI	type I collagen
COL3A1	type III collagen alpha I
Cu	copper
DDW	distilled deionized water
DEAE	Diethylaminoethyl
deH-	dehydro-
DHLNL	dihydroxylysinoonorleucine
DHNL	dihydroxynorleucine
DTT	dithiothreitol
ECM	extracellular matrix
ER	endoplasmic reticulum
EV	empty vector
FACIT	fibril-associated collagen with interrupted triple helices
FBS	fetal bovine serum
FN	fibronectin
Gly	glycine

Glu	glutamine
GRP	glucose-regulated protein
GGT	galactosylhydroxylysyl glucosyltransferase
GT	hydroxylysyl galactosyltransferase
H <sub>2</sub> O <sub>2</sub>	hydrogen peroxide
HEK	human embryonic kidney
HHL	histidinohydroxylysinonorleucine
HHMD	histidinohydroxymerodesmosine
His	histidine
HLNL	hydroxylysinonorleucine
HNL	hydroxynorleucine
HPLC	high performance liquid chromatography
HRP	horseradish peroxidase
HSP	heat shock protein
Hyl	hydroxylysine
Hyl <sup>ald</sup>	hydroxylysine aldehyde
Hyp	hydroxyproline
IGF	insulin-like growth factor
IFN-γ	interferon-gamma
kDa	kilodalton
LAP	latency-associated peptide
LH	lysyl hydroxylase
LLC	large latent complex
LOPP	lysyl oxidase propeptide
LOX	lysyl oxidase
LOXdm	Lysyl oxidase with Lys314 and Tyr349 mutated
LOXL	lysyl oxidase-like
LTBP	latent TGF-β binding proteins
LTQ	lysyl tyrosylquinone
Lys	lysine

Lys <sup>ald</sup>	lysine aldehyde
M	molar
Man <sub>n</sub>	high-mannose N-linked oligosaccharide
MC, MC3T3-E1	osteoblastic cell line from mouse calvaria
mRNA	messenger ribonucleic acid
mTLD	mammalian tolloid
mTLL	mammalian tolloid-like
N-	amino-
NaB <sup>3</sup> H <sub>4</sub>	tritiated sodium borohydride
NF-κB	nuclear factor-kappa B
NH <sub>3</sub>	ammonia
OPG	osteoprotegerin
PAGE	polyacrylamide gel electrophoresis
PBS	phosphate buffered saline
PCP	procollagen C-proteinase
PCR	polymerase chain reaction
PDI	protein disulfide isomerase
PH	prolyl hydroxylase
pI	Isoelectric point
PNP	procollagen N-proteinase
PPI	peptidyl-prolyl cis-trans isomerase
Prl	pyrrole
Pro	proline
Pyr	pyridinoline
RANK	receptor/activator of NF-κB
RANKL	receptor/activator of NF-κB ligand
res	residue
<i>rrg</i>	ras recision gene
S clone	MC3T3-E1 cells derived clones expressing higher level of LOX
Ser	serine

SLC	small latent complex
Smad	small mothers against decapentaplegic protein
SrcR	scavenger receptor cysteine-rich region
TGF- $\beta$ 1	transforming growth factor-beta 1
TNF- $\alpha$	tumor necrosis factor-alpha
$\alpha$ -MEM	alpha minimum essential medium
$\beta$ APN	$\beta$ -aminopropionitrile
$\alpha$	alpha
$\beta$	beta
$\delta$	delta
$\gamma$	gamma
$\varepsilon$	epsilon
$\mu$	micro
m	milli
n	nano
+/+	homozygous wildtype
+/-	heterozygous
-/-	homozygous deficiency
C	cysteine
D	aspartic acid
E	glutamic acid
G	glycine
L	leucine
K	lysine
P	proline
Q	glutamine
R	arginine
S	serine
W	tryptophan
Y	tyrosine

## **CHAPTER I**

### **Introduction**

#### **Biology of bone**

Bone is a specialized form of connective tissue in vertebrates. It serves both mechanical and metabolic functions and is composed of two components, cellular and matrix components. The cellular components include bone lining cells, osteoblasts, osteocytes and osteoclasts while its matrix components contain organic and inorganic components (1, 2). Morphologically, bone is characterized either as cortical (compact) or as cancellous (spongy, trabecular) bone. Functionally, cortical bone provides mechanical resistance and strength while cancellous bone serves for mineral homeostasis and mechanical strength. The bone homeostatic events include bone formation, resorption and remodeling.

#### ***Cellular components of bone***

The cellular components of bone are osteoblasts, osteocytes, bone lining cells and osteoclasts (1, 3). Osteoblasts, osteocytes and bone lining cells are derived from mesenchymal stem cells known as osteoprogenitor cells, whereas osteoclasts are derived from hematopoietic stem cells. Osteoblasts, osteocytes and bone lining cells are located along the surface of bone while osteocytes are located in lacuna inside the bone matrix (2, 3). Osteoblasts are derived from undifferentiated mesenchymal cells or preosteoblasts that are located in the bone marrow, endosteum and periosteum (see review in (4)). Bone lining cells cover most surfaces in the mature bone. They are

inactive and sometimes called resting osteoblasts (1, 3). The third cell type, osteocyte, is estimated to make up more than 90% of the bone cells in an adult bone. Immature osteocytes are surrounded in shallow bone matrix and closely resemble osteoblasts. As these cells mature and more matrices are laid down, they become located deeper within the bone matrix and lose their cytoplasm. They are located within a space or lacuna and have long cytoplasmic processes that project through canaliculi within the matrix and that contact processes of adjacent cells. The processes are thought to be for cellular communication and nutrition within a mineralized matrix (1, 2, 5). The fourth cellular component is the osteoclast. It is a multinucleated giant cell responsible for bone resorption under normal and pathological conditions. It contains many lysosomal vacuoles exhibiting the common description of the foamy cytoplasm. The plasma membrane of the active osteoclast has an infolded appearance known as a ruffled border. It works as a seal to create microenvironment for bone resorption (3, 6). For the development of osteoclast, crosstalk between osteoblasts and osteoclasts must exist to coordinate the process of bone formation and resorption. Osteoprotegerin (OPG) was discovered to be secreted by osteoblasts and acts as a soluble competitive binding partner for RANKL (receptor/activator of NF- $\kappa$ B ligand), which inhibits osteoclast formation and consequently bone resorption. Both OPG and RANKL can bind to RANK (receptor/activator of NF- $\kappa$ B); a transmembranous receptor expressed on osteoclast precursor cells. Interaction between RANKL and RANK initiates a signaling and gene expression cascade resulting in the promotion of osteoclast formation from the precursor pool (7-9).

### ***Extracellular components of bone***

The extracellular matrix (ECM) in bone is composed of organic and inorganic components. The organic matrix accounts for approximately 35% of the total weight of bone tissue compared with 65% for the inorganic part (3).

The inorganic component is generally referred to as hydroxyapatite ( $\text{Ca}_{10}(\text{PO}_4)_6(\text{OH})_2$ ), a plate-like crystal 20-80 nm in length and 2-5 nm thick. Because bone apatite is four times smaller than naturally occurring apatites and less perfect in structure, it is more reactive and soluble and facilitates chemical turnover (10).

The freshly synthesized matrix prior to its mineralization, osteoid, consists primarily (approximately 94%) of collagen type I and is secreted by osteoblasts. Major non-collagenous proteins in bone consist of proteoglycans. In addition to their role in defining the spatial organization of the ECM, type I collagen interacts with growth factors during the development (11). Osteocalcin, osteopontin, osteonectin and matrix-gla protein play roles during the mineralization process (12, 13). Other proteins such as bone morphogenic proteins, growth factors, cytokines, and adhesion molecules also play roles in bone homeostasis (11).

### ***Collagens in bone***

Collagens are a large family of structurally related proteins that assemble in the ECM and contain one or more domain(s) of unique triple helices (collagenous domain). This collagenous domain, the hallmark of these proteins, is a coiled-coil right-handed triple helix composed of three polypeptide chains, called  $\alpha$  chains. The non-triple helical domains are called non-collagenous domains. Each  $\alpha$  chain in the molecule is coiled into an extended left-handed polyproline II-type helix and then the three left-handed helical  $\alpha$

chains are intertwined to one another and folded into a ropelike right-handed triple helix structure (14). The triple helical structure is stabilized by the high content of imino acids, i.e. proline (Pro) and hydroxyproline (Hyp) and the presence of Hyp is essential for interchain hydrogen bonds that further stabilize the triple helical structure. Collagen molecules consist of the repetitive sequences of amino acids  $[\text{Gly}(\text{glycine})\text{-XY}]_n$  (X and Y can be any amino acid but often X is Pro and Y Hyp) are required. Every third amino acid is situated in the center of the triple helix in a very restricted space where only Gly, the smallest amino acid, can fit (15). Collagen is the most abundant protein in vertebrates accounting for about 30% of the body's total proteins and is present in essentially all tissues and organs of the body. The collagen superfamily consists of 27 different genetic types and these distinct types of collagen show marked diversity and complexity in the structure, their biological function and tissue distribution. The collagen superfamily can be divided roughly into 3 groups: fibril forming (type I, II, III, V, XI, XXIV and XXVII), fibril-associated collagen with interrupted triple helices (FACIT) (type IX, XII, XIV, XVI, XIX, XX, XXI, XXII and XXVI), and non-fibril forming (type IV, VI, VII, VIII, X, XIII, XV, XVII, XVIII, XXIII, XXV and XXVI)(15-19). In bone, type I collagen is the most predominant type of collagen and type V collagen is present as a minor type. Type I collagen is a heterotrimeric molecule composed of two  $\alpha 1$  chains and one  $\alpha 2$  chain,  $[\alpha 1(\text{I})]_2\alpha 2(\text{I})$ , although a homotrimeric form of  $\alpha 1$  chains  $[\alpha 1(\text{I})]_3$ , does exist as a minor form. The precursor molecule called tropocollagen consists of three domains: the  $\text{NH}_2$ -terminal nontriple helical (N-telopeptide), the central triple helical and the  $\text{COOH}$ -terminal nontriple helical (C-telopeptide) domains. The procollagen is secreted outside the cell as its precursor form. Proteolytic cleavage of the propeptides results in mature collagen molecules and can assemble into fibrils (20-22). The biosynthesis of procollagen is a complex process in which several enzymes and molecular chaperones assist its folding

and trimerization (23, 24). A number of posttranslational modifications occur both at intra- and extracellular locations. Protein disulphide isomerase (PDI) induces the formation of inter- and intrachain disulphide bonds within the C-propeptide, allowing the association between procollagen chains (25, 26). The C-propeptide ensures the association between monomeric and heteromeric procollagen chains. Newly synthesized procollagen chains are associated in trimers through their C-propeptides, leading to nucleation and folding in a C-to-N direction to form a triple helix. The biosynthesis of procollagen involves different posttranslational modifications that occur in the endoplasmic reticulum: peptidylproline cis-trans isomerase is required to convert the proline residues to the trans form (27, 28), and prolyl 4-hydroxylase is required to convert proline into hydroxyproline residues (29, 30). The family of lysyl hydroxylase (LH) contributes to the formation of hydroxylysine, which specific residues at telopeptide can subsequently be further modified by lysyl oxidases (LOXs). The collagen chaperone heat shock protein (HSP) 47 is also required for the folding of the collagen (31, 32). All of the enzymes responsible for these modifications work in a coordinated fashion to ensure the folding and assembly of a correctly aligned and thermally stable triple-helical molecule. During the secretion of these molecules into the ECM, propeptides are removed by procollagen N- and C- proteinases (NCP and PCP), thereby allowing spontaneous self-assembly of collagen molecules into fibrils (33). Finally, the triple-helical structure is stabilized by an important posttranslational modification that allows intra/intermolecular cross-links to take place as a result of the catalysis of lysyl oxidase (LOX), which oxidizes the specific lysine (Lys) and hydroxylysine (Hyl) residues at the telopeptidyl domains of collagen molecules (Figure 1.1)(15, 34-36).

# Collagen biosynthesis.

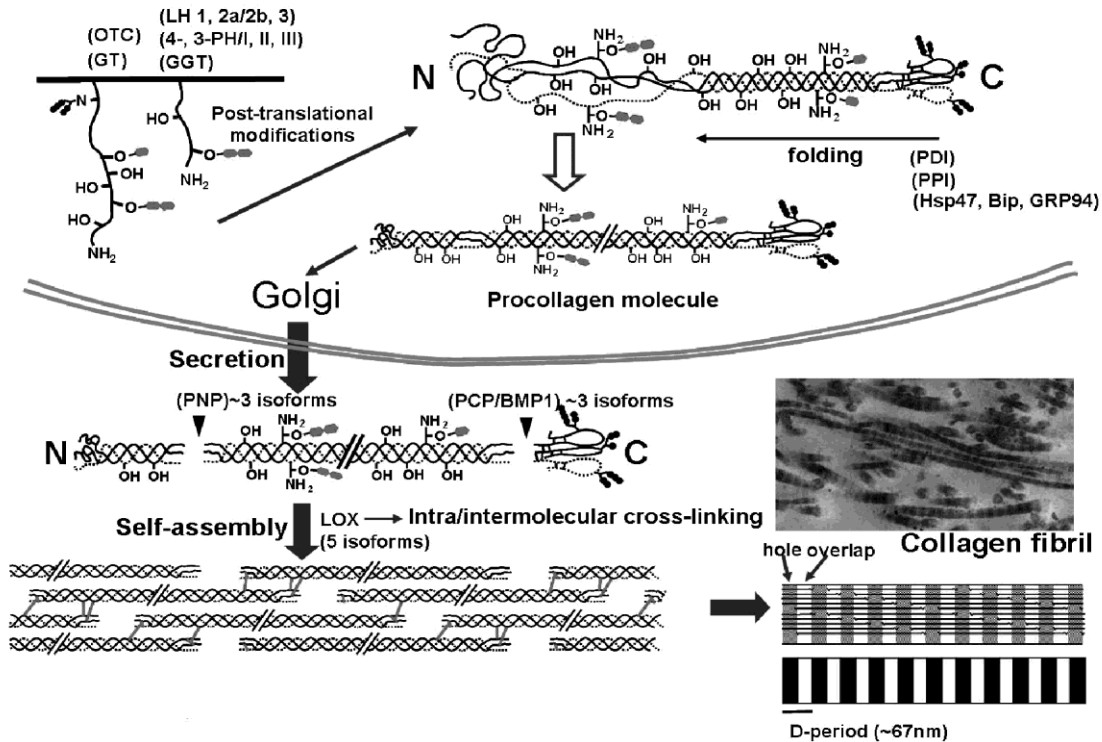


**Figure 1.1** Schematic for the biosynthesis of type I collagen. The upper part shows the intracellular events and the lower part shows the extracellular events. The intracellular events include extensive post-translational modifications such as Pro- or Lys- hydroxylation, glycosylation, association of pro  $\alpha$  chains and folding into a triple helical molecule from the C- to N-terminus. The extracellular events involve the removal of both N- and C-propeptides, self-assembly of collagen molecules into fibril, enzymatic oxidative deamination of lysine and hydroxylysine residues by lysyl oxidase (LOX) and subsequent intra- and intermolecular covalent cross-linking (15).

## Cross-linking pathway

The process of cross-linking is initiated by the oxidative deamination of  $\epsilon$ -amino groups on peptidyl Lys and Hyl residues in the N- and C-terminal telopeptides of collagen and Lys in elastin (34, 37). This reaction generates 5-amino-5-carboxypentanal [( $\alpha$ -aminoadipic acid- $\delta$ -semialdehyde) ( $\text{Lys}^{\text{ald}}$ )] and 2-hydroxy-5-amino-5-

carboxypentanal [( $\delta$ -hydroxy,  $\alpha$ -amino)adipic acid- $\delta$ -semialdehyde) (Hyl<sup>ald</sup>)] and ammonia (NH<sub>3</sub>) and hydrogen peroxide (H<sub>2</sub>O<sub>2</sub>) (Figure 1.2), and initiates a series of condensation reactions forming covalent intra- and intermolecular cross-links (15, 38, 39). Covalent intermolecular cross-linking is essential to provide the tissues with mechanical properties to perform their structural functions. In collagen, once the aldehydes (either Lys<sup>ald</sup> or Hyl<sup>ald</sup>) are formed by the action of LOX in the C- and the N- telopeptide domains, they undergo a series of condensation reactions involving another aldehyde in the same molecule and/or the juxtaposed Lys, Hyl and histidine (His) residues on the neighboring molecules. The results are the formation of covalent intra- and intermolecular cross-links as shown in figure 1.3 (15, 38-40). The cross-linking chemistry/pattern varies from tissue to tissue rather than particular collagen types since a number of tissue specific factors govern the chemistries. Depending on the state of hydroxylation of Lys residues at telopeptides, two major cross-linking pathways evolved Lys<sup>ald</sup> and Hyl<sup>ald</sup> pathways. Besides the enzymatic cross-linking mentioned above, the non-enzymatic cross-linking of collagen has also been taken place (see review in (41-44)).

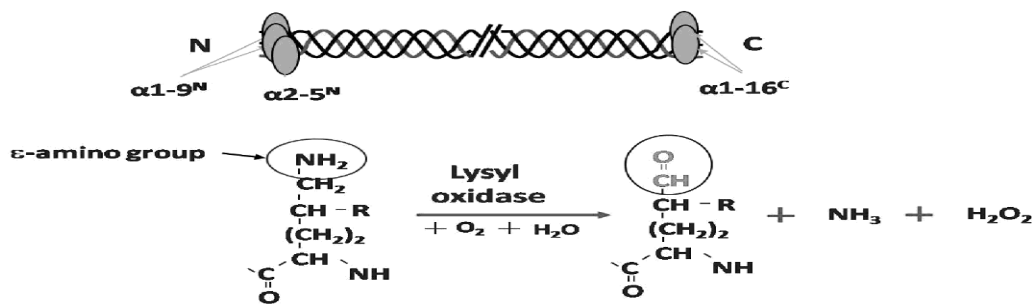


**Figure 1.2** The sites and reaction of LOX on collagen molecules. The specific Lys or Hyl at telopeptidyl domain of a collagen molecule which can be oxidized by LOX and the reaction of LOX oxidation in the presence of oxygen (O<sub>2</sub>) and water (H<sub>2</sub>O). The end products are Lys<sup>ald</sup> or Hyl<sup>ald</sup>, ammonia (NH<sub>3</sub>) and hydrogen peroxide (H<sub>2</sub>O<sub>2</sub>)(15).

The Lys<sup>ald</sup> pathway, a major cross-link pathway in non-mineralized tissues, leads to the formation of a tetravalent cross-link, dehydrohistidinohydroxymerodesmosine (deH-HHMD, Lys<sup>ald</sup> x Lys<sup>ald</sup> x His x Hyl) via intramolecular aldol condensation product (ACP), and a trivalent stable cross-link, histidinohydroxylysionorleucine (HHL, Lys<sup>ald</sup> x Hyl x His) via the iminium cross-link, dehydro-hydroxylysionorleucine (deH-HLNL, Lys<sup>ald</sup> x Hyl). ACP ( $\alpha,\beta$ -unsaturated aldol) occurs as an intramolecular cross-link located in the N-telopeptide domain of the molecule (45, 46). Then Michael addition of N3 imidazole of His to the  $\beta$ -carbon of ACP resulting as aldolhistidine and further condenses with  $\epsilon$ -amino group of Hyl forming an iminium bond to produce deH-HHMD (46). The deH-HHMD is abundant in skin. Lys<sup>ald</sup> located in the C- and N-telopeptide domains can also cross-link to the juxtaposed  $\epsilon$ -amino group of helical Hyl or Lys on the neighboring molecules to form iminium intermolecular cross-links, deH-HLNL. Then deH-HLNL further condenses with a helical His residue and forms the HHL cross-link (47). This HHL cross-link is abundant in skin and cornea (48) but minimal in skeletal tissues such as dentin, bone, ligament and tendon (49).

The Hyl<sup>ald</sup> pathway, a major cross-link pathway in skeletal tissues such as bone, cartilage, tendon and dentin leads to the formation of bifunctional cross-links; dehydro-dihydroxylysionorleucine (deH-DHLNL, Hyl<sup>ald</sup> x Hyl) and deH-HLNL (Hyl<sup>ald</sup> x Lys), and condenses to tri-functional cross-links; pyridinoline (Pyr, Hyl<sup>ald</sup> x Hyl x Hyl<sup>ald</sup>), pyrrole (PrI, Hyl<sup>ald</sup> x Hyl x Lys<sup>ald</sup>), deoxy-pyridinoline (d-Pyr, Hyl<sup>ald</sup> x Lys x Hyl<sup>ald</sup>), and deoxy-pyrrole (d-PrI, Hyl<sup>ald</sup> x Lys x Lys<sup>ald</sup>) (15). The deH-DHLNL can spontaneously form its ketoamines by Amadori arrangement, and further matures into Pyr by involving Hyl<sup>ald</sup> or another deH-DHLNL/or its ketoamine (38). PrI can be formed by pairing deH-DHLNL with Lys<sup>ald</sup>. This cross-link pathway also leads to deH-HLNL (Hyl<sup>ald</sup> x Lys) which further condenses with Hyl<sup>ald</sup> to form d-Pyr or condenses with Lys<sup>ald</sup> to form d-PrI (15). As

described above, the final post-translational modification of collagen is cross-linking formation and this process is initiated by LOX enzymes.

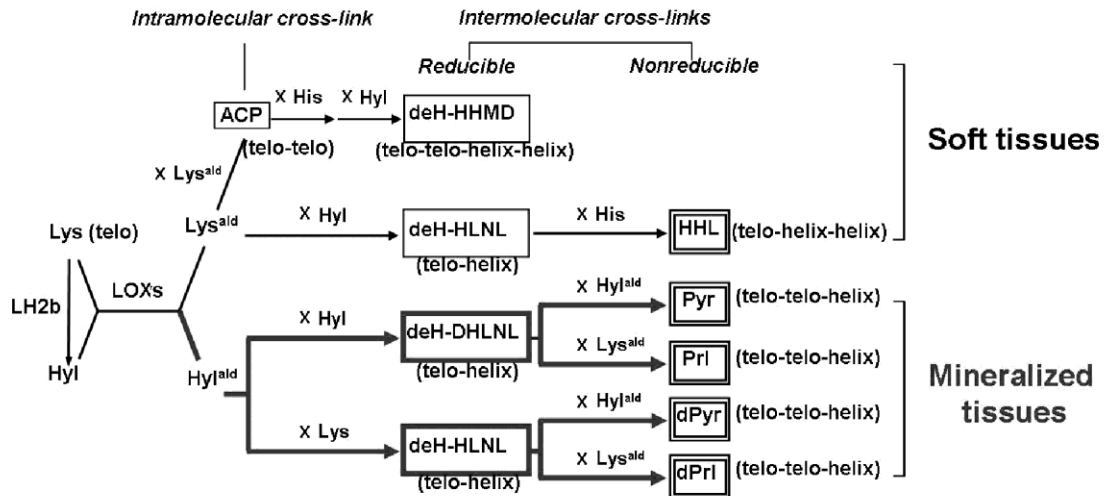


**Figure 1.3** Major cross-linking pathways in type I collagen. L.H.: Lysyl hydroxylase, LOX: Lysyl oxidase, ACP: Aldol condensation product (Intramolecular cross-link), deH: dehydro HLNL: hydroxylysinoxonorleucine, DHLNL: dihydroxylysinoxonorleucine, HHMD: histidinohydroxymerodesmosine, HHL: histidinohydroxylysinoxonorleucine, Pyr: pyridinoline, d-: deoxy, Prl: pyrrole. (15)

## Lysyl oxidases

Lysyl oxidases (LOXs; EC1.4.3.13; protein-lysine 6-oxidases) are extracellular copper ( $\text{Cu}^{2+}$ )-dependent amine oxidases that oxidize the  $\epsilon$ -amino groups on the specific Lys and Hyl of collagen and Lys in elastin (34, 37). This enzyme was first demonstrated its activity *in vitro* in 1968 (50) but many studies on this enzyme were limited by its marked insolubility and aggregation which later was solved by solubility and stability in urea (51). The molecular mass of the enzyme from tissues such as cartilage, aorta, lung, placenta and skin was found to be approximately 32 kDa (52-56). Lysyl oxidase extracted from several tissues resolved upon DEAE chromatography into multiple forms

(57). This suggested the existence of alternative spliced or the presence of isozymes with similar but not identical properties. The human LOX gene is located in chromosome 5q23.3-31.2 encoding a 417 amino acid polypeptide, of which the first 21 residues correspond to the signal peptide (58, 59) and the mRNA for human LOX is found as multiple species with sizes of 5.5, 4.3, 2.4 and 2.0 kb due to the use of alternate polyadenylation sites, and partially to the existence of multiple transcription initiation sites (58-60). The mouse Lox gene has been mapped to chromosome 18 (61-63).

### ***Biosynthesis and processing of the LOX precursor***

LOX protein is secreted into the extracellular space (64-68). The biosynthesis of LOX proenzyme has been first proved by immunoprecipitation of a 46 kDa cell-free translation product of a rat smooth muscle cell LOX mRNA, using an antibody raised against the 32 kDa bovine enzyme (69, 70), and a 48 kDa product, using mRNA isolated from fibrotic rat liver (71). Three forms of LOX with molecular masses of 50, 47, and 32 kDa were identified by immunoprecipitation of media and cell layer extracts of cultured rat smooth muscle cells, which were pulse-labelled with [35S] methionine (72). The 50 kDa product was found both as a secreted protein in the cell medium and in the intracellular fraction, and pulse-chase studies revealed that it is converted to a 32 kDa protein in the medium. The LOX protein is synthesized as a N-glycosylated derivative of the 45 kDa proprotein (72), ~50 kDa proLOX by various cell types including normal/transformed fibroblasts, endothelial cells, smooth muscle cells and osteoblasts (73-79). The mouse and rat propeptide domain contains two consensus sites for the posttranslational N-glycosylation (72). The 32 kDa active enzyme, LOX, contains the 10 cysteine residues of proLOX, all of which exist in disulfide linkage (80). The secreted proLOX is catalytically quiescent but is activated through proteolytic cleavage by procollagen C-proteinases (PCP/BMP1) between residue Gly<sub>168</sub> and Asp<sub>169</sub> (numbered

according to the human sequence) (81, 82), that may occur at cell surface in a bound complex with cellular fibronectin (83). It was also found that other extracellular proteases, including mammalian tolloid (mTLD) and tolloid-like-1 and 2 proteases (mTLL-1 and -2) cleaved proLOX at the correct physiological site but at lower efficiency (84). The N-terminal propeptide of LOX has been implicated in regulating the localization of the enzyme within the specific matrix (85) and reversion of ras-transformed cells to the non-oncogenic phenotype (86).

The C-terminal of human LOX is homologous to the N-terminal extracellular domain of the growth factor and cytokine receptor superfamily and this domain overlaps the catalytic site. The consensus sequence found in the N-terminal modules of Class 1 receptors, C-X<sub>9</sub>-C-x-W-X<sub>26-32</sub>-C-X<sub>10-13</sub>-C (where C is cysteine, W is tryptophan, and X<sub>n</sub> is a defined number of any amino acid), is conserved in human LOX (87). The cytokine receptor module is known to play an adhesion role in several proteins of the growth factor and cytokine receptor superfamily. Based on structure prediction, the cytokine receptor-like domain in the LOX protein forms a partial receptor site and it is questionable if it binds cytokines in the same way (88).

### ***Catalytic mechanism***

#### *Cofactor*

The activity of (mature) LOX requires two cofactors, copper (Cu<sup>2+</sup>) and lysyl tyrosylquinone (LTQ). Direct evidence that copper is a component of LOX was obtained from enzyme isolated from chick bone (89, 90), chick aorta (91, 92), and bovine aorta (93). Studies have demonstrated that approximately one tightly bound copper atom is present in the mature 32 kDa and the removal of the copper ion leads to a catalytically inactive apoenzyme. Electron spin resonance studies have indicated that the copper in

the resting enzyme is in the Cu(II) state, and is bound tetragonally distorted, octahedrally coordinated ligand field (93). The sequence WEWHSCHQHYH in human has been suggested to be the actual copper-binding region, which provides four histidine residues that are involved in the copper-binding coordination complex (94). In addition to the tightly bound Cu ion, purified LOX preparations have been shown to contain 5-9 atoms of loosely bound copper per enzyme molecule (93). Experiments in a cell free transcription/translation system *in vitro* have shown that the unprocessed 50 kDa LOX precursor binds copper (95). A study showed that protein synthesis was important for the incorporation of copper into enzyme but N-linked glycosylation had no effect on secretion of the copper that was bound to LOX. In addition, an inhibition of processing of the 50 kDa LOX precursor into the 32kDa active form with a PCP inhibitor had minimal effect on the amount of copper that was bound to LOX in the cell media (95). Kagan et. al. in 1995 (96) has shown that the propeptide region is not essential to the folding and secretion of the functional enzyme. A truncated rat LOX cDNA lacking sequences which encode for the bulk of the propeptide region was transfected into Chinese hamster ovary cells. The 29 kDa form of mature LOX which catalyzed the deamination of human recombinant tropoelastin and alkylamines was secreted and this secreted enzyme could be inhibited by  $\beta$ -aminopropionitrile ( $\beta$ APN). However, the expression analysis of recombinant LOX in myofibroblast-like cells showed that propeptide region was important for the secretion (97). These controversial data might be due to the difference of type of promoter of the vectors used in the study. These results indicated that copper is incorporated into proLOX in the endoplasmic reticulum or during protein trafficking through the Golgi elements and independent to glycosylation (95, 98).

In addition to copper, LOX was known to possess a covalently bound carbonyl prosthetic group called LTQ (99-104). LTQ is likely the product of a self-processing

reaction involving  $\text{Cu}^{2+}$ -mediated/assisted oxidation of a specific peptidyl tyrosine (res 345 in ratLOX) followed by covalent cross-linking with the  $\epsilon$ -amino group of a conserved peptidyl Lys (res 314 in rat LOX)(105, 106). This unique intramolecular cross-link, LTQ, together with several disulfide linkages within the LOX molecules, most likely contributes to the remarkable physicochemical stability of LOX (34, 104). The covalently linked lysyl component of LTQ of LOX might play an important role in the preference of LOX for peptidyl lysine substrates in cationic protein microenvironments both as a result of its donation of anionic charge to the active site and possibly by restricting the rotation of the LTQ ring in a manner that properly orients the carbonyl cofactor with respect to peptidyl lysine substrates (104). LTQ could be formed in the endoplasmic reticulum or during protein trafficking through the Golgi apparatus (98)(Figure 1.4)

The mechanism of action of LOX has been described in many studies (93, 100, 107-109). The  $\epsilon$ -amino group of the substrate lysine residue condenses with one of the two carbonyls of LTQ to form a Schiff base. The Schiff base linkage coupled with general base-assisted abstraction of hydrogen on carbon 6 of the substrate lysine residue permits the flow of two electrons into LTQ generating the reduced peptidyl lysine tyrosyl aminoquinol. A histidine has been suggested to act as the general base in LOX (110). Hydrolysis of the resulting imine linkage releases the peptidyl aldehyde product from the reduced cofactor. This reactive aldehyde product can then react spontaneously to form lysine- or hydroxylysine-derived cross-links. Subsequent reoxidation of the peptidyl aminoquinol occurs by transfer of two electrons to molecular oxygen, forming and releasing hydrogen peroxide. The quinoeimine so formed is then hydrolyzed to regenerate LTQ and to release the free ammonia product of the reaction (111).

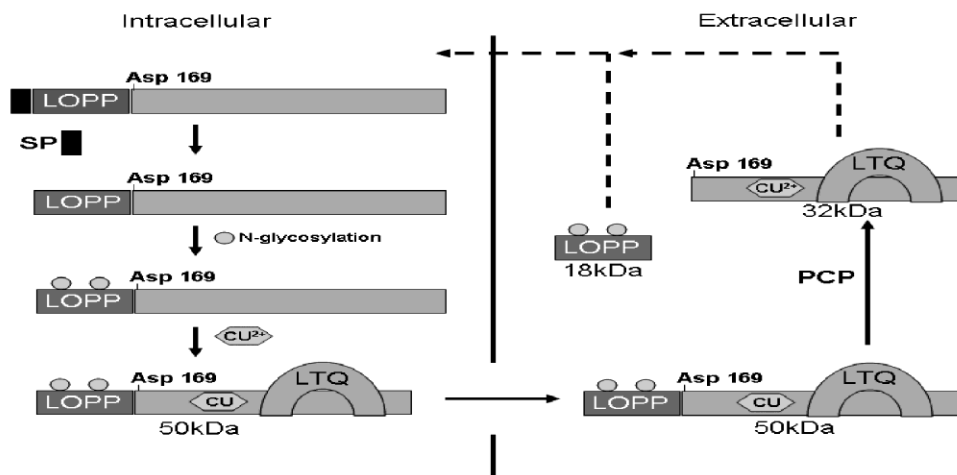


**Figure 1.3** Pathway for LOX biosynthesis. The LOX precursor is trafficked into the rough endoplasmic reticulum where its signal peptide is cleaved. The precursor is glycosylated within the endoplasmic reticulum at two possible Asn residues located in the propeptide region. The addition of copper ( $\text{Cu}^{2+}$ ) and the formation of LTQ cofactor consequently occur. After secretion of the LOX precursor into the ECM, the propeptide region is cleaved by procollagen C-proteinase (PCP) between Gly-168 and Asp-169 to obtain an active 32 kDa enzyme. Lysyl oxidase propeptide (LOPP) and mature LOX has been reported to enter the cell and nucleus after secretion. Molecular mass of LOX polypeptide is indicated according to human LOX enzyme. (69, 70, 112, 113). Cu: Copper, LTQ: Lysyl tyrosylquinone.

### ***Inhibitors***

$\beta$ APN, a potent lathyrogen which can inhibit cross-linkage formation *in vivo*, was recognized before the identification of LOX activity *in vitro* (114).  $\beta$ APN was identified as an active agent in *Lathyrus oderatus* peas causing abnormalities in animals including aortic aneurysm, skin abnormalities, bone and joint weakness (115). Administration of  $\beta$ APN to growing animals results in a condition known as lathyrism, which is characterized by an increased fragility of all connective tissues and an increased solubility of collagen from the tissues (see section osteolathyrism). It has been first demonstrated that micromolar of  $\beta$ APN irreversibly inhibited the activity of LOX *in vitro*

(50).  $\beta$ APN was found to be a potent irreversible inhibitor and its inhibition was temperature- and time-dependent (116).  $\beta$ APN binds to the LTQ, the active site of LOX, and forms a dead-end complex. A free aldehyde product was not generated and the copper content of LOX was not altered upon incubation with  $\beta$ APN (117, 118).  $\beta$ APN has been used to specifically as a lysyl oxidase inhibitor.  $\beta$ -haloamines and  $\beta$ -nitroethylamine are also reported as mechanism-based irreversible inhibitors of LOX similar to  $\beta$ APN (119). Benzylamine derivatives containing para substituents of increased electronegativity and isomers of aminomethylpyridine are also identified as reversible ground state inhibitors by forming LOX-bound intermediates that are not completely processed into aldehydes (107). Vicinal diamines like cis-1,2-diaminocyclohexane and ethylenediamine are potent irreversible inhibitors (120). LOX is inhibited by heparin (121), N-(5-aminopentyl) azidine (122), and trans-2-phenylcyclopropylamine (123). LOX is inhibited by homocysteine thiolactone and its selenium and oxygen analogs in an active-site-directed and irreversible manner (124). LOX is inhibited by ascorbic, and esthonic acids and 3,4-dihydroxybenzoate by possibly the ascorbic acid structure (125).

### ***Substrate specificity***

It was long believed that soluble precursors and immature elastin and fibrillar collagen were the only biological substrate of LOX. This knowledge has been revised when *in vitro* assays demonstrated that the purified LOX oxidized a number of basic globular proteins with pI values  $\geq 8.0$ , but did not oxidize neutral or acidic globular proteins with pI value  $< 8.0$  (126). The electrostatic potential between LOX and its basic protein substrates was essential to productive catalysis. LOX also oxidizes non-peptidyl amine substrates such as n-butylamine and 1,5-diaminopentane leading to the

development of fluorescence-based assay for LOX-dependent H<sub>2</sub>O<sub>2</sub> production (127, 128).

The sequence region within the LTQ domain between Lys314 and Tyr349 are enriched in anionic residues. Once these two regions of LOX become covalently cross-linked to each other as the LTQ cofactor is generated, both of these regions would cooperatively provide an abundance of negatively charged sites in the microenvironment of the active site. It is likely that such an arrangement underlies the strong preference of LOX for cationic protein substrates (104). Interestingly, the sequences surrounding the susceptible lysines in collagen are in hydrophilic sequences containing anionic residues. For example, the lysine residue within the Asp-Glu-Lys-Ser sequence which occurs at the N-terminal region of the  $\alpha 1(I)$  collagen chain within the mature type I collagen molecule is oxidized by LOX *in vivo*. However, a collagen-like synthetic peptide which contains the similar sequence was not a good substrate in assays *in vitro* and oxidation occurred if the Asp residue was replaced with a Gly residue (129). This observation leads to the suggestion that collagen molecules must form into microfibrils before their oxidation by LOX (130) and binding domain of LOX is located in the helical portion of collagen molecule (131). These results led to the hypothesis that the unfavorable negative charge contributed by this Asp residue can be neutralized by a specific cationic site in the neighboring collagen molecule within the quarter-staggered microfibril, thus allowing lysine oxidation by LOX (129). It has been reported that the propeptide regions of recombinant proenzyme of LOX mediated the binding of these enzymes to soluble precursor and fibrous form of elastin in the cultures of transfected RFL-6 fibroblasts. It leads to the conclusion that the binding of the LOX proenzymes to elastin substrates was essential for the oxidation of lysine in elastin by the activated LOX (85). It has been reported that proLOX can bind to fibronectin (FN) to be proteolytically activated to the

functional catalyst (83). Histone H1 and H2 have been demonstrated to have an interaction with LOX *in vitro* (132) and incubation of Histone H1 with LOX results in the catalytic formation of hydrogen peroxide implicating that histone H1 is a substrate of LOX (133). Basic fibroblast growth factor was reported to be a substrate of LOX as the oxidation of lysine residues in bFGF by LOX resulted in the covalent cross-linking of bFGF monomers to form dimers and higher order oligomers and dramatically altered its biological properties (134). Recently, LOX has been reported to be essential for hypoxia-induced metastasis because the administration of  $\beta$ APN, specific anti LOX antibody or short hair-pin RNA could inhibit the metastasis in animal model. It is still unclear whether LOX might oxidize an unknown key protein and inhibit its function in the cancer metastasis, or whether the by-product  $H_2O_2$  from the oxidation plays a role in the inhibition of cancer metastasis (135).

### ***Regulation of LOX***

The factors that were reported to play roles in the regulation of LOX gene expression are transcriptional factors and growth factors as shown in Table 1.1.

**Table 1.1** The various regulators and effects on LOX mRNA and enzymatic activity.

Effector (reference)	Cell or tissue	Effect
IFN- $\gamma$ (136)	Rat aortic smooth muscle cells	Down regulation of mRNA; decreased mRNA half-life
bFGF (75)	Mouse osteoblastic cells	Decreased mRNA level (1-10nM) upregulated of mRNA (0.01-0.2 nM)
FGF-2 and IGF-1 (137)	Inflamed oral tissue, rat fibroblastic mesenchymal cells	Increased of mRNA
PGE <sub>2</sub> (138-140)	Rat lung fibroblasts Human embryonic lung fibroblasts	Unchanged mRNA level; reduction in enzyme activity Downregulation of mRNA

TGF- $\beta$ 1 (75, 76, 138, 139, 141-146)	Rat aortic smooth muscle cells human gingival fibroblast, flexor reticulum cells, renal cell lines, rat lung fibroblasts, kidney tubular epithelial cells, mouse osteoblasts	Increased mRNA level and enzyme activity
BMP-2 (147)	Murine pre-myoblast cells	Increased mRNA level
TNF- $\alpha$ (79, 148)	Mouse osteoblastic cells  Aortic endothelial cells	Decreased mRNA, protein level and enzymatic activity  Decreased mRNA and level and enzymatic activity
Cadmium (149)	Mouse fibroblasts  Mouse cadmium-resistant fibroblasts	Decreased mRNA level  Increased mRNA level
Testosterone (150, 151)	Calf aortic smooth muscle cells, rat granulosa cells	Increased enzyme activity and increase mRNA expression
Follicle stimulating hormone (151)	Rat granulosa cells	Decrease mRNA expression and enzyme activity
Growth differentiation factor-9 (151)	Rat granulosa cells	Increase mRNA expression and enzyme activity
Activin A (151)	Rat granulosa cells	Increase mRNA expression and enzyme activity
Bleomycin (152)	Human lung fibroblasts  Human dermal fibroblasts	Increased mRNA level  Decreased mRNA level
Hydralazine (152)	Human dermal fibroblasts	Increased mRNA level
Minoxidil (152)	Human dermal fibroblasts	Increased mRNA level
Adriamycin (153)	Rat kidney glomeruli, medulla	Increased mRNA level
cAMP (140, 154)	Rat and human vascular smooth muscle cells	Upregulated of transcription
PDGF (155)	Rat vascular smooth muscle cells	Upregulation of mRNA
Dexamethasone (156)	Cultured fetal murine lungs	Upregulation of mRNA
Retinoic acid (157)	Adipocytes in early adipogenesis	Prevents downregulation of mRNA and enzyme activity.
Hypoxia inducible factor-1 (158)	Breast cancer cells	Increased mRNA and protein level but decreased enzymatic activity
Hypoxia/reoxygenation	Breast cancer cells	Increase mRNA, protein level

(158)		and enzyme activity
Low density lipoprotein (77)	Vascular endothelial cells	Decrease mRNA expression and enzyme activity
Homocysteine (159)	Vascular endothelial cells	Decrease LOX activity (35 $\mu$ M) Decrease LOX mRNA expression and LOX promoter activity (250 $\mu$ M)
Pulsed ultrasound (160)	Mouse osteoblastic cells	Increase LOX mRNA expression and enzyme activity (30 mW/cm <sup>2</sup> )
Metavanadate (161)	Rat fibroblast	Decrease LOX activity

Modified from (88, 162)

### ***Animal models***

The consequence of inactivation of the *Lox* gene in mice results in neonatal lethality (162-164). The mice develop to full term but are not viable. The autopsy revealed large aneurysms in aorta, which the diameter of aneurysm was 3 times larger than in the aortas of the wild-type littermates and the wall of the aorta in the *Lox*<sup>-/-</sup> animals was significantly thicker but the diameter of the aortic lumen was significantly smaller than those in the wild-type littermates. The *Lox*<sup>-/-</sup> animal had a congenital diaphragmatic hernia and a large hemorrhage in the upper chest region. Microscopic analysis showed abnormal elastic lamellae with fragmented elastic fibers and discontinuity in the smooth muscle cell layers in *Lox*<sup>-/-</sup> fetuses (162, 163). Another report on *Lox*<sup>-/-</sup> animals reported the similar phenotypes as that the animal died soon after parturition, exhibiting cardiovascular instability with ruptured arterial aneurysms and diaphragmatic rupture. Microscopic analysis of the aorta demonstrated fragmented elastic fiber architecture in homozygous mutant null mice. LOX activity, as assessed by desmosine (elastin cross-link) analysis, was reduced by approximately 60% in the aorta and lungs of homozygous mutant animals compared with wild type mice. Immature collagen content in aorta and lungs of the animals were decreased 74% and 68%

respectively compared with those of wild-type littermates. There were significant decreases in DHLNL and HLNL of 43 and 39% respectively in the *Lox*<sup>-/-</sup> animals as compared with wild type total body collagen cross-links. Interestingly in *Lox*<sup>+/-</sup> mice, DHLNL was 100% of wild type, while HLNL was only 64% of wild type content. This could represent a greater role for LOX in HLNL cross-links. Moreover, DHLNL in lung of *Lox*<sup>-/-</sup> animals was not different among genotypes while decreased in HLNL in *Lox*<sup>+/-</sup> and *Lox*<sup>-/-</sup> was 14 and 32% respectively (164).

### ***Lysyl oxidase isoenzymes***

Isoenzymes or isozymes are defined as isoforms of enzymes in biochemistry. They are the enzymes that differ in amino acid sequence but catalyze the same chemical reaction (165). They are present in different tissues, cell types, or developmental stages of the same or different tissues or organs. Four LOX-like (LOXL) proteins varying degree of similarity to LOX have been discovered and identified; lysyl oxidase-like protein (LOXL1) (87, 166), lysyl oxidase-like 2 protein (LOXL2) (167, 168), lysyl oxidase-like 3 protein (LOXL3) (162, 169-172), and lysyl oxidase-like 4 protein (LOXL4) (162, 173-175). Polypeptides of all these isozymes are highly conserved within their C-terminal ends, which include the copper-binding sites, cytokine receptor-like domains, and LTQ cofactor sites (88). All LOXL proteins possess amine oxidase activity (174, 176-178). In LOXL2, 3 and 4, repeated scavenger-receptor cysteine-rich (SRCR) domains are present as conserved domain. These domains have the potential to interact with other proteins. The SRCR domain contains either six or eight cysteine residues located at highly conserved positions important for tertiary conformation and is found in cell surface protein or secreted protein associated with the immune system. The comparison of LOX family member is shown in the table 2 (adapted from Hornstra et al 2003(164)).

**Table 1.2** The comparison of LOX family member.

Family member	Human Chr.	Mouse Chr.	mRNA and protein size	Highest mRNA tissue distribution	Protein domains	%similarity to LOX domain	%similarity to LOXL2 domain
LOX	5	18	6.8, 4.8 kb 417 res.	Lung, skeletal muscle, kidney, heart	Amine oxidase	100	63
LOXL1	15	9	2.4 kb 574 res.	Lung, heart, spleen skeletal muscle, pancreas	Amine oxidase	85	63
LOXL2	8	14	4.0 kb 774 res.	Lung, thymus, skin, testis, ovary	4 SRCR, Amine oxidase	58	100
LOXL3	2	6	3.3 kb 753 res.	Heart, uterus, testis, ovary	4 SRCR, Amine oxidase	65	78
LOXL4	10	19	3.5 kb 756 res.	Skeletal muscle, testis, pancreas	4 SRCR, Amine oxidase	62	79

*Lysyl oxidase-like protein (LOXL1)*

LOXL1 has been first discovered from a novel human cDNA with a predicted protein similar to LOX. The LOXL1 cDNA corresponds to a single polyadenylated mRNA species of 2.5 kb, which shows a concomitant expression with LOX mRNA in several human tissues (87). The LOXL1 polypeptide consists of 574 amino acids, with a calculated mass of 63 kDa. It shows 76% similarity with LOX at its C-terminal region (87, 166), which includes the copper-binding site and the four histidine residues with the conserved sequence (WEWHSCHQHYYH) that are involved in the copper binding complex. In addition the cytokine receptor-like sequences are present in this C-terminal region in both LOX and LOXL1 polypeptides. The LOXL1 gene contains 7 exons and has been mapped to chromosome 15q24 in humans (179) and chromosome 9 in mice

(180, 181). LOXL1 protein is a secretory protein that is expressed in active fibrotic diseases and in the early stromal reaction of breast cancer (182). Coincident appearance of increased steady-state levels of LOXL1 and COL3A1 mRNAs was detected in the early development of liver fibrosis, suggesting that LOXL1 protein is involved in the development of lysine-derived cross-links in collagenous substrates. In contrast, steady-state levels of LOX mRNA were increased throughout the onset of hepatic fibrosis and appeared in parallel with increased steady-state level of COL1A1 mRNA (183). A specific antibody against LOXL1 has been used to identify proteins immunochemically distinct from LOX in various cells and in bovine aorta. The species of the protein are approximately 68, 52, 42 and 30 kDa (182). A 56 kDa LOXL1 protein was isolated from bovine aorta and the precursor needs to be cleaved by BMP-1 to be active (176). The mice lacking LOXL1 do not deposit normal elastic fibers in the uterine tract post partum and develop pelvic organ prolapse, enlarged airspaces of the lung, loose skin and vascular abnormalities with concomitant tropoelastin accumulation. Distinct from the prototypic LOX, LOXL1 localizes specifically to sites of elastogenesis and interacts with fibulin-5. Thus elastin polymer deposition is a crucial aspect of elastic fiber maintenance and is dependent on LOXL1, which serves both as a cross-linking enzyme and an element of the scaffold to ensure spatially defined deposition of elastin (184).

#### *Lysyl oxidase-like protein 2 (LOXL2)*

LOXL2 was originally cloned, characterized, and named as WS9-14 for its possible association with Werner syndrome (167). Later it was found that WS9-14 mRNA corresponds to LOXL2 mRNA but WS9-14 transcript encodes one additional SRCR domain in its 5' end region (88, 168). LOXL2 mRNA encodes an 87 kDa polypeptide, which contains four SRCR domains that are found in several secreted and cell surface proteins (167). LOXL2 polypeptide shares a 48% similarity with the LOX

polypeptide in its amino acid sequence from residue 546 to 751 in its C-terminal region. This region contains all conserved amino acid sequences needed for the proper function of the mature 32 kDa form of LOX enzyme (167, 168). LOXL2 gene has been mapped to chromosome 8p21 in humans (185) and chromosome 14 in mice (186), and it consists of at least 11 exons (168). LOXL2 is abundantly expressed in senescent fibroblasts and several adherent tumor cell lines, but is down-regulated in several non-adherent tumor cells. This suggests that it may be involved in cell adhesion and that a loss of this protein may be associated with the loss of tumor cell adhesion leading to tumor metastasis. LOXL2 shows similar spatial expression with LOX and LOXL in human placenta and fetal tissues in early pregnancy. However, this pattern diverges during gestation (187). In full-term human placenta, LOX is expressed predominantly in the amniotic epithelium, with little expression in the placenta, while LOXL shows the highest expression in the placenta and lowest expression in the amnion. LOXL2 expression differs in that it is detected predominantly in chorionic cytotrophoblasts of the membranes with only low expression levels in the amnion and placenta (168, 187, 188).

#### *Lysyl oxidase-like protein 3 (LOXL3)*

LOXL3 was detected as an osteoblast-derived EST and later in other tissue panels (171). LOXL3 mRNA encodes a predicted mass of 80.3 kDa protein with a putative signal peptide in the N-terminus. The nonprocessed LOXL3 polypeptide shared a 55% amino acid sequence similarity with the LOXL2 polypeptide and the C-terminal residues showed a high degree similarity with the LOX, LOXL and LOXL2 polypeptides, 51%, 53% and 69% respectively. The N-terminal region of the LOXL3 polypeptide contains a bipartite nuclear localization signal (KKQQQSKPQGGEARVRLKG), which is not found in any other LOX isozyme. Despite the presence of the nuclear localization signal, there was no evidence to show any role of LOXL3 in the nucleus, which has been

shown to be due in part to the LOX polypeptide (112) or LOXL (189). LOXL3 gene has been mapped to chromosome 2p13 in humans (170) and chromosome 6 in mice (171, 172). LOXL3 is expressed highly in placenta, heart, ovary, testis, small intestine and spleen (162, 171).

#### *Lysyl oxidase-like protein 4 (LOXL4)*

LOXL4 was cloned from placental, kidney, fetal tissues and chondroblast and osteoblast cDNA (173-175). The deduced 756-amino acid protein contains an N-terminal signal sequence, 4 scavenger receptor cysteine-rich (SRCR) domains, lysyl and tyrosyl residues that form the carbonyl cofactor within the catalytic site, and a cytokine receptor-like domain at the C terminus. LOXL4 shares 51% and 54% amino acid identity with LOXL2 and LOXL3, respectively. LOXL4 gene has been mapped to chromosome 10q24 in humans (175) and chromosome 19 in mice (162, 173). LOXL4 is highly expressed in skeletal muscle, testis and pancreas and not expressed in leukocytes (173).

### **Novel biological functions of LOX**

#### ***LOX in tumor suppression***

LOX was reported to show tumor suppression in 1990 (190). A cDNA species named as *ras reversion gene (rrg)* was identified when mouse NIH 3T3 cells were transformed with LTR-c-H-ras. This DNA was markedly down-regulated and restored when the transformed cell line (RS485) was treated with interferon to obtain a persistent revertant cell line (PR4). The revertant cells are phenotypically non-transformed and non-tumorigenic. Once an *rrg* antisense RNA was transfected into PR4 cells, the reappearance of the tumorigenic and transformed phenotype was observed. Subcutaneous administration on these antisense cells into athymic mice induced tumor formation. The cDNA sequences of the mouse *rrg* and rat *Lox* were subsequently found

to be identical, indicating that *rrg* encodes *Lox* (191), the activity of which was already known to be markedly low in the medium of malignantly transformed cultured human cell lines (192). Expression of LOX was down-regulated in immortalized rat 208F fibroblasts after transformation by activated H-*ras* (193, 194) and up-regulated in spontaneous phenotype revertants that continued to express the *ras* oncogene (193). In spontaneous phenotypic revertant, LOX expression was found to be irreversibly and coordinately regulated with type I collagen expression (193). A tumor suppressor role of LOX was demonstrated by stable transfection of a LOX cDNA in antisense orientation to normal rat kidney fibroblasts (NRK-49F). The transfected cells exhibited a loose attachment to plate, anchorage-independent growth, and high tumorigenicity in nude mice, and also showed an impaired response of the PDGF and IGF-1 receptors to their ligands (195). Several malignant transformed human cell lines showed low level of LOX mRNA and enzyme activity (196). The LOX gene was identified as a target for the anti-oncogenic transcription factor (IRF-1), which manifests tumor suppressor activity and contributes to the development of human hematopoietic malignancies (197). In malignant human breast carcinomas, LOX was highly expressed in myofibroblasts and myoepithelial cells surrounding the *in situ* tumor and in the reactive fibrosis facing the invasion front of infiltrating tumors (198) and type I, III and IV collagens and elastin were found to be co-distributed with LOX resulting in the formation of a scar-like peritumor barrier (198). In contrast, LOX was found to be absent from the carcinoma cells suggesting a possible host defense mechanism for cancer. Interestingly a late stromal reaction lacking of LOX favors tumor dispersion (198). In mouse prostate cancer model, LOX was expressed in normal epithelium, but lost in primary prostate cancer and associated metastatic lesions (199). In broncho-pulmonary carcinoma, a strong expression of LOX is associated with the hypertrophic scar-like stromal reaction found at the front of tumor progression. In contrast, little or no expression was found within the stromal reaction of invasion

carcinomas, small cell carcinomas and neuro-endocrine carcinoma (200). It has been demonstrated that a loss or reduction of LOX function during tumor development may be a direct consequence of somatic mutations and may be associated with the pathogenesis of colon cancer (201). The LOX gene is located in chromosome region 5q23, which is known to be deleted in a high frequency in many different types of cancer (202). LOX was reported to inhibit ras-mediated transformation by preventing the activation of NF-Kappa B (NF- $\kappa$ B) (203). Lysyl oxidase propeptide (LOPP) was also reported to have tumor suppression ability by inhibiting Erk1/2 Map kinase activation (86, 204) and recently by inhibiting Akt activity and BCL2, a tissue-specific NF- $\kappa$ B target gene (205).

### ***LOX dependent chemotaxis***

$\beta$ APN has been reported to inhibit fibroblast migration in a dose-dependent fashion without inhibiting proliferation (206). Purified 32 kDa mature LOX was shown to play a role as a potent chemoattractant for human peripheral blood mononuclear cells, with a 237% increase in migration over the enzyme-free or catalytically inhibited LOX controls seen at  $10^{-9}$  M LOX (207). The result showed that  $H_2O_2$  product of the LOX-catalytic reaction appeared to mediate the chemotactic response since the observed result was not detected when the LOX was inactivated or absent from the reaction (208). The result also suggested that the chemotactic effect was not due to the reaction of LOX with secreted protein in the media but more likely due to the direct access of LOX to cell-associated substrates. The cellular responses after addition of LOX showed elevated level of intracellular  $H_2O_2$ , enhanced stress fiber formation, and increased focal adhesion assembly, consistent with the induction of chemotactic response. The chemotactic response was prevented by the prior addition of catalase, indicating the crucial role of the  $H_2O_2$  product of the LOX-catalytic reaction (208). In breast cancer studies, LOX and

its isoform mRNA levels are upregulated in invasive type compared to those of non-invasive type and the invasion phenotype was facilitated by active but not inactive LOX. In addition, the invasion was inhibited when the antisense mRNA of LOX was transfected or  $\beta$ APN was added into the cultured (209). A further report from the same group demonstrated that this LOX-dependent chemotactic response of breast cancer cells was elicited by the  $H_2O_2$  product of the LOX-catalytic reaction on unidentified substrates (210). Recently it has been shown that actin stress fiber formation and Rho activity in breast cancer cell line are increased through the p130 (Cas)/Crk/DOCK180 signaling complex by inhibition of LOX in these cells (211). It suggests that the down-regulation of LOX activity could limit the invasiveness of breast cancer. Other isozymes have been reported that their expression are high in metastatic breast cancer cells and correlate with increased tumor malignancy and increased fibrotic foci (209, 212). The elevation of LOX under hypoxic condition in head and neck tumor cells appeared to be essential for the hypoxia-induced metastatic response of these cells and the increased invasiveness was prevented by treatment of  $\beta$ APN, LOX antisense oligonucleotides, LOX antibody or short hairpin RNA expression but not with LOX sense oligonucleotides (135). This study did not show the role of  $H_2O_2$  product of the LOX-catalytic reaction. Another study showed that LOX interacts with hormone placental lactogen and synergistically promotes breast epithelial cell proliferation and migration. However, the study showed that lactogen was neither a substrate nor an inhibitor so the  $H_2O_2$  from the oxidative reaction was not generated but their coexpression resulted in a 240% increase in cell migration (213). Recently, LOX has been reported to be correlated with focal adhesion kinase (FAK)/paxillin activation and migration in invasive astrocytes. Tyrosine phosphorylation of FAK/paxillin was inhibited by  $\beta$ APN treatment and catalase addition (214).

### ***Intracellular and intranuclear activities***

LOX was reported to be associated with cytoskeleton protein in cytoplasm in cultured fibroblasts (215). It was not conclusive that the observed LOX represented the proenzyme and/or mature LOX since the molecular weight of the LOX was not determined. It has been reported that an intracellularly expressed recombinant mature 32 kDa LOX might regulate the activity of COL3A1 gene promoter (195). The coinjection of LOX with oncogenic p21-*ras*<sup>val12</sup> into *Xenopus laevis* oocytes suggests one possible intracellular role for LOX in antagonizing a Ras-induced meiotic maturation of these cells. It has been suggested that a LOX-dependent block in oocyte maturation may be downstream of Erk2, a member of the mitogen-activated protein kinases (216).

A mature LOX 32kDa was observed by immunocytochemistry and Western blot analysis in the nucleus of rat vascular smooth muscle cells and 3T3 fibroblast (112). In addition, the nucleus of the vascular smooth muscle cells contained lysinonorleucine (LNL), which is the adduct formed during cross-linking formation of LOX and the formation of LNL was prevented by administration of  $\beta$ APN, confirming a role of LOX in the reaction (112). It was demonstrated that a purified bovine 32 kDa LOX polypeptide fluorescent-labeled with rhodamine was able to enter into the cytosol and become rapidly concentrated into the nuclei of cultured smooth muscle cells. The intracellular uptake and distribution of intranuclear LOX were not altered by  $\beta$ APN showing its independency from the amine oxidase activity of LOX (217). The intracellular LOX was reported to activate the transcription activity of human collagene III promoter via possible involvement of Ku antigen (218). LOX has been reported to locate in cytoplasm of MDCK II kidney cells and MCF-10A breast cancer cells however, the lysyl oxidase activity from the cell lysate could not be detected (189). Another report from a different group showed a stage-dependent intracellular distribution of mature LOX 32kDa and

LOPP 18kDa in osteoblasts. In proliferating cells, mature LOX located in nucleus and perinuclear region while LOPP associated with Golgi and endoplasmic reticulum. In differentiating cells, mature LOX and LOPP colocalized with the microtubule network (113). However, the mechanism of how LOX and LOPP can be uptaken intracellularly or intranuclearly remains unelucidated (112). Recently LOX has been reported to regulate elastin promoter via intracellular effects of transforming growth factor- $\beta$ 1 (TGF- $\beta$ 1). The author showed the reduction of Smad 3 and 4 in the addition of TGF- $\beta$ 1 when the coding sequence of mature LOX without signal peptides was transfected in 293T cells. The cross control mechanism remains unclear (219).

### ***Growth factor and cellular modulation***

In addition to collagen and elastin, purified LOX oxidized a number of basic globular proteins *in vitro* with pI values  $\geq 8.0$ , but did not oxidize neutral or acidic globular proteins with pI value  $< 8.0$  (126). The study demonstrated Histone H1 as a substrate of LOX by detecting the increase of lysinonorleucine cross-link and ACP in histone H1 sample after incubation with purified LOX. Histones are involved in chromatin packing in nucleus and can be oxidized by LOX. The histone oxidation might modulate the packing state of nuclear chromatin (220). Basic fibroblast growth factor (bFGF) was reported to be a substrate of LOX *in vitro*. The oxidation of lysine residues in bFGF by LOX resulted in the covalent cross-linking of bFGF monomers to form dimers and higher order oligomers. The fluorescence LOX assay showed temperature dependent of amine oxidase activity of LOX in which LOX oxidized 14 lysine residues at 55°C, and 5-6 residues at 37°C. The biological effect of LOX oxidized bFGF resulted in the inhibition of bFGF nuclear localization, and the inhibited FGF-2 mediated cell cycling, resulting in cell growth suppression (134).

## **Lysyl oxidases in an osteoblast cell culture systems and in mineralized tissues**

LOX was first identified in bone from saline extract in 1968 (50). Several reports have shown that the activity of purified bone LOX was inhibited by  $\beta$ APN but it was not well characterized (50, 90). LOX was also identified in dentin (221). In chick calvarial osteoblast cultures, once treated with 20  $\mu$ g/ml  $\beta$ APN, total collagen synthesis was increased two folds with no change in mRNA levels for collagen type I but the accumulated collagen in matrix was decreased by 50% and mineral deposit was reduced compared to control. The  $\beta$ APN treated cultures showed a wider diversity of fibril diameters with a larger average collagen fibril diameter compared to control (222). This study implicated the role of collagen cross-link in the collagen deposition, fibrillogenesis and fibril stability. In 3-dimensional cultures of chondrocytes, treated with 0.25 nM  $\beta$ APN, collagen type II synthesis significantly increased and collagen fibril diameters were larger compared to controls. In addition, the expression of other minor collagens, collagen type XI, and aggrecan increased significantly in the presence of  $\beta$ APN (223). A study of LOX expression and activity in osteosarcoma cell line showed that LOX activity was not related closely to LOX mRNA levels among the different cell clones and the activity of LOX was BMP-1 dependent (224). The role of LOX in controlling insoluble collagen deposition in MC3T3-E1 (MC) osteoblastic cells has been also studied and reported that the maximum increase in LOX activity precedes the most efficient phase of insoluble collagen deposition. Once treated with 400  $\mu$ M  $\beta$ APN, the cultures showed a 44% increase of insoluble collagen deposition compared to control cultures. In addition, the collagen fibril diameter showed irregular shapes and a larger average diameter (30%) compared to the control cultures. The authors suggested that the increase of collagen accumulation in the matrix was due to insufficient proteolytic activity to destroy abnormal collagen fibrils (73). The administration of PCP inhibitor

diminished collagen processing and LOX activity; however, the collagen cross-links, Pyr and d-Pyr were not altered. Moreover, a slight increase (10%) of collagen fibril diameter was reported (225). LOX has been also shown to be regulated by bFGF (226), TGF- $\beta$ 1 (75) and TNF- $\alpha$  (79) in MC3T3-E1 (MC) cells. The expression of LOX and its isoforms in MC cells have recently been investigated and the result showed that LOX and all LOXLs except LOXL2 were expressed in this cell line and the expression during the cell differentiation and matrix mineralization was distinct from one another (74). The stage-dependent intracellular distribution of mature LOX 32kDa and LOPP 18kDa was investigated in MC cells. In proliferating cells, mature LOX located in nucleus and perinuclear region while LOPP associated with Golgi and endoplasmic reticulum. In differentiating cells, mature LOX and LOPP colocalized with the microtubule network (113).

### ***Osteolathyrism***

Osteolathyrism is caused by chronic ingestion of the sweet pea *Lathyrus odoratus*, which contains  $\beta$ -( $\gamma$ -glutamyl)aminopropionitrile, a potent irreversible inhibitor of LOX when metabolized to  $\beta$ APN (115, 227). Other inhibitors are ureides, semicarbazide and thiosemicarbazide, which are believed to chelate the prosthetic Cu-(II)-bipyridine cofactor complex in LOX (228). LOX inhibition leads to the diminished cross-linking of collagen and elastin and consequently causes weakness and fragility of connective tissue (i.e., skin, bones, and blood vessels [angiolathyrism]) and the paralysis of the lower extremities associated with neurolathyrism. A study in Bangladesh showed that the prevalence of neurolathyrism among neurological patients is 0.14% and the prevalence was higher among young males. The patients always consumed green shoots of *Lathyrus sativus* (229). The prevalence of osteolathyrism in neurolathyritic patients was about 12% (230). The connective tissue manifestations include

kyphoscoliosis, bone deformities, weakening of tendons and ligament attachments, dislocation of joints, weakening of skin and cartilage, hernias and dissecting or saccular aneurysm of the aorta (231). In a rabbit model, osteolathyrism does not become manifest until practically all mature cross-linking that can be affected has been inhibited (232). In experimental osteolathyritic rat model, osteolathyrogens cause a spectrum of tissue alterations in skeleton, soft connective tissue and arteries (233). Ectopic exostoses and aneurysmal-like bone cysts in mandible and long bones were observed (234, 235) due to significantly impaired turnover and remodeling rates of periosteal and endosteal bone (236). Fracture healing in osteolathyritic animals results in excessive callus formation. The vast fracture callus is very fragile and consists of irregular cartilage and premature woven bone (237, 238). Fractured tibias in the animal developed excessive amounts of mechanically weak callus tissue with irregular cartilage and showed reduced glycosaminoglycan accumulation. In lathyritic calluses, the maximal mRNA of type II and IX collagens and aggrecan core protein was peaked 4 days earlier than in controls reflecting the less well control of endochondral ossification in lathyritic calluses. Interestingly the expression of TGF- $\beta$ 1 mRNA in lathyritic calluses was already peaked at the early time-points while that of control was relatively low and increased gradually at later time-points of study (239).

### **TGF- $\beta$ in bone and its potential regulation by LOX**

TGF- $\beta$  is one of the most potent pleiotropic growth factors controlling a diverse set of cellular processes, e.g. cell growth, differentiation, migration, apoptosis, and synthesis of ECM proteins including collagen (240-245). The TGF- $\beta$  superfamily comprises over 35 structurally related polypeptides in vertebrates including TGF- $\beta$ s, activins, nodal, bone morphogenetic proteins (BMPs) and some other related proteins, and those have crucial roles in development and in tissue homeostasis (246). All of

these members share a cluster of conserved cysteine residues forming a characteristic cysteine knot. They are synthesized as precursors with a large N-terminal propeptides that is proteolytically cleaved from a mature C-terminal domain peptide.

TGF- $\beta$ 1 is the prototypic member of the TGF- $\beta$  superfamily, and bone ECM is a major storage site in the body for this growth factor (247). Though TGF- $\beta$ 2 and 3 are also present in bone, TGF- $\beta$ 1 is the predominant isoform (>90%) at the level of 200-700  $\mu$ g/Kg in this tissue (248, 249). In bone, TGF- $\beta$ 1 plays pivotal roles in many, if not all, aspects of the tissue development, remodeling, mechanical properties and aging (250-252). Numerous studies, though not always consistent, have shown that TGF- $\beta$ 1 stimulates recruitment and proliferation of osteoblast progenitors (253, 254), stimulates matrix production such as collagen, fibronectin, osteopontin, osteonectin, proteoglycans, but inhibits osteocalcin (250, 255), inhibits late stage of osteoblast differentiation and matrix mineralization (256, 257), and modulates osteoclast differentiation (258). The abundance of this growth factor with such potent effects on cells predicts the need for tight regulation of its biological activities. Indeed, several studies have shown that deregulation/overactivation of TGF- $\beta$  could be detrimental to osteoblastogenesis and bone formation causing bone defects (259-261).

TGF- $\beta$ 1 is secreted as a latent complex that needs to be activated before being capable of eliciting biological effects (262, 263), and it appears that it is the only growth factor known to be produced in a latent/inactive form. The latency is achieved by noncovalent association between TGF- $\beta$  and its propeptide, called latency-associated peptide (LAP), forming a ~100 kDa small latent complex (SLC). For this association, thus, to confer “latency” to TGF- $\beta$ , res 50-85 near the N-terminus of LAP is important (264). More recently, it has been reported that the LSKL sequence (res 54-57) in this region of LAP is critical for its association with mature TGF- $\beta$  (265). In the same report,

the authors also identified the RKPK sequence near the C-terminus of mature TGF- $\beta$  as a potential recognition sequence for LSKL. Interestingly, the C-terminus of the mature TGF- $\beta$  (res 83-112) including the RKPK sequence has also been demonstrated to be the critical site for the binding to its type II receptor (T $\beta$ RII) that initiates the signaling cascade of TGF- $\beta$  (241, 266, 267). Thus, the association of LSKL of LAP and RKPK of TGF- $\beta$  may sterically prevent receptor binding (265). It is of interest to note that the vicinity of the critical regions of LAP and TGF- $\beta$  for their association and the region of TGF- $\beta$  to bind T $\beta$ RII for signaling are enriched in basic amino acids, including several Lys residues, yielding high pI values (e.g. estimated pI for res 50-85 of LAP is 9.98, and for res 83-112 of mature TGF- $\beta$ 1 is 9.24). In many cell types, LAP is further disulfide-bonded by latent TGF- $\beta$  binding proteins (LTBPs) to form a ~290kDa large latent complex (LLC) prior to secretion, and in the ECM, LLC is stored possibly by covalently linked to matrix components (263, 268). LTBP is thought to be important for efficient secretion, storage of TGF- $\beta$  in ECM and TGF- $\beta$  activation (268). Although almost all nonmalignant cells secrete TGF- $\beta$  as a part of LLC, bone cells form an exception as they efficiently secrete SLC, thus, lacking LTBP (269-271). At least 50% of the latent TGF- $\beta$  forms produced by bone cells was found to be SLC (272) indicating its specific role in bone biology. Bone cells also produce LLC like other cell types (273) where LTBP may play dual roles in matrix storage and structural element for bone formation (272). The latent TGF- $\beta$  can be activated by plasmin, thrombospondin-1,  $\alpha_v\beta_6$  integrin, heat, low pH, etc. (263). Such low pH can be generated by osteoclasts during bone resorption to activate TGF- $\beta$  (7, 274). Since bone is a dynamic, constantly remodeling tissue, tight regulation of TGF- $\beta$  activity (either in a free or a complex form) is crucial. The regulation can be done by: 1. stable TGF- $\beta$  binding molecules limiting the bioavailability of this growth factor during remodeling, and/or 2. TGF- $\beta$  modifications that reduces its potency as a growth factor or stabilizes its latency. In bone matrix, there are several TGF- $\beta$

binding molecules including small leucine-rich proteoglycans, decorin and biglycan (260, 275, 276) that may sequester TGF- $\beta$  in the matrix and/or diminish TGF- $\beta$  binding to its cell receptor (277). However, the significance of these interactions in bone ECM is not known. Furthermore, potential extracellular modification of TGF- $\beta$  that may change and/or stabilize the potency is unknown.

During the course of my study on the biological significance of the post-translational modifications of collagen in bone, I discovered that in an osteoblastic cell culture system, higher LOX expression resulted in less collagen production and suppressed TGF- $\beta$ 1 signaling while lower LOX expression exhibited more collagen production and enhanced TGF- $\beta$ 1 signaling. This intriguing finding prompted me to examine the potential interaction between LOX and this growth factor. When these two proteins were co-expressed in 293 cells, the binding was detected in a dose-dependent manner. No binding was identified between LOX and BMPs tested or LAP. Furthermore, TGF- $\beta$ 1 was found to be bound LOX in the mineralized bone matrix. Considering the facts that LOX possesses a strong preference towards basic proteins as its substrates and TGF- $\beta$ 1 (and LAP) is a basic protein, especially its critical domain for “latency” and “signal transduction” is enriched in basic amino acids including Lys residues, it is then possible that LOX may bind and oxidize TGF- $\beta$ 1 in bone. This may result in limiting bioavailability and activity of this growth factor.

## **CHAPTER II**

### **Hypothesis**

Lysyl oxidase regulates TGF- $\beta$ 1 function in bone via its amine oxidase activity.

## **CHAPTER III**

### **STUDY I**

#### **Lysyl oxidase regulates collagen quality and quantity in osteoblasts**

Phimon Atsawasuwan, Yoshiyuki Mochida, Michitsuna Katafuchi, Mitsuo Yamauchi

#### **Specific aims**

1. To establish several MC cell clones that express higher or lower levels of LOX by overexpression or antisense approaches.
2. To characterize collagen cross-linking, production, fibrillogenesis and matrix mineralization in the clones.

## ABSTRACT

Fibrillar type I collagen controls spatial aspects of mineralization by providing a stable template in most mineralized tissues. The stability of the fibril is primarily derived from covalent intermolecular cross-linking initiated by lysyl oxidase (LOX). In this study, MC cell-derived clones expressing higher (S) or lower (AS) levels of LOX were generated, and the effects on collagen production, fibrillogenesis and mineralization were characterized *in vitro*. In comparison to controls (parental MC3T3-E1 cells (MC) and empty vector (EV) clones), the S clones showed significant decreases in total collagen production and increases in pyridinoline cross-link and total aldehydes, AS clones showed the opposite phenotypes. The numbers and diameter of collagen fibrils of S clones were markedly less and smaller while the diameter of fibrils of AS clones were larger than those of controls. The onset of mineralization was delayed in both S and AS clones in comparison with the controls indicating defective matrix mineralization. CONCLUSION: These results indicate that LOX is critical in regulating not only quality but quantity of collagen and mineralization in an osteoblastic cell culture system.

## INTRODUCTION

Mineralization is a multifactorial process orchestrated by cells and a number of matrix molecules. In bone, fibrillar type I collagen regulates spatial aspects of mineralization by providing a 3-dimensional template for minerals to deposit and grow. One of the characteristics of collagen is its large number of post-translational modifications, many of which are unique to collagens (15, 35). Covalent intermolecular cross-linking is the final modification essential for the stability of the fibrils, thus, for the functional fibrils. The stability and adaptability of the fibril attained by specific covalent intermolecular cross-linking seem to be essential and the alterations of collagen cross-linking were indeed observed in numerous bone disorders (38, 278, 279). The process of collagen cross-linking is initiated by the conversion of telopeptidyl lysine and hydroxylysine residues to aldehyde through the action of an enzyme, lysyl oxidase (EC 1.4.3.13, protein-lysine 6-oxidases, LOX) (15, 34). The aldehyde produced then undergoes a series of condensation reactions to form intra- and intermolecular cross-links that are essential for the stability of collagen fibrils (15). A study of LOX in MC3T3E-1 (MC) cells showed that the maximum increase in lysyl oxidase activity precedes the most efficient phase of insoluble collagen deposition. Once treated with 400 $\mu$ M  $\beta$ APN, the cultures showed a 44% increase of insoluble collagen deposition compared to control cultures. In addition, the collagen fibril diameter showed irregular shapes and a higher average diameter (30%) compared to the control cultures (73). Recently we have reported that LOX and all LOXLs, except LOXL2, were expressed in MC cells, a osteoblastic cell line, and that the expression pattern during cell differentiation and matrix mineralization was distinct from one another (74). The expression of LOX mRNA is the highest form among its family and the expression pattern corresponds to that of type I collagen in this cell line. To obtain further insights

into the function of this enzyme in osteoblastic cells, we generated several MC cells-derived clones that express higher or lower levels of LOX and investigated the effects on collagen matrix in their respective cultures. Here we have demonstrated that LOX has significant effects on collagen fibrillogenesis and mineralization *in vitro*.

## EXPERIMENTAL PROCEDURES

*Cell Lines and Culture Conditions*– MC cells subclone 4, (280) were purchased from American Type Culture Collection (CRL-2593) and maintained in  $\alpha$ -minimum essential medium (Gibco) containing 10% FBS (Atlanta Biologicals) and supplemented with 100 U/ml penicillin G sodium (Gibco), 100  $\mu$ g/ml streptomycin sulfate (Gibco) in a 5% CO<sub>2</sub> atmosphere at 37 °C. The medium was changed twice a week.

*Isolation of LOX cDNA and generation of constructs*– Total RNA was isolated from MC cells using TRIzol reagent (Invitrogen) according to the manufacturer's protocol. Two  $\mu$ g of total RNA was used for reverse transcription and the cDNA was synthesized using the Omniscript Reverse Transcriptase kit (Qiagen). Specific primers for the coding region of the mouse LOX (Genbank accession NM010728) was as follows; forward primer, 5'-CCCGGTCTTCCTTTTCTCCTAGCC-3' and reverse primer, 5'-ATACGGTGAAATTGTGCAGCCTGA-3'. PCR amplification was performed by ProofStart DNA polymerase (Qiagen) with an annealing temperature of 62 °C for 35 cycles. After adding 3'A-overhangs, the PCR products were then ligated into the pcDNA3.1/V5-His-TOPO mammalian expression vector (Invitrogen) generating the plasmid containing LOX (pcDNA3.1/V5-His/LOX) construct. The orientation and molecular weight of the ligated insert were analyzed by *Hind*III (Roche) restriction enzyme digestion followed by 1.2% agarose gel electrophoresis. Plasmids containing digested inserted of the 996 bp, i.e. in a sense (S) or 343 bp, i.e. antisense orientation (AS) orientation were sequenced at the UNC-CH DNA sequencing facility (University of North Carolina, Chapel Hill, NC). A search in the database confirmed that the ligated PCR product was 100% identical to the mouse LOX sequence from Genbank.

*Transfection and generation of stable cell clones*– MC cells were transfected with pcDNA3.1/V5-His/LOX constructs (S and AS orientation) or pcDNA 3.1/V5-His A vector (empty vector [EV]; Invitrogen) using Fugene 6 transfection reagent (Roche). After 48 h, cells were trypsinized and plated at a low density. Single cell-derived clones (S and AS clones) were isolated and maintained in the presence of 400 µg/ml G418 (Invitrogen) for up to 4 weeks.

*Immunoprecipitation and Western blot analysis of the S and AS clones*– MC, EV, S and AS clones were plated onto 10-cm dishes (Falcon) at a density of  $2.0 \times 10^5$ /dish and cultured in  $\alpha$ -minimum essential medium ( $\alpha$ -MEM, Gibco containing 10% FBS) with the same supplements described above. After 7 days of cell culture, culture media were collected and incubated with anti-LOX antibody (Imgenex) at 4 °C overnight. After the addition of rec-Protein G-Sepharose conjugate beads (Zymed laboratories) and incubation at 4°C for 30 min, the samples were washed with lysis buffer containing 150mM NaCl, 20 mM Tris-HCl pH 7.5, 10mM EDTA, 1% Triton X-100, 1% deoxycholate, 1.5% aprotinin, and 1mM phenylmethylsulfonyl fluoride three times. Protein bound to the beads were dissolved in SDS sample buffer (100mM Tris HCl, pH 8.8, 0.01% bromophenol blue, 36% glycerol, and 4% SDS) in the presence of 10mM dithiothreitol (DTT), applied to 4-12% gradient SDS-PAGE (Invitrogen), transferred onto a polyvinylidene fluoride membrane (Immobilon-P, Millipore Corp.), and subjected to Western blot analysis with anti LOX antibody and a secondary antibody, an anti-rabbit IgG conjugated to alkaline phosphatase [(ALP), Pierce Biotechnology]. The immunoreactivity was visualized by an ALP conjugate substrate kit (Bio-Rad Laboratories).

*Proliferation assay*– MC, EV, S and AS clones were plated in triplicate at a density of  $5 \times 10^4$  cells /ml in a 96-well plate, and cultured with  $\alpha$ -MEM and 10% FBS. At

day 2, 4 and 6 days of cell culture, the cells were subjected to MTS cell proliferation assay (CellTier 96®, Promega) according to the manufacturer's protocol. Briefly, 100 µl of MTS solution was added into each well and incubated at 37 °C for 4 hrs. The amounts of formazan compound, 3-(4,5-dimethylthiazol-2-yl)-5-(3-carboxymethoxyphenyl)-2-(4-sulfophenyl)-2H-tetrazolium), MTS, produced by metabolically active cells were measured by absorbance at 490 nm.

*Quantitative Collagen Cross-link Analysis*– MC, EV, S and AS clones were cultured in α-MEM, 10% FBS and 50µg/ml ascorbic acid. After 2 weeks of culture, cells/matrices were washed with phosphate buffered saline (PBS), scraped into a 1.8 ml eppendorf tube and washed with PBS, distilled deionized water (DDW) twice then lyophilized. Two milligrams of the lyophilized samples were suspended in 0.15M N-trismethyl-2-aminoethanesulfonic acid and 0.05M Tris-HCl buffer (pH 7.4) and reduced with standardized NaB<sup>3</sup>H<sub>4</sub> (281), hydrolyzed with 6 N HCl *in vacuo*, after flushing with N<sub>2</sub> at 105°C for 22 h. The hydrolysates were dried by a speed vacuum concentrator (Savant Instruments Inc), dissolved in 300 µl of DDW and filtered through a 0.22 µm membrane (Costar, Corning Inc) and kept in 4°C. Aliquots were subjected to amino acid analysis to determine Hyp and the hydrolysates with known amounts of Hyp were analyzed for cross-links on a cation-exchange column (AA-991; Transgenomic) linked to a fluorescence detector (FP1520; Jasco Spectroscopic) and a liquid scintillation analyzer (500TR series; Packard Instrument) as reported previously (282). All reducible cross-links and aldehydes were measured as their reduced forms. The major reducible cross-links, dihydroxylysinonorleucine and hydroxylysinonorleucine (DHLNL, HLNL) and precursor aldehydes and non-reducible cross-links, pyridinoline and deoxypyridinoline (Pyr, d-Pyr) were simultaneously quantified by the cross-link analyzer. The quantities of the collagen cross-links were expressed as moles/mole of collagen (283). The analyses

were done in triplicate and the values are means $\pm$ SD. To confirm the reproducibility of the results, three independent experiments were performed.

*Collagen content determination*– MC, EV, S and AS clones were cultured as described above. At day 3 and 7, cell culture medium were collected and cell/matrix layers were collected and lyophilized as described above. The dry cells/matrices and lyophilized medium were hydrolyzed with 300  $\mu$ l of 6 N HCl (Pierce) *in vacuo*, after flushing with N<sub>2</sub>, for 22 h at 105°C, dried, dissolved in 300  $\mu$ l of distilled water, filtered with 0.22  $\mu$ m filter unit and kept in 4°C. An aliquot of each hydrolysate was subjected to amino acid analysis on a Varian high-performance liquid chromatography (HPLC) system (9050/9012; Varian Associates Inc) using ninhydrin (Pickering laboratories) for color development at 135°C to determine hydroxyproline residue (282). The collagen content in the cells/matrices was calculated using a value of 300 residues of Hyp per collagen molecule. The total collagen content in the medium and matrices was calculated and normalized with the number of the cells in each dish. To confirm the reproducibility of the results, three independent experiments were performed.

*Transmission electron microscopy*– The cell/matrix layers of MC, EV, S and AS clones at week 3 of study were washed with PBS, fixed with 3% glutaraldehyde and 1% tannic acid in 0.1 M cacodylate buffer, pH 7.4 for 90 mins. The specimens were then post-fixed in 1% osmium tetroxide in 0.1M sodium cacodylate, pH 7.4 for 1 hour at room temperature. The samples were dehydrated with ethanol, embedded in Polybed 812 epoxy resin (Polysciences) and ultrathin sectioned at 70 nm with a diamond knife. The sections were stained with 4% aqueous uranyl acetate for 20 min, followed by Reynolds lead citrate for 8 min. The sections were observed at 80 kV using a Leo EM 910 transmission electron microscope (LEO Electron Microscopy). Digital images were acquired at 40,000X magnification using a Gatan Bioscan CCD camera and Digital

Micrograph software (Gatan, Inc). For each sample, a total of 500 collagen fibril diameters and the number of fibrils per  $\mu\text{m}^2$  were measured randomly using Scion Image software (Scion Corporation).

*In vitro mineralization assay*– MC, EV, S and AS clones were plated on 35 mm plastic dishes at the density of  $2 \times 10^5$  cells/dish (Falcon) and cultured until confluence. The medium was then replaced with the one supplemented with 50  $\mu\text{g/ml}$  of ascorbic acid and 2 mM of  $\beta$ -glycerophosphate (mineralization medium), and maintained for up to 4 weeks. *In vitro* mineralization assay was performed at the end of week 2 and 4. At each time point, cell/matrix layers were washed with 1X PBS twice, fixed with 100% cold methanol, stained with 1% Alizarin Red S (Sigma) for 15 min and washed with DDW and dried at room temperature(74). At week 4, the calcium contents were quantified by measuring the amount of Alizarin red S bound to mineralization nodules in the cultures. Briefly, after staining with Alizarin red S, the cultures were washed with 10% (w/v) cetylpyridinium chloride in 10 mM sodium phosphate, pH 7.0 for 15 min. The dye concentration in the extracts were subjected to spectrophotometer at absorbance 562 nm (284, 285) to compare the amount of alizarin and normalized with cell numbers. To confirm the reproducibility of the results, three independent experiments were performed.

*Statistical analyses*– All statistical analyses were performed using Sigma stat software. Data are expressed as mean $\pm$ SD. Statistical differences were determined by one-way ANOVA followed by a Tukey-Kramer multiple comparison test at  $P=0.05$ .

## RESULTS

*Generation of the S and AS clones*– The immunoprecipitation/Western blot analysis of three S, three AS clones and the controls are shown in Figure 2.1. S3 showed the highest level of LOX (S3: 2.34, S2: 2.25 and S1: 1.47 fold) while AS1 showed the lowest level of LOX (AS1: 0.49, AS2: 0.73, AS3: 0.85 fold) compared to the average expression level of MC and EV. Using MTS assay, the proliferation rate of S clones were comparable with controls (MC and EV) while those of AS clones were slightly lower compared to controls at the same timepoint of study but there is no statistically difference among the clones and when compared to controls ( $P>0.05$ ) (Figure 2.2).

*Quantitative collagen cross-link analysis*–To confirm if the generated S and AS clones secreted functional recombinant LOX, the collagen cross-links in each clones were quantified. The collagen cross-links produced in MC, EV, S, and AS clones at 2 weeks of culture were bifunctional reducible cross-links, i.e. DHLNL and HLNL and a trivalent nonreducible cross-link, Pyr. The cross-link analysis of S clone exhibited higher levels of total aldehydes (DHLNL+HLNL+2xPyr), DHLNL and Pyr whereas that of AS exhibited lower levels of total aldehydes, DHLNL and Pyr (Figure 2.3). The Pyr contents in S clones were constantly higher (157, 206 and 260 % increase) whereas those in AS clones lower (64, 57and 42% decrease) than those of controls ( $P<0.05$ ) (Table 2.1). The data from cross-link analysis is consistent with the level of LOX in S and AS clones (Figure 2.1).

*Collagen content determination*– The total collagen content in each clone at day 3 and 7 of the study was shown in Figure 2.4. After normalized with cell numbers in each dish, the results demonstrated that the total collagen content (in medium and matrix) in

all S clones was significantly lower than those of controls (MC and EV) at both time-point of study ( $P<0.05$ ) while that in all AS clones was comparable to those of the controls at day 3 but significantly higher than those of controls at day 7 in AS1 and AS2 clones ( $P<0.05$ ).

*Ultrastructural analysis of collagen fibrils*– Cross-sectional views of collagen fibrils obtained from cultures of S (S1, S2, S3) and AS (AS1, AS2, AS3) clones and the controls (MC, EV) are shown in Figure 2.5. As shown in histogram, MC cells had a mean diameter of  $46.2\pm 9.4$  nm with a range of 29.2-87.5 nm, which is similar to that of the EV clone (mean  $42.3\pm 6.8$  nm; range 29.2-62.5 nm). In all S clones, the mean fibril diameters and their range were significantly smaller than those of controls ( $P<0.05$ ). Among the S clones, S3 that exhibited the highest level of LOX overexpression (Fig 2.1) showed the smallest fibril diameter (mean  $21.1\pm 7.9$  nm; range 3.7-46.6 nm) followed by S2 clones (mean  $24.2\pm 9.97$  nm; range 3.7-44.1 nm) and S1 clones that exhibited the lowest level of LOX overexpression (mean  $30.1\pm 4.4$  nm; range 3.7-44.1 nm). In all AS clones, the mean fibril diameters and their range were significantly larger than those of controls ( $P<0.05$ ). Among AS clones, AS1 that exhibited the lowest level of LOX showed the largest fibril diameter (mean  $99.1\pm 43.2$  nm; range 31.3-226.7 nm) followed by AS2 clones (mean  $66.9\pm 21.6$  nm; range 22.2-170.8 nm) and AS3 clones that exhibited LOX only slightly lower than controls (mean  $58.4\pm 19.6$  nm; range 16.7-129.2 nm) (Figure 2.6). Therefore, the fibril diameter and distribution range were inversely correlated with the level of LOX expression in the clones. The number of collagen fibrils were counted per square micron randomly from 6 areas and presented in Table 2.2. The number of fibrils in all S clones were significantly lower than those of the controls ( $P<0.05$ ).

*In vitro mineralization assay*– The result of *in vitro* mineralization assay is shown in Fig 2.7. The mineralization pattern of two controls, MC cells and EV clone, was

essentially identical to each other. In both cases, the formation of mineralized nodules was present at 2 weeks of culture and the number and size of mineralized nodule increased thereafter. In S clones, mineralized nodules were not observed in any clones even at week 4. In AS clones, a small number of mineralized nodules were observed at 2 weeks of cultures and increased there after; however, the amounts of nodules in all AS clones were less than those of controls (Fig 2.7A). The quantitative analysis of Alizarin Red S stain extracted from the mineralized matrix confirmed the defective matrix mineralization observed in S and AS clones. The level of Alizarin Red extracted dye from the MC and EV were comparable but higher than those from S and AS clones (Figure 2.7B) ( $P < 0.05$ ).

**Table 2.1** The amount (moles/mole collagen) of total aldehydes and reducible and, non-reducible cross-links in each clone are expressed as mean $\pm$ S.D. ( - : decrease, \* P<0.05, ANOVA)

	<b>DHLNL</b>	<b>HLNL</b>	<b>PYR</b>	<b>Total Aldehydes</b>	<b>% change of PYR</b>
<b>AS1</b>	0.354 $\pm$ 0.064*	0.123 $\pm$ 0.007	0.012 $\pm$ 0.005*	0.500	-64.61
<b>AS2</b>	0.448 $\pm$ 0.023	0.138 $\pm$ 0.025	0.014 $\pm$ 0.003*	0.614	-56.92
<b>AS3</b>	0.463 $\pm$ 0.013	0.079 $\pm$ 0.015*	0.019 $\pm$ 0.010	0.580	-41.54
<b>MC</b>	0.475 $\pm$ 0.010	0.168 $\pm$ 0.030	0.029 $\pm$ 0.007	0.701	0
<b>EV</b>	0.476 $\pm$ 0.032	0.172 $\pm$ 0.024	0.036 $\pm$ 0.015	0.719	0
<b>S1</b>	0.487 $\pm$ 0.052	0.130 $\pm$ 0.001	0.084 $\pm$ 0.008*	0.783	156.92
<b>S2</b>	0.514 $\pm$ 0.021	0.140 $\pm$ 0.022	0.100 $\pm$ 0.013*	0.853	206.15
<b>S3</b>	0.609 $\pm$ 0.126*	0.127 $\pm$ 0.003	0.117 $\pm$ 0.010*	0.970	260.0

**Table 2.2** The fibril density (number fibrils per square micrometer) from each clone is expressed as mean $\pm$ S.D. (\* P<0.05, ANOVA)

<b>Clones</b>	<b>Mean <math>\pm</math> S.D.</b>
<b>AS1</b>	93.2 $\pm$ 48.2
<b>AS2</b>	122.2 $\pm$ 26.9
<b>AS3</b>	132.7 $\pm$ 27.4
<b>MC</b>	129.8 $\pm$ 49.2
<b>EV</b>	130.5 $\pm$ 42.0
<b>S1</b>	59.0 $\pm$ 24.0*
<b>S2</b>	70.0 $\pm$ 25.6*
<b>S3</b>	72.7 $\pm$ 17.6*

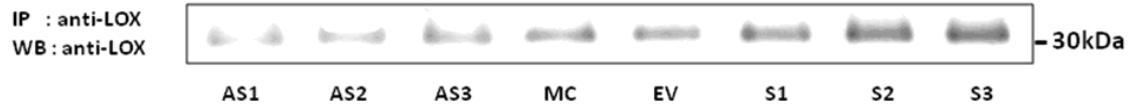


**Figure 2.1** The level of LOX protein expression per dish in stable clones and controls. Cultured medium pooled during the first week of culture were analyzed by IP-WB analysis using anti LOX antibody. The immunoreactive bands at ~35 kDa can be detected in all stable clones and controls. S clones, S1, S2 and S3, possessed higher levels of LOX ( $S3 > S2 > S1$ ) compared to controls, MC cells or EV clone. AS clones, AS1, AS2 and AS3, synthesized lower levels of LOX ( $AS3 > AS2 > AS1$ ) compared to that of controls.

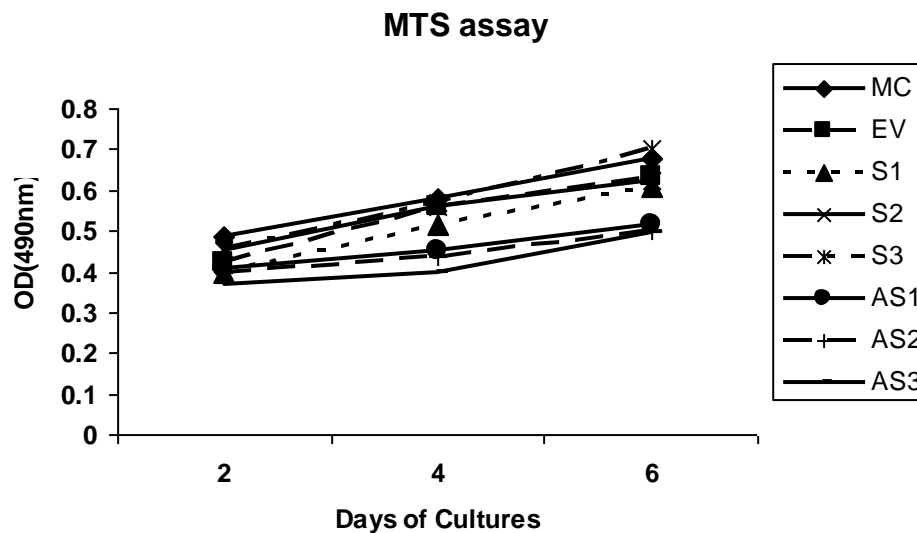


**Figure 2.2** Cell proliferation rate of S and AS clones. Cell proliferation of each clones and controls were assessed by MTS cell proliferation assay. Note that cell proliferation was comparable among all cell types. ( $P > 0.05$ , ANOVA)

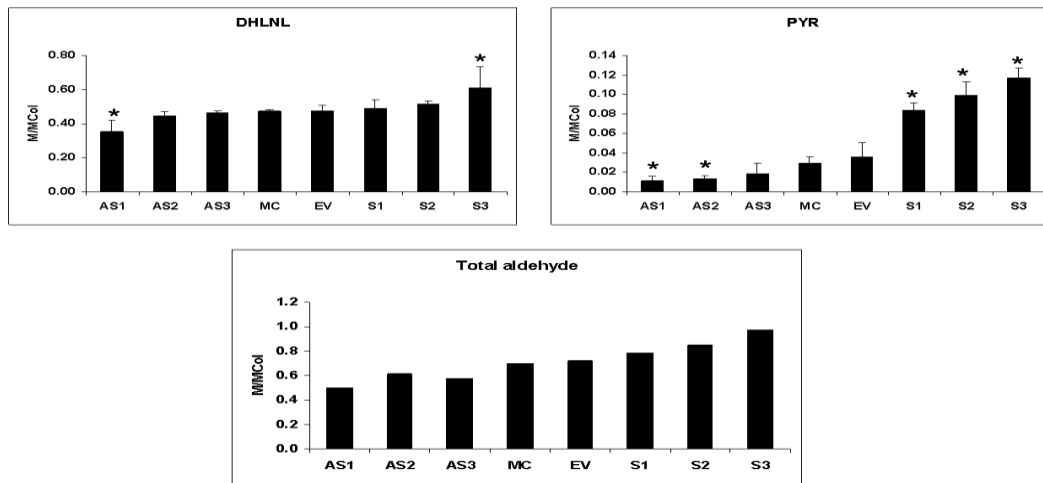


**Figure 2.3** Amounts of collagen cross-links and their precursor expressed in moles/mole of collagen at 2 weeks of cultures. Total aldehydes and DHLNL in all AS clones were lower and in all S clones were higher than those of controls. Non reducible crosslink represented as Pyr in clones and controls was shown as bar graph. S1, S2 and S3 clones exhibited significantly higher level while AS 1 and 2 exhibited significantly lower level than that of controls (\* P<0.05, ANOVA).

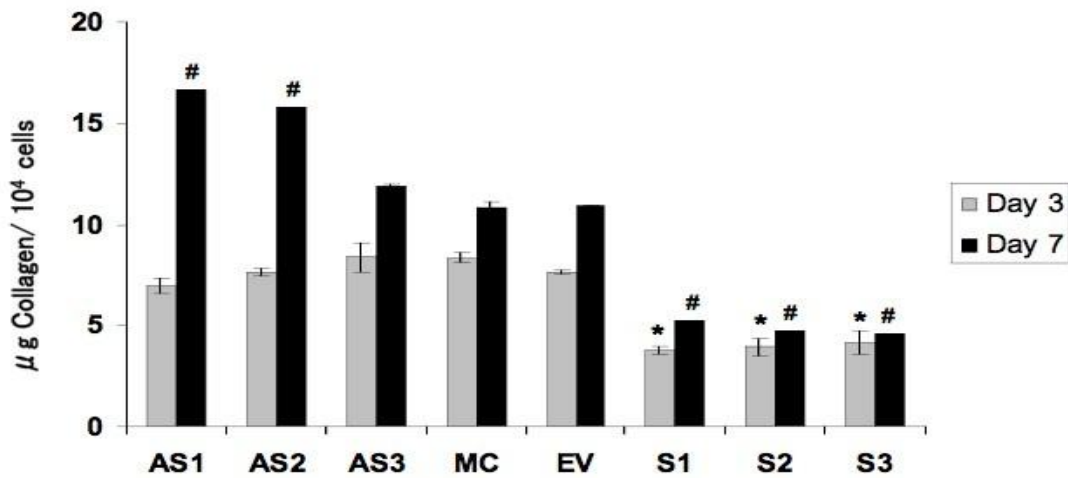


**Figure 2.4** Total collagen content from culture matrix and medium at day 3 and 7 of the cultures expressed as microgram of collagen per 10<sup>4</sup> cells in each dish. All S clones showed significantly lower collagen production compared to those of controls at each timepoint of study (\*, # P<0.05, ANOVA) while AS1 and 2 produced more collagen significantly at day 7 (# P<0.05, ANOVA).

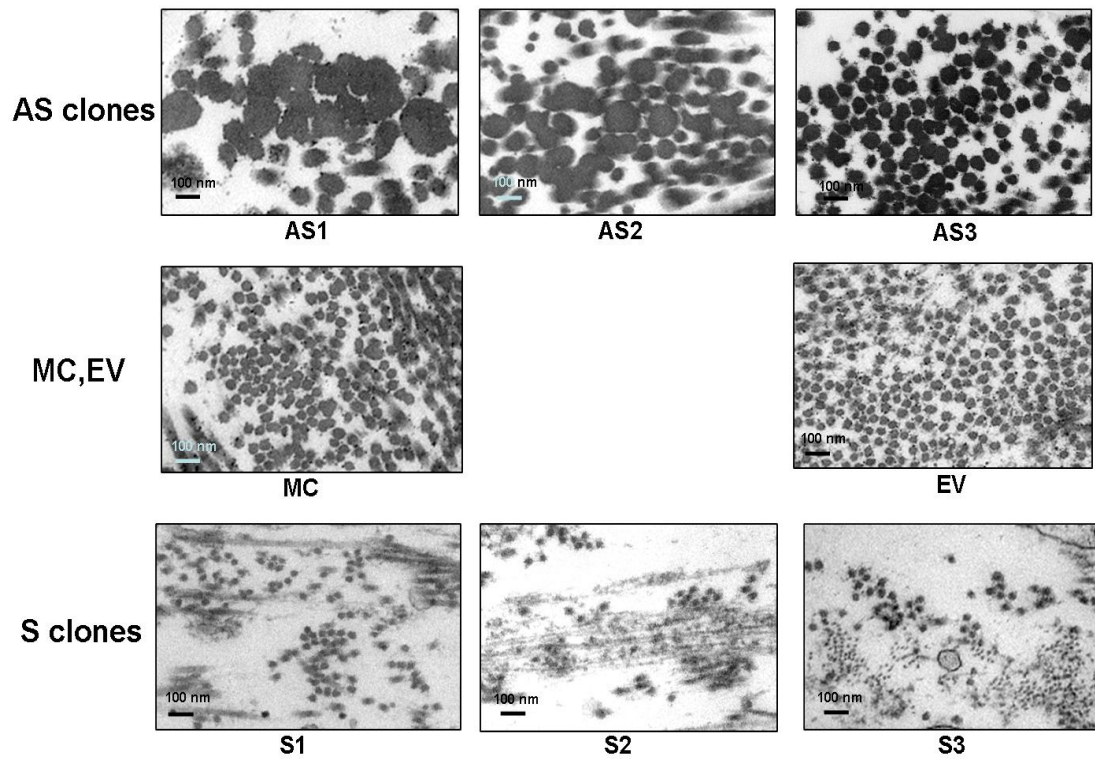


**Figure 2.5** Cross-section of the collagen fibrils in the ECM at 3 weeks of cultures observed under TEM and their diameter. All S clones produced smaller collagen fibrils while all AS clones produced larger collagen fibrils than those of the controls. The S3 clone, highest LOX level, produced the smallest collagen fibrils while the AS1 clone, lowest LOX level, produced the largest collagen fibrils. (bar = 100 nm).

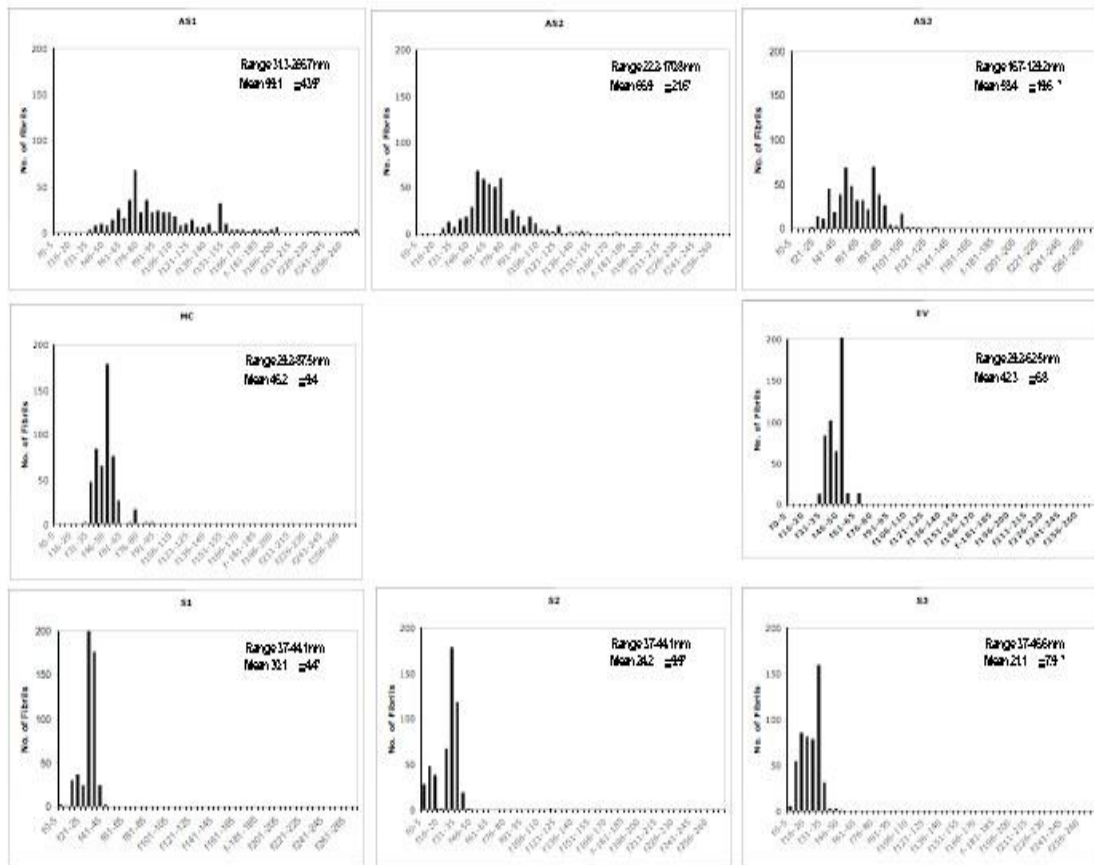


**Figure 2.6** Distribution of the collagen fibril diameter in the ECM at 3 weeks of cultures observed under TEM and their diameter distribution, based on total numbers of 500 fibrils. The fibril diameter in all S clones were significantly smaller while those of all AS clones were significantly larger than those of the controls (\*  $P < 0.05$ , ANOVA). The S3 clone, highest LOX level, produced the smallest collagen fibrils while the AS1 clone, lowest LOX level, produced the largest collagen fibrils.

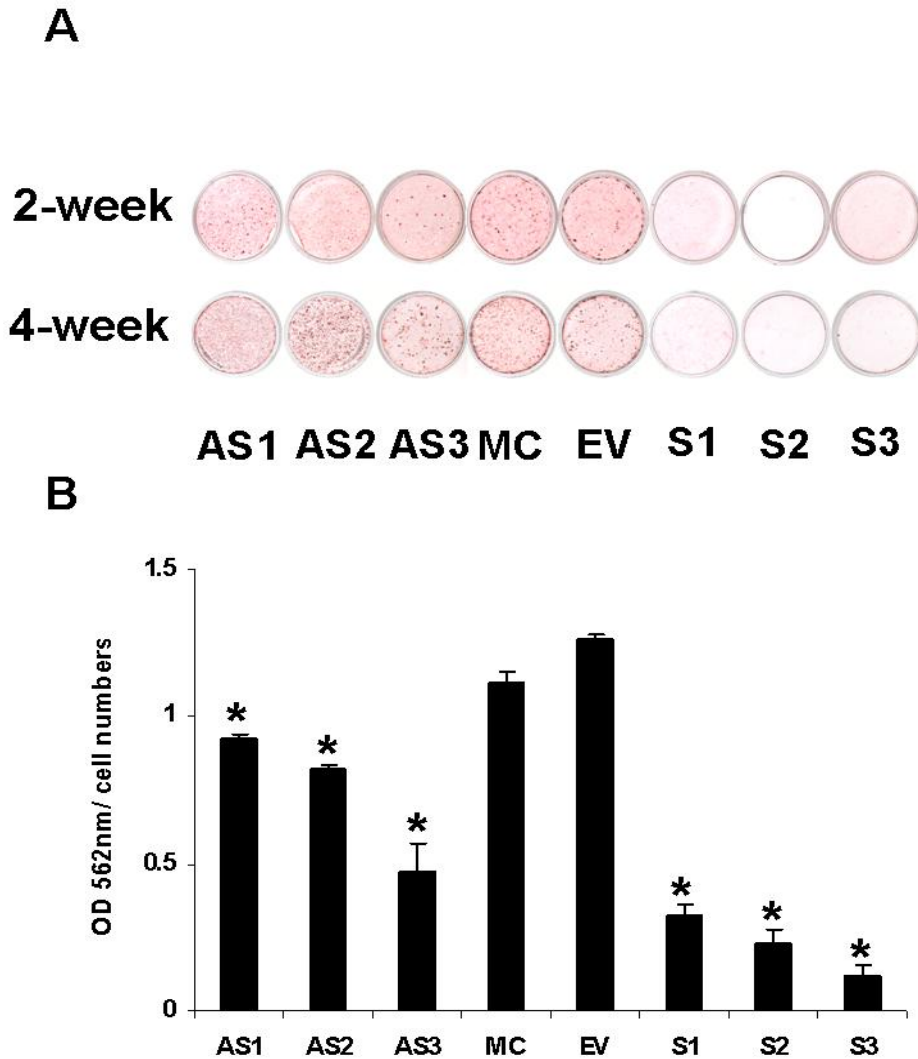


**Figure 2.7** *In vitro* mineralization assay. A. Mineralized nodules formed by the controls (MC and EV) at 2 and 4 weeks of cell culture from the clones (S and AS) and the controls (MC and EV). In S clones, mineralized nodules were not observed in any clones at any time-point of study while in the AS clones, the formed nodules were formed at week 2 of cultures and increased thereafter. The nodules of AS clones were lesser than those of controls. B. The quantitative assay at week 4 of cultures confirmed the defective mineralization in S and AS clones. (\* $P < 0.05$ , ANOVA)

## DISCUSSION

In bone, a specific spatial relationship between the two predominant components, collagen fibrils and mineral, is critical for the mechanical function (286, 287), and the collagen fibrils apparently regulate the manner of mineral deposition and growth (288, 289). A number of studies indicate that the covalent intermolecular cross-linking formed at the edge of the hole zones of the fibril, the putative nucleation sites, plays a crucial role in collagen mineralization (283, 290-292). We have reported that the manipulation of cross-linking pattern in MC cells through lysyl hydroxylase 2b affects the collagen fibrillogenesis, and matrix mineralization (293). The study indicates the importance of the type of collagen cross-links is an important factor to regulate collagen fibrillogenesis and matrix mineralization. Up to now, however, the effect of the quantity of collagen cross-links on mineralization has never been directly investigated. As described, LOX family enzymes are the only known family enzyme to initiate the process of cross-linking by oxidative deaminating the  $\epsilon$ -amino groups on peptidyl Lys and Hyl residues in the N- and C-terminal telopeptides of collagen. In this study, by establishing and characterizing MC cell derived clones expressing higher and lower levels of LOX, we examined if the level of collagen cross-links plays a role in collagen fibrillogenesis and subsequent matrix mineralization.

The collagen phenotype produced by S and AS clones was investigated by analyzing the quantity and quality using HPLC and TEM. The total collagen content in culture media and matrix in S clones was markedly decreased while that in AS clones was increased. The collagen fibril observed under TEM in S clones was significantly smaller and those in AS clones showed diversified diameter and larger than those of controls. The findings in AS clones were similar to those treated with  $\beta$ APN (73, 222) or a procollagen C-proteinase inhibitor (225). In  $\beta$ APN treated cultures, the total collagen

synthesis was increased and collagen fibril diameters were diversified and larger than those observed in control group (73, 222). In PCP inhibitor treated cultures, an increase of collagen fibril diameters was detected while LOX activity was decreased (225). In S clones, however, the total collagen content and its fibril diameter showed opposite to those found in AS clones, i.e. decreased collagen content and larger fibril diameter compared to controls. These results indicate the effect of LOX on collagen production, fibrillogenesis and mineralization. Altered collagen fibrillogenesis and mineralization might be the consequence of altered collagen cross-linking as its pattern is associated with those processes (293-295). However, the underlying mechanism of how LOX controls the collagen production is not clear. The altered level of collagen production at as early as day 3 can be hardly explained by an increase or a decrease of collagen cross-linking since even immature cross-links begin to accumulate only after 1-2 weeks in osteoblast cultures (222, 295, 296). The increased collagen expression/production by the treatment of  $\beta$ APN have also been reported in chondrocyte cultures (223, 297). These data clearly indicate that LOX inhibition affects “early” cellular functions associated with increased collagen expression/synthesis. The upregulation of collagen mRNA seen in lathyritic animals during the early phase of bone fracture healing (239) also supports this notion. Thus, the effect of LOX on collagen production might be related to its recently identified cellular functions (134). Future studies need to be investigated to clarify this speculation.

The *in vitro* mineralization was severely impaired in all S clones and, to a certain extent, in AS clones. This phenotype might be explained based on the template stability, morphology proposed by Landis et al 1993 (289). However, the result in this study showed the critical importance of LOX for the physiological matrix mineralization.

In conclusion, this study showed potential roles of LOX in modulating collagen production, fibrillogenesis and matrix mineralization in osteoblastic cultures. Some of those effects may be associated with the cellular function of LOX.

## **CHAPTER IV**

### **STUDY II**

#### **Lysyl oxidase regulates transforming growth factor- $\beta$ 1 function in bone via its amine oxidase activity.**

Phimon Atsawasuwan, Michitsuna Katafuchi, Yoshiyuki Mochida, Masaru Kaku,

Mitsuo Yamauchi

#### **Specific aims**

1. To elucidate the binding between LOX and TGF- $\beta$ 1 *in vitro* and in bone matrix.
2. To evaluate the role of LOX on TGF- $\beta$  activity by determination of the level of Smad 3 phosphorylation and TGF- $\beta$ 1 induced matrix molecule mRNA expression.

## ABSTRACT

Lysyl oxidase (LOX), an amine oxidase critical for the initiation of collagen and elastin cross-linking, has recently been shown to regulate cellular activities possibly by modulating growth factor activity. In this study, we investigated the interaction of LOX with transforming growth factor- $\beta$ 1 (TGF- $\beta$ 1), a potent growth factor abundant in bone, and evaluated the effect of this interaction. The specific binding between LOX and TGF- $\beta$ 1 was demonstrated both by immunoprecipitation and glutathione-S-transferase pull down assay. Both molecules were co-localized in the extracellular matrix in culture and the binding complex was identified in the mineral-associated fraction of bone matrix. Furthermore, LOX suppressed TGF- $\beta$ 1 induced Smad3 phosphorylation and collagen (I/IV) expression but the effects were nullified by  $\beta$ -aminopropionitrile. The suppression of Smad3 phosphorylation was not affected in the presence of catalase. The data indicate that LOX may bind to mature TGF- $\beta$ 1 and regulate its signaling via its amine oxidase activity in bone, thus, may play an important role in bone remodelling and mineralization.

## INTRODUCTION

Lysyl oxidase (LOX) is a copper-dependent amine oxidase that initiates the process of covalent intra- and intermolecular cross-linking in collagen and elastin (34). The critical role of LOX in tissue stability is well exemplified by “lathyrism”, the condition where deleterious effects in connective tissues are caused by lathyrogens such as  $\beta$ -aminopropionitrile ( $\beta$ APN) (298). In lathyrotic animals, bone is one of the most severely affected tissues revealing kyphoscoliosis, bone deformities, weakening of tendons and ligament attachments, dislocation of joints, weakening of skin and cartilage, hernias and dissecting or saccular aneurysm of the aorta (233-235, 239).  $\beta$ APN is a potent and irreversible inhibitor of LOX, and prevents cross-linking of immature collagen and elastin into mature, stable insoluble fibers. Therefore, it has been thought that the phenotypes seen in lathyrotic animals are due to the lack of cross-linking. Several reports showed that  $\beta$ APN treated osteoblasts exhibited an increase in collagen production and abnormal fibrillogenesis (73, 222). Moreover, the similar collagen phenotypes were observed in  $\beta$ APN treated chondrocytes (223, 297). These examples of abnormal collagen production can be hardly explained by a decrease of collagen cross-linking since even immature cross-links begin to accumulate only after 1-2 weeks in osteoblast cultures (222, 295, 296). The upregulation of collagen mRNA was observed in lathyrotic animals during the early phase of bone fracture healing as well (239).

Recent reports, however, have revealed novel functions for LOX including the regulation of gene transcription and cellular functions. Though the mechanisms are still not clear, those functions could be associated with its ability to oxidize substrates other than collagen and elastin, such as Histone H1 and H2 (132), basic fibroblast growth factor (bFGF) (134), and hypoxia induced factor (299). Thus, lathyrotic phenotypes may also be due in part to the loss of LOX control of cellular functions.

Our previous study (chapter III) has demonstrated that LOX expression is inversely correlated with collagen production in an osteoblastic cell culture system. This could be due to the LOX interaction/regulation of growth factors that regulate collagen expression, as some studies suggested (104, 134). Thus, we next investigated the potential LOX regulation of growth factors that are known to regulate collagen expression in bone. In bone, there are several major growth factors such as transforming growth factor- $\beta$  (TGF- $\beta$ ), bone morphogenic proteins (BMPs), insulin-like growth factors (IGFs) and platelet derived growth factor (PDGF), tumor necrosis factor- $\alpha$  (TNF- $\alpha$ ) and basic fibroblast growth factor (bFGF). Several studies has reported that insulin-like growth factors (IGF1 and 2) and TNF- $\alpha$  play some roles in collagen production (300-307). Concerning the effects on collagen synthesis, bFGF and PDGF showed inconsistent results (303, 304, 308-311). However, considering the fact that LOX has a strong preference for basic proteins as its substrate (126), IGF1/2 (pI ~6.46 and 7.76) and TNF-  $\alpha$  (pI ~7.02) may not be substrates for LOX. Type I collagen has been reported as a target gene of TGF- $\beta$ 1 and BMPs in bone (252, 312-314) and that both are basic proteins (pI~8.59 and 8.5). During our initial study on the interaction between LOX and TGF- $\beta$ 1/BMPs, we have found that LOX specifically binds to mature TGF- $\beta$ 1 and suppresses its signaling. TGF- $\beta$ 1 is one of the most potent growth factors enriched in bone matrix modulating many aspects of bone physiology (see a review in (252)). TGF- $\beta$ 1 is secreted and stored as a small or large latent complex in bone matrix that can be released and activated by the action of osteoclasts (262, 263) and through other mechanisms. Numerous studies, though not always consistent, have shown that TGF- $\beta$ 1 stimulates recruitment and proliferation of osteoblast progenitors (254, 315) and stimulates matrix production including collagen, but rather inhibits late stage of osteoblast differentiation and matrix mineralization (256, 257) and osteocalcin expression (250, 316). It is also involved in the modulation of osteoclast differentiation

(258). The abundance of this growth factor with such potent effects on cells in a dynamic environment of bone clearly predicts the need for tight regulation of its biological activities.

In this study, we have demonstrated that LOX binds to mature TGF- $\beta$ 1 and inhibits its signaling through an amine oxidase activity. Furthermore, LOX and TGF- $\beta$ 1 form a complex in the mineralized matrix fraction in bone. Thus, LOX may play a pivotal role not only in collagen stability but also in regulation of TGF- $\beta$  activity which is critical for bone physiology and pathology.

## EXPERIMENTAL PROCEDURES

*Antibodies and Proteins Used-* These following antibodies were used in this study: Anti-V5 antibody (Invitrogen), anti-hemagglutinin (HA) antibody (Roche Diagnostics), anti-phosphoSmad3 antibody (Biosource), anti-glutathione S-transferase (GST) antibody (Sigma-aldrich), anti-Smad3, anti-phosphoSmad1,5,8, anti- $\beta$ -actin antibodies (Cell signaling technologies), and anti-TGF- $\beta$ 1 antibody (R&D systems). Two types of polyclonal anti-LOX antibodies were used, one purchased from Imgenex (anti-LOXi) and another described in previous studies (anti-LOXh) (83, 317). Recombinant human TGF- $\beta$ 1 protein (rhTGF- $\beta$ 1) and recombinant human BMP-2 (rhBMP-2) were purchased from R&D systems.

*Cell Lines and Culture Conditions-* The human embryonic kidney (HEK) 293 cells were purchased from Clontech and maintained in Dulbecco' s modified Eagle medium (Gibco) supplemented with 10% fetal bovine serum (Atlanta Biologicals), 100 U/ml penicillin (Gibco), and 100  $\mu$ g/ml streptomycin (Gibco) in a 5% CO<sub>2</sub> atmosphere at 37 °C. The medium was changed twice a week. The mouse calvaria-derived MC3T3-E1 (MC) cells were purchased from American Type Culture Collection (CRL-2593) and maintained in  $\alpha$ -minimum essential medium (Gibco) with the same supplements as above. The medium was changed twice a week.

*Molecular cloning of mouse LOX cDNA-* Total RNA was isolated from MC cells using TRIzol (Invitrogen). Two  $\mu$ g of total RNA was used for reverse transcription and the cDNA was synthesized using the Omniscript RT kit (Qiagen). The cDNA containing the coding region of the mouse LOX (Genbank accession NM\_010728) was generated by PCR using Hotstar *Taq* polymerase (Qiagen). The sequences of the primers were designed as shown in Table 3.1. The PCR product was then ligated into the

pcDNA3.1/V5-His-TOPO mammalian expression vector (Invitrogen), sequenced at the UNC-CH DNA sequencing facility (University of North Carolina, Chapel Hill, NC), and the plasmid containing LOX cDNA in a sense orientation (pcDNA3.1/V5-His/LOX) was obtained. To generate pcDNA3/V5-His/LOXdm (LOX with Lys314 and Tyr349 mutated resulting in an inactive LOX) (105), the coding sequences of LOX was subcloned from pcDNA3.1/V5-His/LOX by PCR and another additional two sets of primers for the mutation of Lys314 and Tyr 349 were designed using primers in Table 3.1. To generate pcDNA3/HA/LOX and pcDNA3/HA/LOXdm, the coding sequences of LOX was subcloned from pcDNA3.1/V5-His/LOX and pcDNA3/V5-His/LOXdm by PCR and the primers designed were shown in Table 3.1. The PCR products were digested with BamH I and Xho I and ligated into pcDNA3/HA mammalian expression vector (318), sequenced at the UNC-CH DNA sequencing facility. Two additional deletion mutant constructs of LOX, i.e. mature LOX (signal peptide-residue 1-16 and 162-411, LOX-HA) and LOX propeptide (signal peptide and propeptide: residue 1-161, LOPP-HA) were generated using 2 additional sets of primers as shown in Table 3.1, subcloned from pcDNA3/HA/LOX and sequenced at the UNC-CH DNA sequencing facility.

*Transfection, Immunoprecipitation and Western Blotting-* 293 cells cotransfected with pcDNA3/HA/LOX vector and pcDNA3.1/V5-His vector harboring BMP-2, -4, -6, -7 (318) or pcDNA3.1-V5-His/TGF- $\beta$ 1 using a FuGENE6 transfection reagent (Roche Diagnostics) according to the manufacturer's instructions. pcDNA3.1-V5-His/TGF- $\beta$ 1 was generated as described. Briefly, PCR products were amplified using the normal mouse kidney cDNA (BD Bioscience) as a cDNA template, purified and ligated into the pcDNA3.1/V5-His-TOPO mammalian expression vector, sequenced at the UNC-CH DNA sequencing facility, and the plasmid containing TGF- $\beta$ 1 cDNA in a sense orientation (pcDNA3.1/V5-His/TGF- $\beta$ 1) was obtained. The sequences of the

primers were designed and shown in Table 3.1. After transfection, the cultured media were collected, immunoprecipitated with either anti-V5 or anti-HA antibody. The samples were then incubated with protein A-sepharose 4B conjugate beads (Zymed Laboratories) for 30 min and the beads were washed twice with lysis buffer containing 150mM NaCl, 20 mM Tris-HCl pH 7.5, 10mM EDTA, 1% Triton X-100, 1% deoxycholate, 1.5% aprotinin, and 1mM phenylmethylsulfonyl fluoride three times. Protein bound to the beads were dissolved in SDS sample buffer (100mM Tris HCl, pH 8.8, 0.01% bromophenol blue, 36% glycerol, and 4% SDS) in the presence of 10mM dithiothreitol (DTT), applied to 4-12% gradient SDS-PAGE, transferred onto a polyvinylidene fluoride membrane (Immobilon-P, Millipore), and subjected to Western blot analysis with anti-V5 or anti-HA antibody. The immunoreactivity was visualized by an alkaline phosphatase (ALP) conjugate substrate kit (Bio-Rad). To determine whether LOX binds to LAP or mature TGF- $\beta$ , 293 cells were transiently transfected with the pcDNA3/HA/LOX, and either pcDNA3.1/V5-His/TGF- $\beta$  1 or pcDNA3.1/V5-His/LAP, using Fugene6 transfection reagent. pcDNA3.1/V5-His/LAP was subcloned from pcDNA3.1/V5-His/TGF- $\beta$ 1 by PCR and the primers were shown in Table 3.1. The PCR product was then ligated into the pcDNA3.1/V5-His-TOPO mammalian expression vector, sequenced at the UNC-CH DNA sequencing facility, and the plasmid containing LAP cDNA in a sense orientation (pcDNA3.1/V5-His/LAP) was obtained. The total amounts of plasmid were kept constant (2.5  $\mu$ g) by supplementing pcDNA3.1/V5-HisA (empty vector). The media were collected and subjected to immunoprecipitation and Western blot analysis in the same manner as described above.

*Generation of 293-derived Stable Clones Overexpressing LOX and MC Stable Clones Over/Underexpressing LOX*– HEK293 cells were transfected with either pcDNA3.1/V5-His/LOX or pcDNA3.1/V5-His/LOXdm constructs as described above.

After transfection, cells were cultured in the presence of 400 µg/ml of G418 (Gibco) for 3-4 weeks to select stably transfected clones. Positive clones derived from single G418-resistant cells were then isolated by cloning rings and further grown in the same conditions. As a control, 293 cells were also transfected with an empty pcDNA3.1/V5-His A vector (EV, Invitrogen) and the clones (EV clones) were generated in the same manner.

MC cells were transfected with pcDNA3.1/V5-His/LOX constructs (S and AS orientation) (see Chapter III) and pcDNA 3.1/V5-His A vector (empty vector [EV]; Invitrogen) using Fugene 6 transfection reagent (Roche). After 48 h, cells were trypsinized and plated at a low density. Single cell-derived clones (S and AS clones) were isolated and maintained in the presence of 400 µg/ml G418 (Invitrogen) for up to 4 weeks.

*Purification of LOX-V5/His Fusion Protein* – The 293-derived clones that synthesized the highest level of LOX-V5/His protein were cultured in 15 cm plates for 6 days and the culture media were collected. LOX-V5/His fusion protein (LOX-V5) was purified using a nickel-nitrotriacetic acid-agarose resin (Qiagen) at 4°C, and the purified proteins were pooled, dialyzed against 0.2 M sodium borate pH 8.2 and kept in -20°C until use. The protein concentrations were measured by DC protein assay kit (Bio-Rad). To assess the purity of LOX-V5, aliquots of the sample were dissolved in SDS sample buffer containing 10 mM DTT, separated by 4-12% SDS-PAGE and subjected to Coomassie Brilliant Blue (CBB) R-250 staining or Western Blot analysis. For the latter analysis, two anti-LOX antibodies (anti-LOXi and anti-LOXh, see above) and anti-V5 antibody were used. The major CBB stained protein band on the gel was cut and subjected to matrix assisted laser desorption ionization mass spectrometric analysis (MALDI-MS) at UNC-CH Proteomics Facility. LOXdm-V5/His fusion protein (LOXdm-V5)

was also purified in the same manner and subjected to LOX activity assay to verify the activity nullification of the mutations.

*LOX Activity Assay-* The LOX enzyme activity was measured using the Amplex Ultra Red fluorescence assay (128). Five or ten  $\mu\text{g}$  of LOX-V5 with or without 500  $\mu\text{M}$   $\beta\text{APN}$  were suspended in 2 ml of 0.1 M sodium borate, pH 8.2, containing, 1.2 M urea, 1 unit/ml horseradish peroxidase (HRP) (Biochemika), 10  $\mu\text{M}$  Amplex red (Molecular Probes, Inc.), 10 mM 1,5-diaminopentane dihydrochloride (Sigma). The mixture was incubated for 30 min at 37°C and the fluorescence intensities were measured with excitation and emission wavelength at 563 and 587 nm, respectively, using F2000 spectrofluorometer (Hitachi).

*Glutathione S transferase (GST) Pull-down Assay-* The sequences of the primers were designed to amplify the mature form of TGF- $\beta$ 1 (residue number 279-390) and shown in Table 3.1. The PCR products were amplified using the normal mouse kidney cDNA as a cDNA template, purified and ligated into a pGEX-4T-1 vector (GE Healthcare) and transformed into BL21 strain of *Escherichia coli* (Stratagene). An empty pGEX4T-1 vector was also transformed into the bacterial cells to produce GST protein alone. After DNA purification, plasmids were analyzed by restriction enzyme digestion, sequenced, and the plasmid harboring the mature form of GST-TGF- $\beta$ 1 (pGEX4T-1-TGF- $\beta$ 1) was obtained. After the bacteria transformed with pGEX4T-1-TGF- $\beta$ 1 or pGEX4T-1 were cultured at 37 °C for several hours, 250 $\mu\text{M}$  of isopropyl-D-1-thiogalactopyranoside (IPTG, Sigma-Aldrich) was added to induce the synthesis of GST and GST-TGF- $\beta$ 1 proteins. After incubating for 24 hours at 20°C, the cultures were centrifuged, lysed in a buffer containing PBS and 1% Triton X-100, and sonicated for 20 sec three times with an interval of 3 min on ice. The lysates were collected by centrifugation, incubated with glutathione-sepharose beads (GE Healthcare) overnight at

4°C and the beads were extensively washed with PBS. The recombinant GST-TGF-β1 and GST proteins were then released with the elution buffer (10mM glutathione, 50mM Tris-HCl pH 8.0) at 4 °C. The purity of the recombinant proteins was assessed by SDS-PAGE. The protein concentrations were measured by DC protein assay kit. Then GST pull down was performed in the following manner. Five μg of GST or purified GST-TGF-β1 fusion protein 2.5 or 5 μg were incubated with 10 μg of LOX-V5 in 50 mM Tris-HCl, pH 8.0, with the presence or absence of 500 μM βAPN for 1 h at 4°C. Glutathione-sepharose beads (GE Healthcare) were then added and further incubated for 30 min at 4°C. The beads were then washed three times with TBST buffer (0.02% Tween 20 (Fisher scientific), and the proteins bound were released by boiling for 5 min in SDS sample buffer containing 10mM DTT, and subjected to Western blot analysis with anti-V5 antibody. The immunoreactivity was visualized by ALP conjugate substrate kit.

*Direct binding of LOX and TGF-β1 by immunoprecipitation-* Twenty ng of rhTGF-β1 (R&D systems) were incubated with 10 μg of LOX-V5 in 50 mM Tris-HCl, pH 8.0, containing in the presence or absence of 500 μM βAPN for 1 h at 4°C. The protein G-sepharose 4B conjugate beads (Zymed) were then added to the solutions and further incubated for 30 min. The sepharose-bound complexes were collected by centrifugation, washed three times with TBST buffer, and the proteins bound were released and subjected to Western blot analysis with anti-V5 antibody as described above.

*Laser-scanning Confocal Microscopy* – The potential co-localization of LOX and TGF-β1 was investigated in a MC culture system by a laser-scanning confocal microscopy. MC cells were cultured for 3 weeks as described above, washed with PBS and fixed with 10% formaldehyde for 10 min. Cell/matrix layer was then cut into 1 X 1 cm pieces, placed on a glass slide and dried. The slides were then immersed in PBS and

treated with 20 µg/ml of Proteinase K (Roche Applied Science) for 10 min. Samples were incubated with two primary antibodies, i.e. anti-TGF- $\beta$ 1 and anti-LOXi antibodies, in PBS containing 1.5% goat serum for 30 min, washed with PBS and incubated with species-specific fluorescence-labeled secondary antibodies, mouse Alexa Fluor 594 and rabbit Alexa Fluor 488 (Invitrogen), for 30 min each. After washing with PBS, the specimens were mounted and the immunofluorescence was observed under a Zeiss LSM5 Pascal at UNC-CH microscopy services laboratory.

*Identification of LOX-TGF- $\beta$ 1 complex in bone matrix-* Femurs from fetal bovine animals were purchased from Aries Scientific (Texas) and kept at -80°C until use. Both femoral heads were removed and the mid-shafts were longitudinally cut. After the bone marrow was removed and washed with cold PBS; bones were cut into small pieces, defatted with methylene chloride and methanol solution (2:1) overnight at 4°C, washed with cold DDW and lyophilized. The bone fragments were then pulverized in liquid nitrogen using a freezer mill (Spex Certiprep), washed with cold distilled water, lyophilized and subjected to sequential extraction described by Termine et al. (319) with some modifications (320). Briefly, ~1 g of bone powder was first extracted with 5 ml of 6M guanidine-HCl (GH), pH 7.4, for 2 days at 4°C, the supernatant was separated by centrifugation at 15,000Xg for 30 min, exhaustively dialyzed against cold distilled water and lyophilized (G1 representing the matrix molecules that are not associated with mineral). The residue (mineral-associated) was then demineralized with 0.5M EDTA, pH 7.4, for 2 weeks at 4°C with several changes of EDTA, the supernatant was separated by centrifugation as described above, dialyzed against cold distilled water and lyophilized (E representing soluble matrix molecules associated with mineral). The residue was further extracted with 5 ml of 6 M GH, pH 7.4, for 2 days at 4°C, the extract was collected by centrifugation, dialyzed and lyophilized as described above (G2

including mineral-associated, insoluble matrix). All fractions were weighed, dissolved in lysis buffer and centrifuged. The protein concentration in the supernatant was determined by a DC protein assay kit. Fifteen  $\mu\text{g}$  of proteins in each fraction was dissolved in SDS sample buffer and subjected to WB analysis with either anti-LOXi or anti-TGF- $\beta$ 1 antibodies. The immunoreactivity was visualized by ALP conjugated substrate kit. In order to confirm the specific binding, various amounts of E fraction (500, 1000 and 2000  $\mu\text{g}$  of protein) was immunoprecipitated with either 5  $\mu\text{l}$  of anti-LOXi or anti-LOXh antibodies or 5  $\mu\text{l}$  of rabbit non-immune serum (negative control) in lysis buffer overnight at 4°C. Then protein G-sepharose 4B conjugate beads were added, incubated for 15 min at 4°C and the beads were washed 3 times with lysis buffer. The immunocomplex was then released from the beads and subjected to Western blot analysis with anti-TGF- $\beta$ 1 antibody. The immunoreactivity was visualized by ALP conjugate substrate kit.

*Effect of LOX on Smad phosphorylation-* To determine the effect of LOX on the TGF- $\beta$ 1 activity, MC cells were plated onto 35 mm culture dishes at a density of  $2.0 \times 10^5$ /dish in duplicate and cultured in  $\alpha$ -minimum essential medium (Gibco) with the same supplements as described in the culture condition section. MC cells were transiently transfected with 1, 2.5 and 5  $\mu\text{g}$  of the pcDNA3.1/V5-His/LOX using Fugene6 transfection reagent. After 48 hours, cells were treated with rhTGF- $\beta$ 1 (5 ng/ml) for 30 min in the presence or absence of 300  $\mu\text{M}$   $\beta$ APN or 200U/ml of catalase. Another set of the cells was transiently transfected with 5  $\mu\text{g}$  of pcDNA3.1/V5-His/LOXdm and the cells were treated with rhTGF- $\beta$ 1 in the same manner. The cells were lysed with 400  $\mu\text{l}$  RIPA buffer containing 150 mM NaCl, 50 mM Tris-HCl pH 8.0, 1% NP-40, 0.1% SDS, 0.5% deoxycholate, 1% aprotinin, and 1 mM phenylmethylsulfonyl fluoride by continuous shaking for 1 hour at 4°C then centrifuged. The supernatants collected were then

subjected to Western blot analysis with anti-phospho Smad3 (Biosource) and anti Smad3 antibodies (Cell Signaling). The intensity of phospho-Smad3 protein from each sample was normalized by the amount of total Smad3 protein using Scion Image software. LOX in the media was quantified by immunoprecipitation followed by Western blot analysis with anti-LOXi antibody. In a parallel set of experiment, cells were treated with 100 ng/ml of rhBMP-2 instead of rhTGF- $\beta$ 1 and the cell lysates were subjected to Western blot analysis with anti-Smad1,5,8 and anti  $\beta$ -actin (Cell signaling technologies). In another set of experiment, MC cells were cultured as described above. On the following day, 2.5 or 5  $\mu$ g of LOX-V5 or a combination of 5  $\mu$ g of LOX-V5 with or without 300  $\mu$ M of  $\beta$ APN or 300  $\mu$ M  $\beta$ APN alone was added to the cells. Cells were then treated with 5 ng/mL of rhTGF- $\beta$ 1 for 30 min, and the phosphorylation of Smad3 was evaluated in the same manner as described above.

To determine the effect of the level of LOX on the TGF- $\beta$ 1 activity, MC, EV, S and AS clones were plated onto 35 mm culture dishes at a density of  $2.0 \times 10^5$ /dish in duplicate and cultured in  $\alpha$ -minimum essential medium with the same supplements as described in the culture condition section. After 48 hours, cells were treated with rhTGF- $\beta$ 1 (5 ng/ml) for 30 min. The cells were lysed then centrifuged and supernatants collected were then subjected to Western blot analysis with anti-phospho-Smad3 and anti Smad3 antibodies. The intensity of phospho-Smad3 protein from each sample was normalized by the amount of total Smad3 protein using Scion Image software.

*Quantitative Real-time PCR-* MC cells were cultured in the same manner as described in the Smad3 phosphorylation western blotting experiment. On the following day, 2.5 or 5  $\mu$ g of LOX-V5 or a combination of 5  $\mu$ g of LOX and 300  $\mu$ M of  $\beta$ APN was added to the cells. Cells were then treated with 5 ng/mL of rhTGF- $\beta$ 1 and further cultured for 24 hours. Total mRNA was extracted by TRIzol reagent. Two  $\mu$ g of total

RNA was used for reverse transcription and the cDNA was synthesized using the Omniscript RT kit. Real-time PCR was performed using sequence specific primers and ABI Prism 7000 Sequence detection system (Applied Biosystems). Primers used are as follows: COL1a2 (#Mm00483888\_m1) and COL5a1 (#Mm00489342\_m1) and GAPDH (#4308313). The analyses were performed in triplicate for three independent experiments to confirm reproducibility of the results. SB431542, ALK 4,5 and 7 inhibitors, were used as negative controls in the experiment (321). The mRNA expression relative to GAPDH was determined and the fold changes were calculated using the values of rhTGF- $\beta$ 1 addition only as a calibrator by means of  $2^{-\Delta\Delta C_T}$  method (74).

*RNA interference-* MC cells were plated onto 35 mm culture dishes at a density of  $5.0 \times 10^4$ /dish in duplicate and cultured in the same manner as described above. On the following day, cells were transfected with 3.75  $\mu$ g of LOX siRNA ID#156159, 156160, 156161 or Silencer negative control AM4611 (Ambion) using siPORT Amine transfection agent (Ambion). Forty-eight hours after transfection, the cells were treated with 5 ng/ml of rhTGF- $\beta$ 1 for 30 min Smad3 phosphorylation was examined in the same manner as described above. The suppression of LOX protein in the media was verified by immunoprecipitation followed by Western blot analysis with anti-LOX antibodies

*Statistical analyses-* All statistical analyses were performed using Sigma stat software. Data are expressed as mean $\pm$ SD. Statistical differences were determined by one-way ANOVA followed by a Tukey-Kramer multiple comparison test at P=0.05.

**Table 3.1** Primers list of constructs used in the study.

construct	Forward primer Reverse primer
fLLOX-V5/His	5'-CCCGGTCTTCCTTTTTCTCCTAGCC-3' 5'-ATACGGTGAAATTGTGCAGCCTGA-3'
fLLOXdm-V5/His	5'-GCTGAAGGCCACGCAGCAAGCTTCTGT-3' 5'-ACAGAAGCTTGCTGCGTGGCCTTCAGC-3' and 5'-TGTTATGACACCTTTGCGGCAGACATA-3' 5'-TATGTCTGCCGCAAAGGTGTCATAACA-3' and 5'-CCCGGTCTTCCTTTTTCTCCTAGCC-3' 5'-ATACGGTGAAATTGTGCAGCCTGA-3'
fLLOX-HA and fLLOXdm-HA	5'-GCGGATCCATGCGTTTCGCCTGGGCTGTGCTC-3' 5'-GCCTCGAGATACGGTGAAATTGTGCAGCCTGAGGC-3'
LOX-HA	5'-CTTCTCCGCTGCGACGACCCCTACAATCCCTAC-3' 5'-GTAGGGATTGTAGGGGTCGTGCGAGCGGAGAAG-3' and 5'-GCGGATCCATGCGTTTCGCCTGGGCTGTGCTC-3' 5'-GCCTCGAGATACGGTGAAATTGTGCAGCCTGAGGC-3'
LOPP-HA	5'-GCGGATCCATGCGTTTCGCCTGGGCTGTGCTC-3' 5'-GCCTCGAGGCCCAACCATGCGATCTATGTGGCT-3'
TGF- $\beta$ 1-V5	5'-CATGCCGCCCTCGGGGCTG-3' 5'-GCTGCACTTGCAAGGAGCGC-3'.
LAP-V5	5'- GCTGCACTTGCAAGGAGCGC -3' 5'- TCTCCGGTGCCGTGAGCTGTG -3'
Mature GST-TGF- $\beta$ 1	5' GCGAATTCGCCCTGGATACCAACTATTGCTTC 3' 5' GCCTCGAGTCAGCTGCACTTGCAAGGAGCGCAC 3'

## RESULTS

*Mature LOX binds to mature TGF- $\beta$ 1*– The binding of LOX to TGF- $\beta$ 1 and some of the osteogenic TGF- $\beta$  superfamily members, i.e. bone morphogenetic proteins (BMP-2, -4, -6 and -7), was investigated by co-expressing those proteins with two types of tag (HA for LOX and V5 for other proteins) followed by immunoprecipitation (IP) and Western blot (WB) analysis (Fig 3.1A). When IP and WB were performed with either anti-V5 or -HA antibody alone, V5-tagged TGF- $\beta$ 1 (Fig 3.1A, *lane 6*, lower panel), V5-tagged BMPs (Fig 3.1A, *lanes 2-5*, lower panel), or HA-tagged LOX (Fig 3.1A, *lanes 2-7*, middle panel) was detected at the expected molecular weight of each protein demonstrating the presence of those proteins. Of the proteins tested, only TGF- $\beta$ 1 was shown to bind LOX (Fig 3.1A, *lane 6*, upper panel). Any of the BMPs tested did not show appreciable binding (Fig 3.1A, *lanes 2-5*, upper panel). Even when higher levels of BMP2 (2-fold) were expressed; no binding was observed (data not shown). The binding of LOX to TGF- $\beta$ 1 was further characterized. Fig 3.1B showed that the binding of LOX to full-length TGF- $\beta$ 1 occurred in a dose dependent manner (Fig 3.1B, *lanes 3-5*, upper panel) while LAP (propeptide of TGF- $\beta$ 1) alone did not bind to LOX at various doses (Fig 3.1B, *lanes 7-9*, upper, indicating that LOX bound specifically to mature TGF- $\beta$ 1. Then, we generated HA-tagged full length LOX (residue 1-411, fLOX-HA) (Fig 3.2A, 1) and two deletion mutant constructs of LOX, i.e. mature LOX (signal peptide-residue 1-16 and 162-411, LOX-HA) (Fig 3.2A, 2) and LOX propeptide (signal peptide and propeptide: residue 1-161, LOPP-HA) (Fig 3.2A, 3). One of these proteins and TGF- $\beta$ 1-V5 were then transiently co-expressed by 293 cells and the binding was assessed by IP and WB analysis in the same manner as described above. Three different levels of TGF- $\beta$ 1 were expressed for the binding assay (Fig 3.2B, lower panel). The immunoreactive bands were detected in a dose dependent manner for fLOX-HA (Fig 3.2B, upper panel) and

LOX-HA (Fig 3.2B, upper middle panel) but not LOXPP-HA (Fig 3.2B, lower middle panel). When fLOX-HA was expressed, both full length (55 kDa) and mature forms (35 kDa) of LOX were synthesized (shown by an arrow in the upper panel of Fig 3.2B). Though fLOX-HA was partially overlapped with the IgG heavy chain, the dose-dependent binding was readily observed for both fLOX and mature LOX. These results indicate that the binding of LOX to TGF- $\beta$ 1 occurs via the mature form of LOX but not its propeptide domain.

*Direct binding of LOX to TGF- $\beta$  and the effect of  $\beta$ APN* – To determine if LOX binds to TGF- $\beta$ 1 directly, we performed GST pull down assay by using GST fused mature TGF- $\beta$ 1 (GST-TGF- $\beta$ 1) and purified LOX-V5 protein. First the purity of LOX-V5 (both full length and mature) was verified by SDS-PAGE and WB analyses. When stained with CBB, 4 bands were observed at 28 and 35 kDa corresponding to the molecular sizes of mature LOX and 48 and 55 kDa corresponding to those of full-length LOX with V5 tag, respectively. The LOX-V5 was further analyzed by WB analysis using two anti-LOX antibodies (anti-LOXi and anti-LOXh) and anti-V5 antibody (Fig 3.3A, lanes 3, 4 and 5, respectively). The 28 kDa band was indeed immunoreactive to 3 antibodies but not normal rabbit serum (Fig 3.3A, lane 2). The 28 and 35 kDa band were cut and subjected to protein identification using MALDI-MS at UNC-CH Proteomics Facility and four tryptic peptides separated were all identified in both bands as portions of LOX (res 225-231, 246-254, 263-277, 372-391 respectively) (accession protein# NP\_034858.1), thus unequivocally confirming its identity. LOX-V5 was then subjected to amine oxidase assay reported by Palamakumbura AH and Trackman PC (128). The activity increased in a dose-dependent manner and nullified by the addition of  $\beta$ APN demonstrating that the LOX-V5 still retained activity after purification (Fig 3.3B). LOXdm-V5 was also subjected to amine oxidase assay and showed no activity at all (data not shown). After

we obtained active LOX-V5, we performed GST pull down using active LOX-V5 and GST-TGF- $\beta$ 1. The positive immunoreactive bands of LOX-V5 were detected when LOX-V5 was incubated with GST-TGF- $\beta$ 1 in a dose-dependent manner (Fig 3.4A, *lanes* 3 and 4) but not with GST alone (Fig. 3.4A, *lanes* 2 and 5). LOX-V5 was also verified in Fig. 4A, lane 1. The binding of LOX-V5 to GST-TGF- $\beta$ 1 was not affected by the presence of 500  $\mu$ M  $\beta$ APN (Fig. 3.4A, *lanes* 6 and 7). The direct binding was also confirmed by IP-WB analysis using LOX-V5 and rhTGF- $\beta$ 1. When those two proteins were mixed and immunoprecipitated with anti-V5 antibody and subjected to WB analysis with anti-TGF- $\beta$ 1 antibody, the TGF- $\beta$ 1 was detected and it was not interfered in the presence of  $\beta$ APN as well (Fig. 3.4B).

*Co-localization of LOX and TGF- $\beta$ 1 in an osteoblast culture system* –To investigate the endogenous association of LOX with TGF- $\beta$ 1 *in vitro*, we used preosteoblastic cell line, MC cells, and the localization of both proteins was assessed by the laser scanning fluorescence microscopy. In Fig. 3.5, TGF- $\beta$ 1 was shown in red (Fig. 3.5A), LOX in green (Fig. 3.5B) and co-localization of the two in yellow in the merged image (Fig. 3.5D). A fibrous extracellular matrix (ECM) structure between cell bodies was identified in the culture and confirmed by differential interference contrast (DIC) image (Fig 3.5C). The result demonstrated that both molecules were co-localized in the ECM of the culture (Fig. 3.5D) suggesting the close association of both proteins in the preosteoblastic cell matrices (Fig. 3.5E).

*Identification of a LOX-TGF- $\beta$ 1 complex in bone matrix* – To investigate whether or not a LOX-TGF- $\beta$ 1 complex is indeed present in bone, bone matrix was fractionated into G1, E and G2 by sequential extraction. The equal amount of protein from each fraction was subjected to WB analysis with anti-LOXi and anti-TGF- $\beta$ 1 antibodies. Both LOX and TGF- $\beta$ 1 in bone matrix were identified in mineral-associated matrix fractions (E

and G2) but not in G1 fraction though their relative distribution in each fraction was different (Fig. 3.6A). This suggested that LOX and TGF- $\beta$ 1 were both closely associated with mineral in bone matrix. Then various amounts of E fraction (500, 1000 and 2000  $\mu$ g), which is more soluble and abundant than G2, were then subjected to IP with anti LOXi and WB with to investigate their potential endogenous binding in bone matrix. The results shown in Fig. 3.6B demonstrated that the endogenous binding between LOX and TGF- $\beta$ 1 occurs in a dose dependent in bone matrix.

*Effect of LOX enzymatic activity on TGF-  $\beta$ 1 signaling*– Since the binding of LOX to TGF- $\beta$ 1 in both in vitro and in vivo was confirmed, the effect of LOX on TGF- $\beta$ 1 signaling and its potential mechanism were then examined. MC cells were transiently transfected with various amounts of pcDNA3.1/LOX/V5-His in the presence or absence of 300  $\mu$ M BAPN or 200U/ml of catalase. The LOX protein level in each treatment group was evaluated by IP-WB analysis with anti-LOX antibody (Fig 7A,B, *lower panel*). Then rhTGF- $\beta$ 1 was added to those groups and the phosphorylation of Smad3 (phosphoSmad3 protein relative to the total Smad3 protein) was evaluated. Without the addition of rhTGF- $\beta$ 1, cells overexpressing EV, LOX did not induce Smad3 phosphorylation (Fig 3.7A, *lanes 1 and 2*, Fig 3.7B, *lanes 1-3*). The addition of TGF- $\beta$ 1 in the EV group induced Smad3 phosphorylation (Fig 3.7A, *lane 3*). However, the phosphorylation level was diminished with the presence of LOX in a dose-dependent manner (Fig 3.7A, *lanes 4-6*). The LOX-mediated inhibition was not affected in the presence of catalase (Fig 3.7A, *lane 7*) but completely rescued in the presence of  $\beta$ APN (Fig 3.7A, *lane 8*). When MC cells were transfected with pcDNA3.1/LOX/V5 and pcDNA3.1/LOXdm/V5-His in the same amount, in the similar settings, the inhibition of Smad3 phosphorylation was observed in cells overexpressing LOX (Fig 3.7B, *lane 5*) but not in LOXdm (inactive LOX) (Fig 3.7B, *lane 6*) compared to EV group (Fig 3.7B, *lane 4*)

In stable cell clones, without the addition of rhTGF- $\beta$ 1, Smad3 phosphorylation could not be detected (Fig 3.8, *lane 2*). The addition of TGF- $\beta$ 1 significantly induced Smad3 phosphorylation in all groups of cells (Fig 3.8, *lanes 1, 3-9*). Moreover, the phosphorylation level in all S clones were diminished and in all AS clone were enhanced corresponded to the level of LOX expression in each clone (Fig 3.8, *lanes 4-9*) while that in all AS clones were enhanced respectively (Fig 3.8, *lanes 7-9*) compared to controls (MC and EV) (Fig 3.8, *lanes 1 and 3*).

In another set of experiments, using MC cells, the effect of exogenous LOX-V5 addition with or without  $\beta$ APN on TGF- $\beta$ 1 signaling was further evaluated. The results are shown in Fig 3.9. Without TGF- $\beta$ 1 treatment, the presence or absence of LOX or  $\beta$ APN did not induce Smad3 phosphorylation (Fig 3.9, *lanes 1-3*). The phosphorylation was induced with TGF- $\beta$ 1 (Fig 3.9, *lane 4*), but it was significantly diminished with the addition of LOX-V5 in a dose-dependent manner (Fig 3.9, *lanes 6 and 7*). However, this LOX mediated inhibition was rescued in the presence of  $\beta$ APN (Fig 3.9, *lane 7*). Moreover, when  $\beta$ APN without exogenous LOX-V5 was added combined with TGF- $\beta$ 1, Smad3 phosphorylation was slightly more enhanced in comparison to that of TGF- $\beta$ 1 alone (Fig 3.9, *lane 8 vs. 3*). Since  $\beta$ APN alone did not induce Smad3 phosphorylation (Fig 3.9, *lane 3*), this result suggests the presence of endogenous LOX in the cultured medium that was inhibited by  $\beta$ APN.

To confirm that the inhibitory effect of LOX is specific to TGF- $\beta$ 1 not BMPs, the effect of LOX on BMP-2 induced signaling was then examined. MC cells were transiently transfected with various amounts of pcDNA3.1/V5-His/LOX in the presence or absence of 300 $\mu$ M  $\beta$ APN. The LOX protein level in each treatment group was evaluated by IP-WB analysis with anti-V5 antibody (Fig 3.10, *lower panel*). Then rhBMP-2 was added to those groups of cells overexpressing active LOX and the phosphorylation of Smad1,5,8

was evaluated. Regardless the addition of BMP-2, cells overexpressing EV or LOX did not induce Smad1,5,8 phosphorylation either in the presence or absence of  $\beta$ APN (Fig 3.10, upper panel, *lanes 3-8*). The signal of Smad1,5,8 phosphorylation was normalized with the level of  $\beta$ -actin (Fig 3.10, middle panel).

*Effect of LOX on TGF- $\beta$  induced ECM molecules mRNA expression* – Type I and type V collagen mRNA expression were quantified after the addition of exogenous LOX either with or without  $\beta$ APN (Fig 3.11). The expression levels of both types of collagen were upregulated upon TGF- $\beta$ 1 treatment (5ng/ml)(Fig3.11,*lane 4*), however, in the presence of LOX (2.5 and 5 ug), the level was decreased respectively (Fig 3.11, *lane 5, 6*). Moreover, an addition of 300 $\mu$ M  $\beta$ APN rescued LOX-mediated TGF- $\beta$ 1 inhibition (Fig 3.11, *lane 7*). Note that the expression of Col5A1 was more responsive to TGF- $\beta$ 1 addition than that of Col1A2.

*Effect of LOX RNA interference on TGF- $\beta$  signaling* – In addition to verify the effect in AS, another loss-of-function experiment was performed by RNAi technology. MC cells were transiently transfected with Silencer negative control or three different constructs of LOX siRNA. LOX protein levels in the media were lower (20-80%) in the cell groups that were transfected with siRNA than that of negative control (Fig 3.12, *lane 2-5, upper panel*). The LOX level was the lowest when cells were transfected with 3 siRNA constructs combined (Fig 3.12, *lane 2*). In comparison to the negative control (Fig 3.12, *lane 1*), the TGF- $\beta$ 1 induced Smad 3 phosphorylation was significantly increased in all siRNA transfected groups (Fig 3.12, *lane 3, 4 and 5*) and the increase level was the highest in the combined group that exhibited the lowest LOX protein level (Fig 3.12, *lane 2*). Without rhTGF- $\beta$ 1, LOX siRNA transfection alone did not induce Smad3 phosphorylation (Fig 3.12, *lane 6-10*). This result implicated that the knock down of endogenous LOX in the culture leads to the higher levels of TGF- $\beta$ 1 signaling.

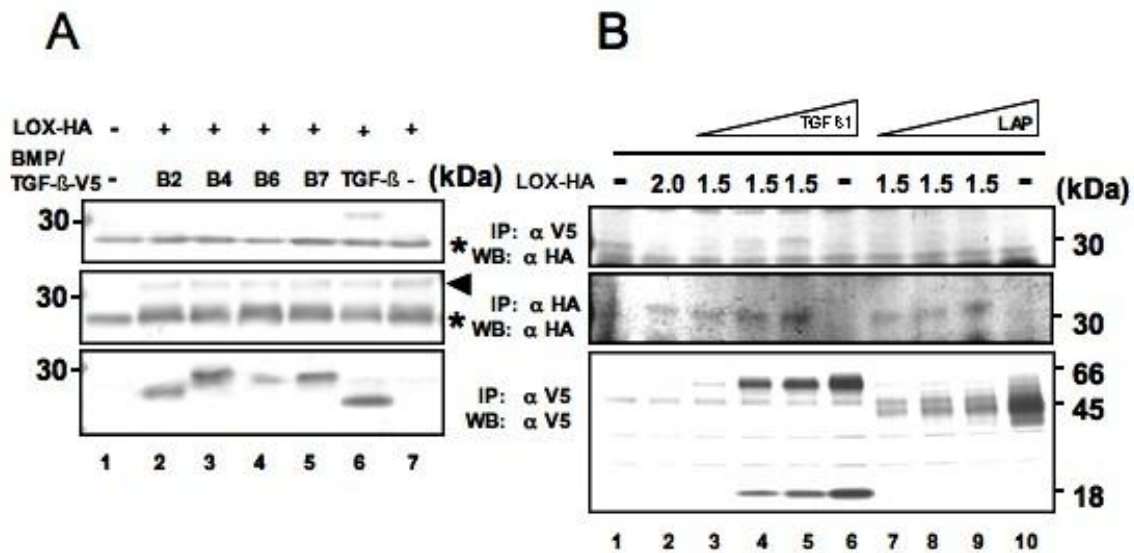


**Figure 3.1** Binding of LOX to TGF- $\beta$ 1/BMPs. A, Binding of LOX to TGF- $\beta$ 1 (upper panel, lane 6), but not to any BMPs (upper panel, lanes 2-5) was clearly observed. The expression levels of LOX and BMPs/TGF- $\beta$ 1 were verified by IP-WB analyses with anti-HA antibody (middle panel) and with anti-V5 antibody (lower panel), respectively. An asterisk indicates Ig light chain. B, Binding of LOX to TGF- $\beta$ 1 in a dose-dependent manner (upper panel, lanes 3-5 indicated by an arrowhead) but not to LAP with any doses tested (upper panel, lane 7-9). The expression levels of LOX and TGF- $\beta$ 1/LAP are shown in the middle and lower panels, respectively. Note that LOX binds to TGF- $\beta$ 1; LAP: latency associated peptide. Molecular weights are shown on the right.

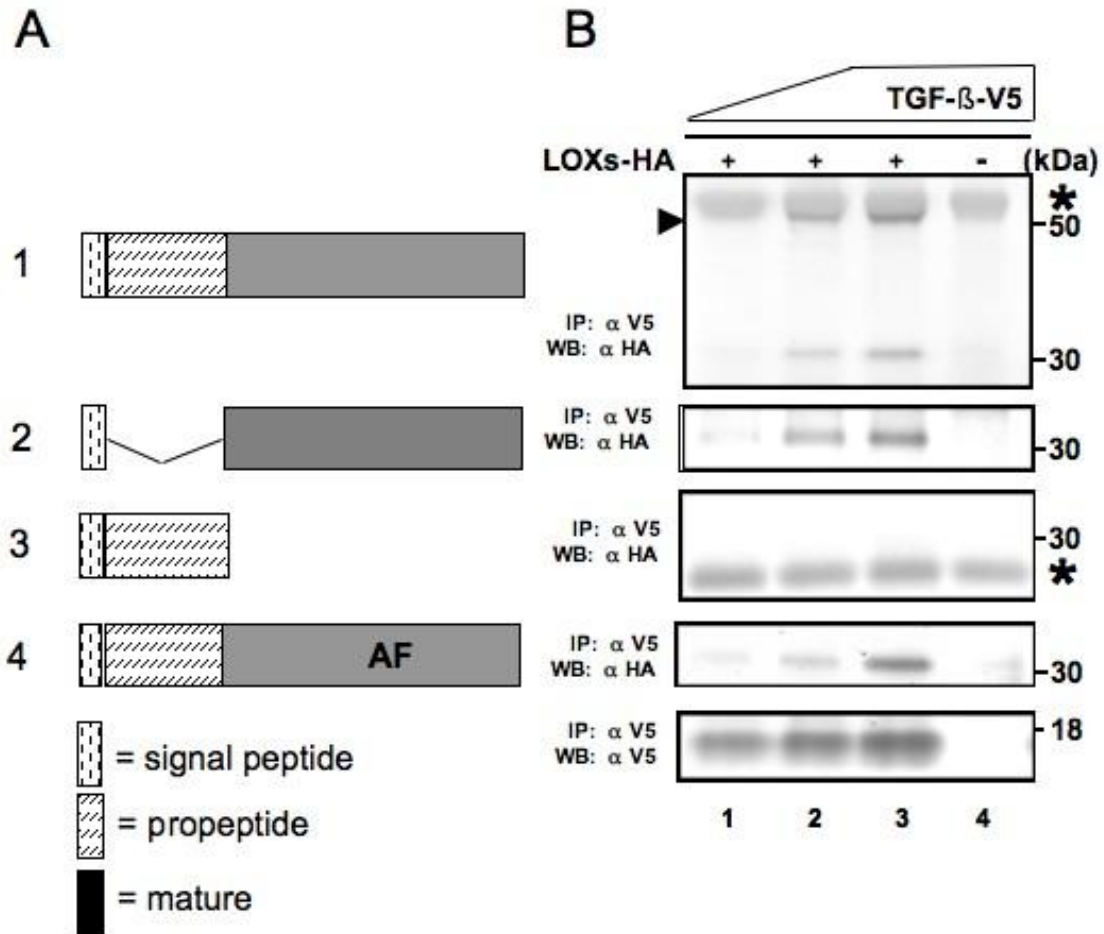


**Figure 3.2** LOX constructs and their binding to TGF- $\beta$ 1 by IP-WB. Left panel: a diagram of LOX constructs. Right panel: the binding between each LOX-HA construct product and TGF- $\beta$ 1-V5/His by IP with anti-V5 antibody followed by WB with anti-HA antibody. Various expression levels of full-length TGF- $\beta$ 1 for the assay are shown by WB with anti-V5 antibody at the bottom. Note that all of the LOX construct products [LOX-HA (1), LOX $\Delta$ pro-HA (2), LOXdm-HA (4)] except LOPP (3) show binding to TGF- $\beta$ 1-V5/His in a dose-dependent manner except LOXpropeptide. Note that LOXdm was shown the similar pattern as LOX-HA and an arrow indicates the full-length LOX but the WB showed only mature form area. Asterisks represent heavy and light chains of IgG. AF represents alanine (A) and phenylalanine (F) which replaced tyrosine and lysine in LTQ domain.

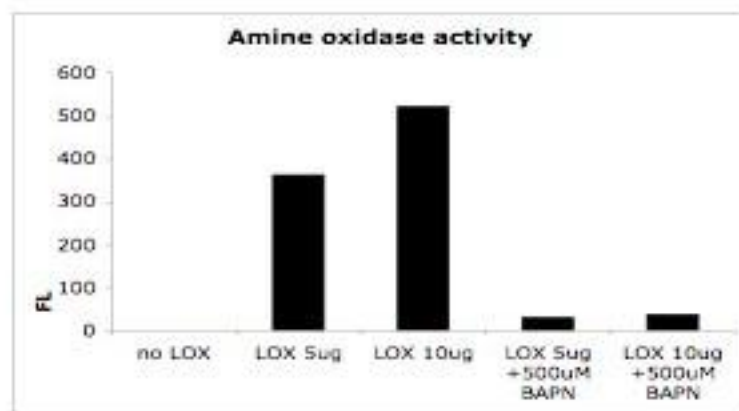
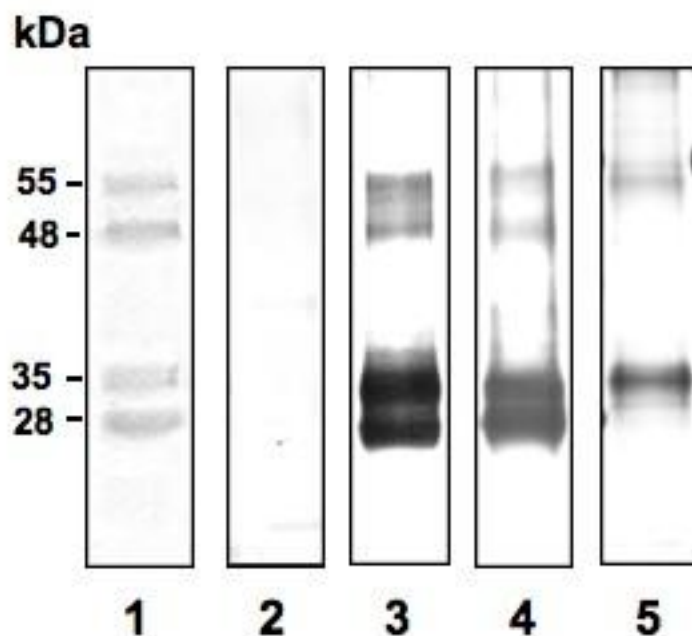


**Figure 3.3** Purity and activity of LOX-V5/His protein. (a) LOX-V5/His protein was stained with CBB (lane 1), immunostained with normal rabbit serum (RS; lane 2), anti-V5 antibody (lane 3), anti-LOX antibody (Imgenex) (lane 4) and that provided by Dr. Csiszar, U Hawaii (lane 5). An immunopositive band at ~35kDa (~30kDa LOX + ~5kDa V-5/His tag) was detected with all the antibodies used except RS. (b) Amine oxidase activity of LOX-V5/His protein. Note that an amine oxidase activity of LOX-V5/His protein is retained and increased in a dose-dependent manner, and the activity was completely blocked with 500 $\mu$ M of  $\beta$ APN.

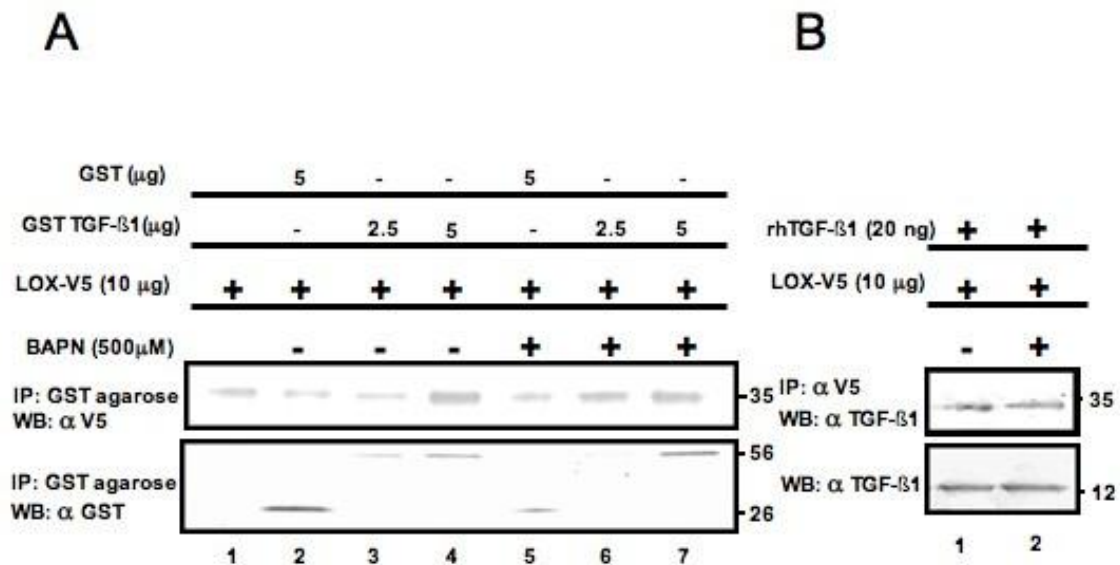


**Figure 3.4** Direct binding of LOX to TGF-β1. A, LOX-V5/His protein was incubated with GST-TGF-β1 or GST alone, and subjected to GST pull down assay. The binding of GST-TGF-β1 (lane 3,4), not GST alone (lane 2), to LOX-V5/His was clearly detected and, moreover, the binding was not affected by the presence of βAPN. Note that the binding is detected in a dose-dependent manner (lanes 6 and 7). Note that LOX-V5 in lane 1 was not pulled down with GST agarose. The amounts of the GST proteins and peptide added (input) are shown in the lower panel. 10μg of LOX-V5 protein added, BAPN: β-aminopropionitrile. B, LOX-V5/His protein was incubated with rhTGF-β1 either in the presence of absence of βAPN. βAPN did not affect the binding between LOX and TGF-β1 (upper panel). The amounts of the rhTGF-β1 (input) are shown in lower panel.

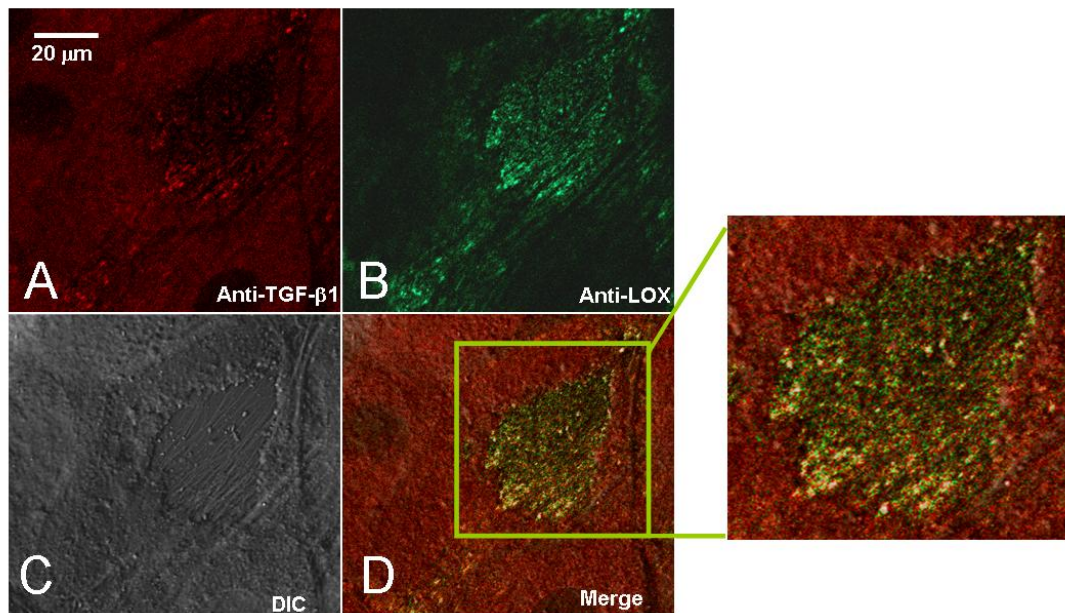


**Figure 3.5** Co-localization of LOX and TGF-β1 in a MC cell culture system. After 3 weeks of culture, immunofluorescence staining for LOX and TGF-β1 was carried out and observed under LSCM (see text for details). (a) TGF-β1 shown in red, (b) LOX in green, (c) Merged image showing co-localization of the two in yellow, (d) Differential interference contrast (DIC) image confirming fibrous ECM (arrowhead).

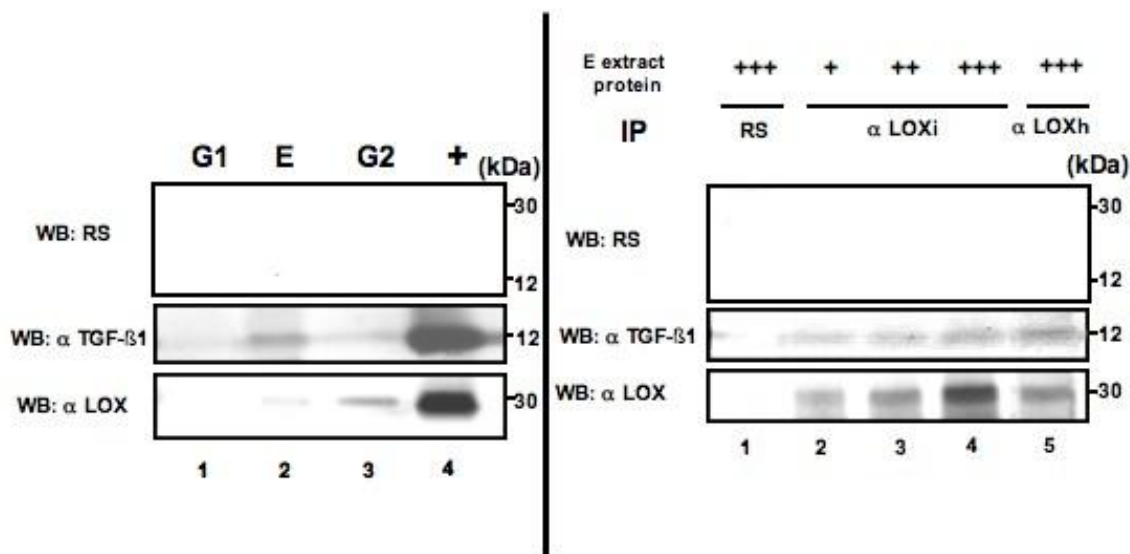


**Figure 3.6** Binding of LOX and TGF- $\beta$ 1 in bone extracellular matrix. A, Presence of LOX and TGF- $\beta$ 1 proteins in bone matrix extracts. WB analyses were performed with anti-LOX antibody (upper panel), anti-TGF- $\beta$ 1 antibody (middle panel), and normal rabbit serum (RS) (upper panel). The immunoreactive bands for LOX and TGF- $\beta$ 1 were identified at the expected molecular weight in E and G2 fraction of bone (lanes 2 and 3), but not in G1 fraction of bone (lane 1). No immunoreactive bands were detected using RS (upper panel). G: guanidine-HCl, E: EDTA, G1: non-mineral associated fraction, E: mineral-associated, soluble fraction, G2: mineral-associated, insoluble fraction. LOX protein or recombinant human TGF- $\beta$ 1 protein was subjected to WB analyses for positive controls (lane 4). B, Presence of LOX-TGF- $\beta$ 1 binding complex in bone E extract. Note that immunopositive bands of TGF- $\beta$ 1 are clearly detected in a dose-dependent manner (Middle panel, lanes 2-4) when IP-WB analyses were performed (IP; anti-LOX antibody, WB; anti-TGF- $\beta$ 1 antibody), but absent from a negative control (normal rabbit serum, lane 1). The immunopositive band was also observed when another anti-LOX antibody was used (lane 5). The amount of LOX is shown in lower panel. +, ++, +++: 500, 1000 and 2000  $\mu$ g of protein.

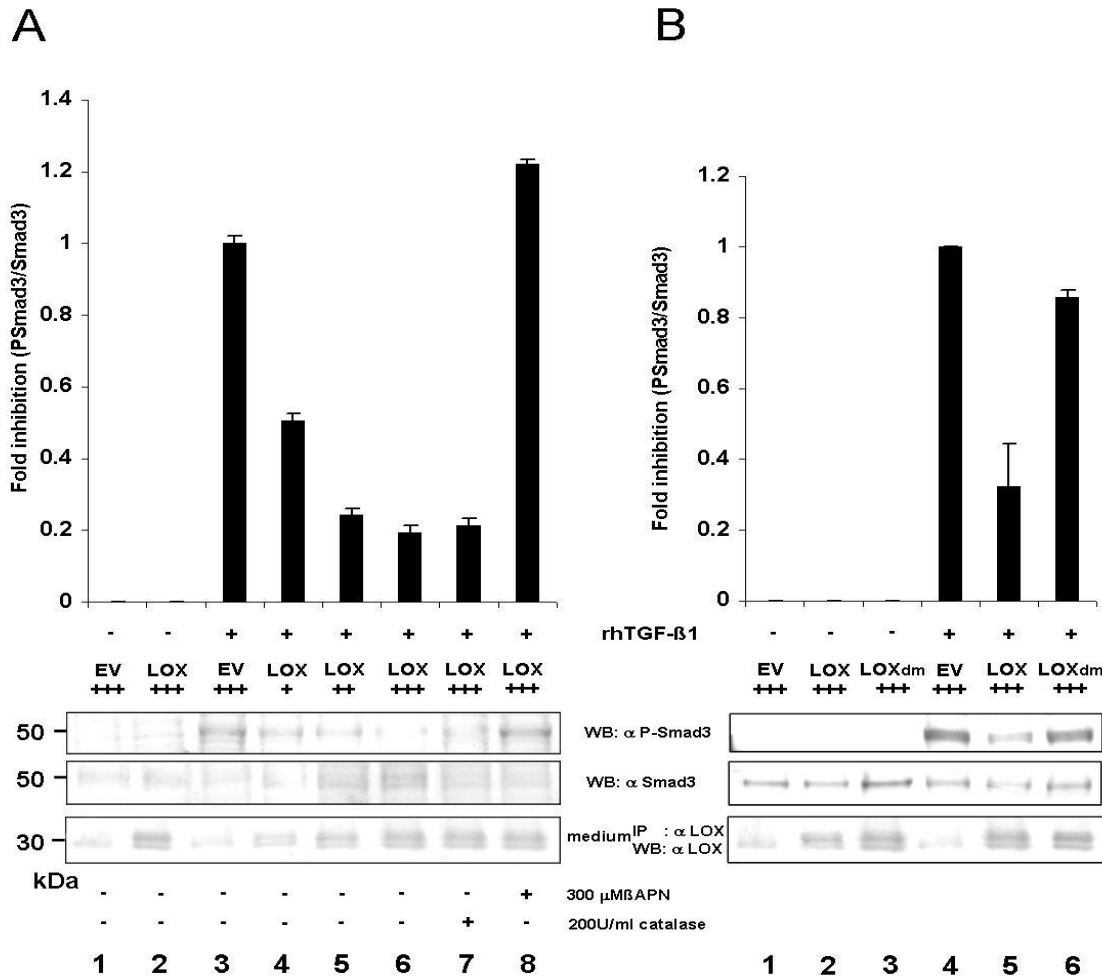


**Figure 3.7** Effect of LOX overexpression on TGF- $\beta$  signaling in osteoblasts (MC). A. The levels of Smad3 phosphorylation upon 30-minute incubation with TGF- $\beta$ 1 (5ng/ml) (upper panel, lanes 4-6) were decreased in a dose dependent manner of LOX compared to those of controls (upper panel, lanes 3). The inhibited Smad3 phosphorylation was enhanced upon TGF- $\beta$ 1 treatment in the presence of 300 $\mu$ M  $\beta$ APN (upper panel, lane 8). The presence of catalase 200U/ml did not affect the inhibition effect of LOX on TGF- $\beta$  signaling (upper panel, lane 7). The levels of Smad 3 phosphorylation were normalized to those of Smad3. The level of LOX expression was determined by IP-WB with anti LOX antibody (lower panel); \* P<0.05 compared to control (lane 3). B. In the cell transfected with LOXdm (upper panel, lane 6), the signal of smad3 phosphorylation was almost comparable to control (upper panel, lane 4) but still inhibited by the presence of LOX (lane 5), \* P<0.05 compared to control (lane 4)

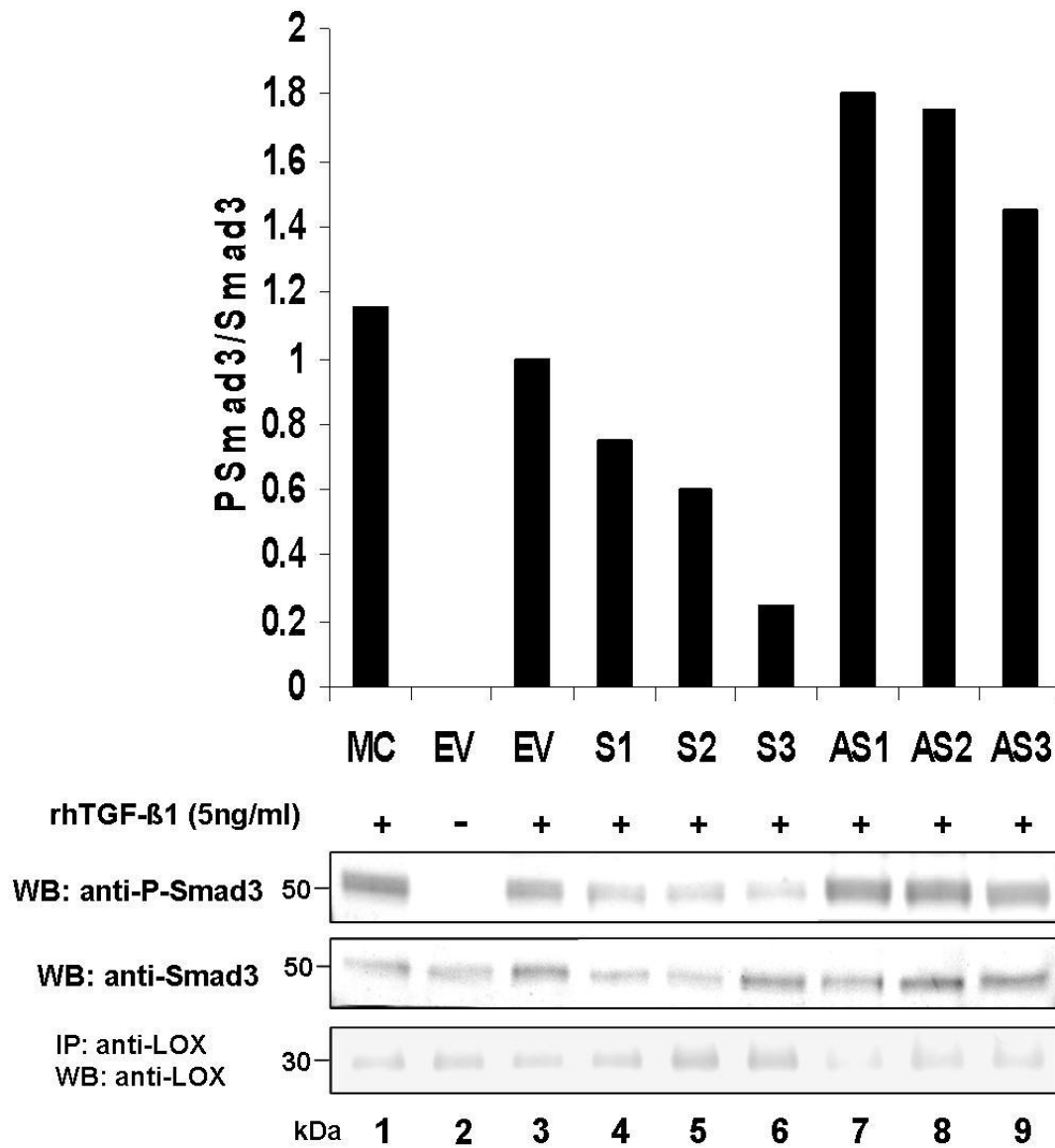


**Figure 3.8** Effect of over/underexpression of LOX on TGF- $\beta$  signaling in MC cells. Note that the expression levels of Smad3 phosphorylation upon 30-minute incubation with TGF- $\beta$ 1 (5ng/ml) after normalized with Smad3 (middle panel) were lower in all S clones (upper panel, lanes 4-6) while those in AS clone were higher (upper panel, lane 7-9) compared to those of control cells, MC and EV (lanes 1 and 3). The LOX level was shown in lower panel.

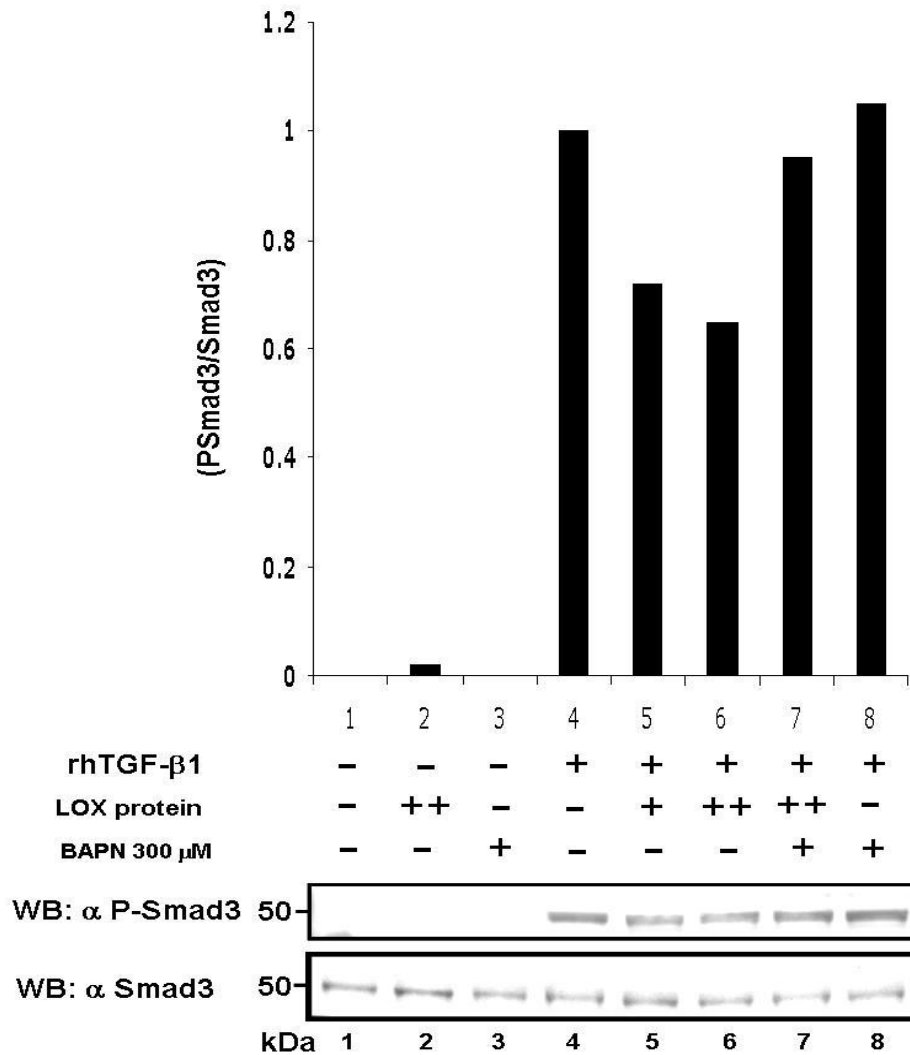


**Figure 3.9** Effect of exogenous LOX protein on TGF-β signaling in osteoblasts (MC). The levels of Smad3 phosphorylation upon 30-minute incubation with TGF-β1 (5ng/ml) (upper panel, lanes 5-6) were decreased in a dose dependent manner of LOX compared to those of controls (upper panel, lanes 4). The inhibited Smad3 phosphorylation was enhanced upon 30 minutes of TGF-β1 treatment in the presence of 300μM βAPN (upper panel, lane7). In the presence of βAPN only, the signal was increased compared to those of controls (upper panel, lane 8). Without TGF-β induction, the levels of Smad 3 phosphorylation were not detected (upper panel, lane 1-3). The levels of Smad3 phosphorylation were normalized to those of Smad3 (lower panel).

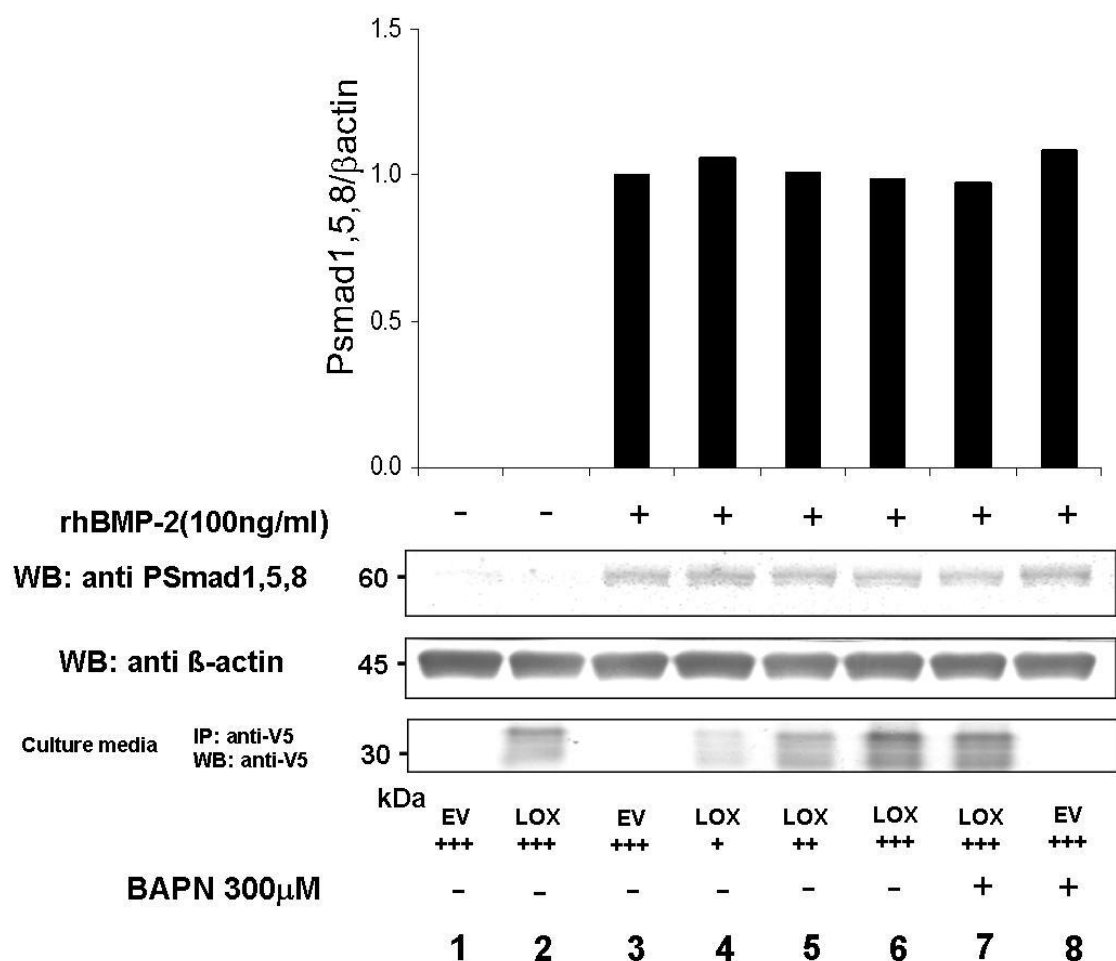


**Figure 3.10** Effect of LOX overexpression on BMP signaling in osteoblasts (MC). The levels of Smad 1,5,8 phosphorylation upon 30-minute incubation with BMP-2 (100ng/ml) (upper panel, lanes 3-8) were investigated. The Smad3 phosphorylation was not changed upon the treatment in any dose of LOX plasmid transfection (upper panel, lane 4-6) compared to those of controls (upper panel, lane 3). The Smad 1,5,8 phosphorylation was not changed upon BMP-2 treatment in the presence of 300 $\mu$ M  $\beta$ APN (upper panel, lane7). The levels of Smad 1,5,8 phosphorylation were normalized to those of  $\beta$ -actin (middle panel).The level of LOX expression was determined by IP-WB with anti V5 antibody (lower panel).

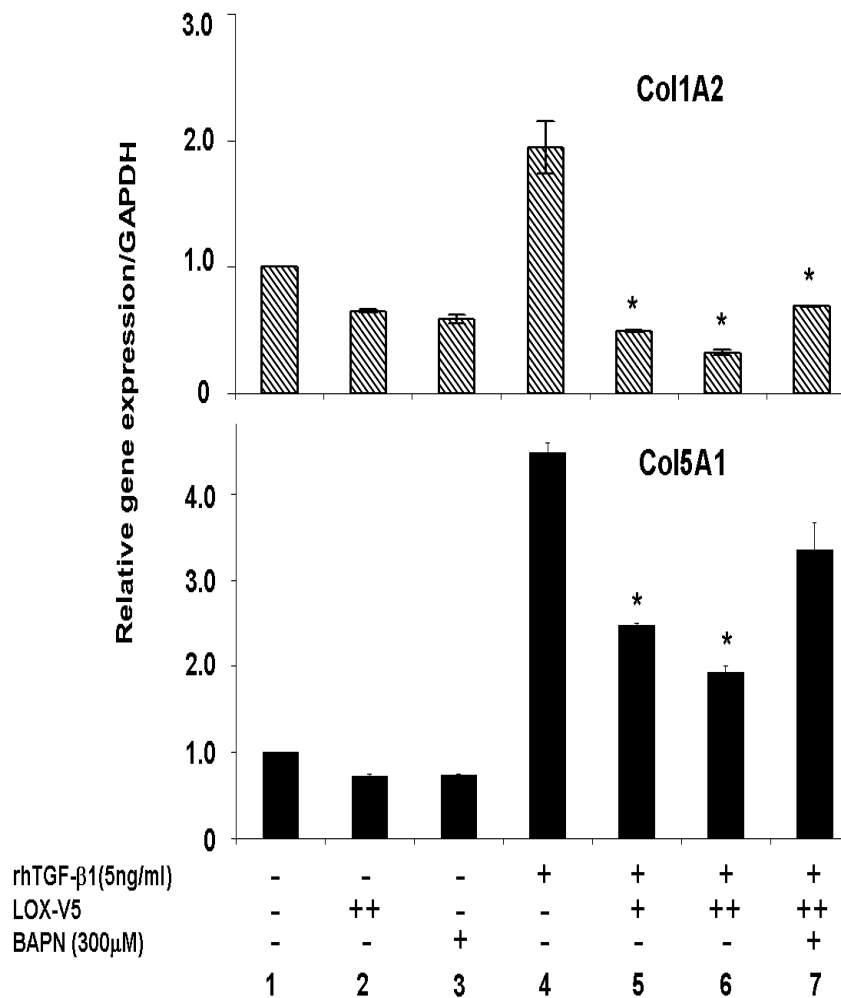


**Figure 3.11** Effect of LOX on TGF- $\beta$  induced type I and type V collagen expression in osteoblasts by *real-time* PCR. Note that the expression levels of both types of collagen were upregulated upon 24-hour incubation with TGF- $\beta$ 1 (5ng/ml)(lane 4), however, in the presence of LOX (2.5 and 5 ug), the level was decreased respectively (lane 5, 6). Moreover, an addition of 300 $\mu$ M  $\beta$ APN rescued LOX-mediated TGF- $\beta$ 1 inhibition (lane 7). LOX: LOX-V5/His protein. \*P<0.05.

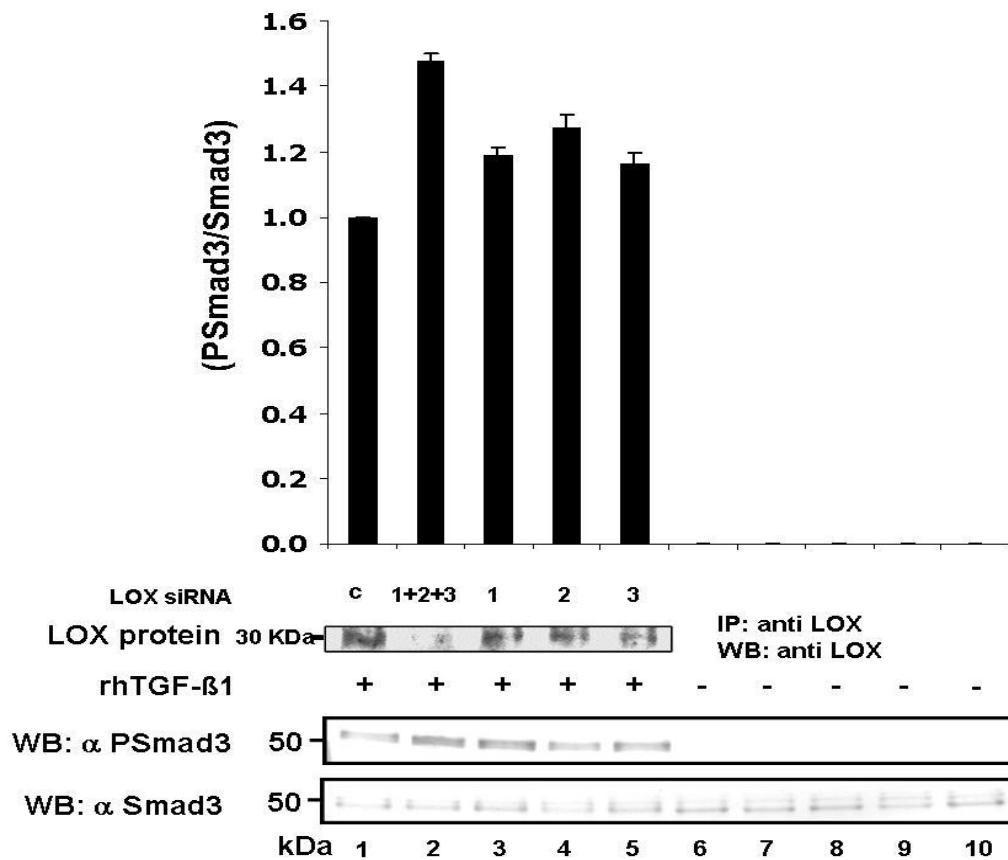


**Figure 3.12** Effects of LOX suppression on TGF-β signaling by RNA interference. The levels of Smad3 phosphorylation upon TGF-β1 treatment (5ng/ml) were higher when LOX siRNA was performed (middle panel, lane 2-4) compared to control siRNA treatment (middle panel, lane 1). Without TGF-β1 induction, the levels of Smad 3 phosphorylation were not detected (middle panel, lane 6-10). The levels of Smad3 phosphorylation were normalized to those of Smad3 (lower panel). The level of LOX expression was determined by IP-WB with anti LOX antibody (upper panel).

## DISCUSSION

Bone matrix is primarily composed of type I collagen and mineral such as hydroxyapatite. Bone matrix has been reported to store high concentrations of several growth factors that can affect the behaviour of connective tissue cells including transforming growth factor- $\beta$  (TGF- $\beta$ ) and a set of bone morphogenic proteins (BMPs). TGF- $\beta$ 1 is the prototypic member of the superfamily, and bone ECM is a major storage site in the body for this growth factor (247). In bone, TGF- $\beta$ 1 plays pivotal roles in many, if not all, aspects of the tissue development, remodeling, mechanical properties and aging (250-252). Numerous studies, though not always consistent, have shown that TGF- $\beta$ 1 stimulates recruitment and proliferation of osteoblast progenitors (253, 254), stimulates matrix production such as collagen, fibronectin, osteopontin, osteonectin, proteoglycans, but inhibits osteocalcin (250, 322), inhibits late stage of osteoblast differentiation and matrix mineralization (257, 323), and modulates osteoclast differentiation (258). The abundance of this growth factor with such potent effects on cells predicts the need for tight regulation of its biological activities. This regulation is thought to be achieved through its latency. Since bone is a dynamic, constantly remodeling tissue, tight regulation of TGF- $\beta$  activity (either in a free or a complex form) is crucial. The regulation can be done by: 1. stable TGF- $\beta$  binding molecules limiting the bioavailability of this growth factor during remodeling, and/or 2. TGF- $\beta$  modifications that reduces its potency as a growth factor or stabilizes its latency. In bone matrix, there are several TGF- $\beta$  binding molecules including small leucine-rich proteoglycans, decorin and biglycan (260, 275, 276) that may sequester TGF- $\beta$  in the matrix and/or diminish TGF- $\beta$  binding to its cell receptor (277). However, the significance of these interactions in bone ECM is not known. Furthermore, potential extracellular modification of TGF- $\beta$  that may change and/or stabilize the potency is unknown.

Here we have demonstrated the direct binding between mature LOX and mature TGF- $\beta$ 1 *in vitro* and in bone matrix and showed that LOX inhibited TGF- $\beta$ 1 activity likely via its amine oxidase activity. In this study we showed that LOX bound to TGF- $\beta$ 1 but not major osteogenic BMPs found in bone. Using co-immunoprecipitation and GST pull-down assay, we found that mature TGF- $\beta$ 1 not LAP was the form that bound directly to LOX. As we tried to identify the TGF- $\beta$ 1 binding site within a LOX molecule, we demonstrated that mature LOX, a 32 kDa form of LOX after cleaved by BMP-1 at specific sequence, contained TGF- $\beta$ 1 binding site but not LOX propeptide. Moreover, the binding was not affected in the presence of  $\beta$ APN, a potent and irreversible inhibitor of LOX. It has been proposed that the inhibition occurs by the formation of a “dead-end” complex between  $\beta$ APN and the carbonyl cofactor of LOX, lysine tyrosylquinone (LTQ) (117, 118). The conformational change due to mutations of specific Lys and Tyr in LTQ cofactor domain did not affect the binding as well. It implicates that LOX indeed binds directly to TGF- $\beta$ 1 and its LTQ domain is not the binding domain.

To the best of our knowledge, in bone, LOX was not well characterized except the measurement of its activity in crude saline extracts (50). LOX has been reported that it can bind to collagen in dentin (221). In preosteoblast culture system, we showed that LOX and TGF- $\beta$ 1 co-localized in the fibrous extracellular matrix. This implicates that TGF- $\beta$ 1 in cultures might be stored closely in the form of SLC and closely associated with collagen matrix in which LOX can bind. In bone matrix, LOX and TGF- $\beta$ 1 appeared to be closely associated to collagen and mineral as both were present in E and G2 fractions of bone matrix. The binding complex of LOX and TGF- $\beta$ 1 has been identified using co-immunoprecipitation in E fraction (mineral-related fraction) indicating the presence of the LOX-TGF- $\beta$ 1 complex in bone.

The expression LOX is known to be regulated by TGF- $\beta$ 1 (75, 76, 138, 141-145) but this study is the first to show that LOX in turn regulates TGF- $\beta$  activity and signaling. It has been well accepted that TGF- $\beta$ 1 regulates the target genes through TGF- $\beta$  signaling cascade i.e. Smad3 phosphorylation. Recently, there was a report on a cross control of LOX on TGF- $\beta$  effects; however, the underlying mechanism was not clear (219). Here we showed that LOX directly bound TGF- $\beta$ 1 and inhibited its signaling through amine oxidation evidenced by decreased Smad3 phosphorylation, decreased TGF- $\beta$  induced gene expression. This was evident since the inhibitory effect was diminished by the presence of  $\beta$ APN, the LOX inhibitor, or when we transfected cells with inactive LOX (LOXdm). In addition the inhibitory effect was not due to H<sub>2</sub>O<sub>2</sub> byproduct of the LOX oxidative reaction since the inhibitory effect was not altered in the presence of catalase, H<sub>2</sub>O<sub>2</sub> scavenger. Previous literature has shown that H<sub>2</sub>O<sub>2</sub> from oxidative stress could enhance TGF- $\beta$  signaling leading to various effects: i.e. the accumulation of extracellular matrix molecules mRNA and protein expression, production of proinflammatory mediators or cellular senescence (324-330). Though H<sub>2</sub>O<sub>2</sub> in this study did not alter the inhibitory effect, it is possible that the H<sub>2</sub>O<sub>2</sub> endproduct from LOX oxidative reaction might alleviate the inhibitory effect on TGF- $\beta$ 1 reflecting a moderate inhibition of LOX i.e. the inhibitory effect in exogenous LOX addition. The inhibitory effects were also confirmed using MC stable clones over/underexpressing LOX and the result showed that Smad3 phosphorylation was enhanced in AS clones (low LOX expression) but inhibited in S clones (high LOX expression) after rhTGF- $\beta$ 1 induction.

In MC derived clones overexpressing LOX exhibited less collagen production while those underexpressing LOX produced more collagen suggesting the effect of LOX on TGF- $\beta$ 1 induced matrix molecule production (see chapter III). Several reports have

shown markedly increased collagen synthesis and abnormal collagen fibrillogenesis in  $\beta$ APN treated osteoblast cultures (73, 222). The increased collagen production can hardly be explained by altered collagen cross-linking since even immature cross-links (thus, early forms of cross-links) begin to accumulate only after 1-2 weeks in osteoblast cultures (295, 296); however, the current study i.e. LOX regulates TGF- $\beta$ 1 signaling, may explain the phenotype seen in the  $\beta$ APN treated osteoblast culture. The upregulation of collagen mRNA was also seen in lathyrotic animals during the early phase of bone fracture healing as well as TGF- $\beta$ 1 mRNA expression (239). This implicates the interaction of LOX and TGF- $\beta$ 1 *in vivo*.

Taken together, our results indicate that for the first time, the signaling of TGF- $\beta$ 1 is inhibited by amine oxidase activity of LOX. This proposed mechanism is different from the previously reported ones i.e: sequestration of mature TGF- $\beta$  to limit the bioavailability of this growth factor to its receptor (275) or inhibition of TGF- $\beta$  processing that decreases its active form or stabilizes its latency (331). This finding represents a novel control mechanism of TGF- $\beta$ 1 function in bone and may provide more insight to the mechanism of bone development and remodeling. It will be important in the future to determine the specific binding domain of LOX to TGF- $\beta$ 1 and also the relevant function of oxidized TGF- $\beta$ 1 in bone biology.

## **CHAPTER V**

### **CONCLUDING REMARKS**

## Concluding remarks

It is now evident that LOX substrates are more than immature collagen and elastin and that LOX is involved in cellular functions. In conjunction to those, we have discovered the followings:

1. In an osteoblastic cell culture system, overexpression of LOX exhibited lower collagen synthesis, smaller collagen fibrils, and markedly delayed mineralization while underexpression of LOX exhibited higher collagen synthesis and larger collagen fibrils compared to control cells, MC cells and EV clones. These phenomena can be partly explained by the fact that the increase of collagen cross-links generated the restricted collagen scaffold leading to defective matrix mineralization.

2. The overexpression of LOX caused suppression of collagen synthesis while the underexpression of LOX caused more collagen synthesis at early time-point. The LOX overexpression coincided with lower signaling of TGF- $\beta$ 1 but the underexpression enhanced the signaling. The phenomena observed in S and AS clones indicate that LOX modulates TGF- $\beta$ 1 function.

3. The mature LOX directly binds mature TGF- $\beta$ 1 both *in vitro* and in bone marix. The binding is not affected by  $\beta$ APN or the mutation of LTQ in LOX indicating that the binding of LOX to TGF- $\beta$ 1 does not require LTQ or the conformation generated by LTQ.

4. The suppression of TGF- $\beta$ 1 signaling induced either by LOX overexpression or an addition of LOX protein was rescued by  $\beta$ APN but not affected by catalase. The enhancement of TGF- $\beta$ 1 signaling was observed when LOX mRNA was silenced by RNA interference or LOX underexpression.

Based on the results that have been observed in the study, it is clear that LOX regulates TGF- $\beta$ 1 signaling through its amine oxidase activity that is important to control collagen matrix production/organization and mineralization. The deregulation of such control may result in overactivation of TGF- $\beta$  signaling leading to bone defects. As TGF- $\beta$ 1 is a potent growth factor involved in bone development and remodeling, the current study may shed new light on our understanding of bone physiology, pathology and treatment.

Though this study has shown the possible mechanism of how LOX regulates TGF- $\beta$ 1, further experiments are clearly warranted i.e. direct evidence to show whether TGF- $\beta$ 1 is a substrate of LOX by *in vitro* LOX activity assay, determination of binding domain of TGF- $\beta$ 1 on LOX molecule, identification of oxidized Lys residues on TGF- $\beta$ 1 molecule to determine if those Lys are indispensable for the TGF- $\beta$ 1 signaling. The biological significance of LOX-TGF- $\beta$ 1 complex in bone may be addressed using *in vivo* animal model. The effects of S or AS clones on collagen production, collagen phenotype and bone formation could be evaluated using an *in vivo* transplantation model (285, 293). The comprehensive analysis of bone phenotypes among LOX deficient animals (conventional or tissue specific conditional knock-out), LOX and TGF- $\beta$ 1 transgenic animals should provide valuable information regarding the biological significance of LOX-TGF- $\beta$ 1 interaction.

## BIBLIOGRAPHY

1. **Marks SCJ, Popoff, S.N.** 1988 Bone cell biology: the regulation of development, structure, and function in the skeleton. *Am J Anat* 183:1-44
2. **Marks SC, Hermey, D.C.** 1996 The structure and development of bone. Academic Press, San Diego, California
3. **Buckwalter JA GM, Cooper RR, Becker R.** 1996 Bone biology, part I: structure, blood supply, cells, matrix and mineralization
4. **Ducy P, Schinke T, Karsenty G** 2000 The osteoblast: a sophisticated fibroblast under central surveillance. *Science* 289:1501-4
5. **Holtrop ME** 1990 Light and electron microscopic structure of bone forming cells. Telford Press Inc, Caldwell, NJ
6. **Holtrop ME** 1991 Light and electronmicroscopic structure of osteoclasts. CRC Press Inc, Boca Raton, Fla
7. **Teitelbaum SL** 2000 Bone resorption by osteoclasts. *Science* 289:1504-8
8. **Teitelbaum SL** 2006 Osteoclasts and integrins. *Ann N Y Acad Sci* 1068:95-9
9. **Hofbauer LC, Khosla S, Dunstan CR, Lacey DL, Boyle WJ, Riggs BL** 2000 The roles of osteoprotegerin and osteoprotegerin ligand in the paracrine regulation of bone resorption. *J Bone Miner Res* 15:2-12
10. **Weiner S, Traub W** 1992 Bone structure: from angstroms to microns. *Faseb J* 6:879-85
11. **Sommerfeldt DW, Rubin CT** 2001 Biology of bone and how it orchestrates the form and function of the skeleton. *Eur Spine J* 10 Suppl 2:S86-95
12. **Ducy P, Desbois C, Boyce B, et al.** 1996 Increased bone formation in osteocalcin-deficient mice. *Nature* 382:448-52
13. **Yagami K, Suh JY, Enomoto-Iwamoto M, et al.** 1999 Matrix GLA protein is a developmental regulator of chondrocyte mineralization and, when constitutively expressed, blocks endochondral and intramembranous ossification in the limb. *J Cell Biol* 147:1097-108
14. **Bateman JF, Lamande, S.R., Ramshaw, J.A.M.** 1996 Collagen superfamily. Harwood Academic Publisher, Amsterdam, Netherland
15. **Yamauchi M** 2002 Collagen Biochemistry: an overview. World Scientific Publishing Co. Pte. Ltd., New Jersey

16. **Sato K, Yomogida K, Wada T, et al.** 2002 Type XXVI collagen, a new member of the collagen family, is specifically expressed in the testis and ovary. *J Biol Chem* 277:37678-84
17. **Koch M, Laub F, Zhou P, et al.** 2003 Collagen XXIV, a vertebrate fibrillar collagen with structural features of invertebrate collagens: selective expression in developing cornea and bone. *J Biol Chem* 278:43236-44
18. **Pace JM, Corrado M, Missero C, Byers PH** 2003 Identification, characterization and expression analysis of a new fibrillar collagen gene, COL27A1. *Matrix Biol* 22:3-14
19. **Boot-Handford RP, Tuckwell DS, Plumb DA, Rock CF, Poulson R** 2003 A novel and highly conserved collagen (pro(alpha)1(XXVII)) with a unique expression pattern and unusual molecular characteristics establishes a new clade within the vertebrate fibrillar collagen family. *J Biol Chem* 278:31067-77
20. **Myllyharju J, Kivirikko KI** 2004 Collagens, modifying enzymes and their mutations in humans, flies and worms. *Trends Genet* 20:33-43
21. **Dominguez LJ, Barbagallo M, Moro L** 2005 Collagen overglycosylation: a biochemical feature that may contribute to bone quality. *Biochem Biophys Res Commun* 330:1-4
22. **Kuznetsova N, Leikin S** 1999 Does the triple helical domain of type I collagen encode molecular recognition and fiber assembly while telopeptides serve as catalytic domains? Effect of proteolytic cleavage on fibrillogenesis and on collagen-collagen interaction in fibers. *J Biol Chem* 274:36083-8
23. **Lamande SR, Bateman JF** 1999 Procollagen folding and assembly: the role of endoplasmic reticulum enzymes and molecular chaperones. *Semin Cell Dev Biol* 10:455-64
24. **Hendershot LM, Bulleid NJ** 2000 Protein-specific chaperones: the role of hsp47 begins to gel. *Curr Biol* 10:R912-5
25. **Bulleid NJ, Dalley JA, Lees JF** 1997 The C-propeptide domain of procollagen can be replaced with a transmembrane domain without affecting trimer formation or collagen triple helix folding during biosynthesis. *Embo J* 16:6694-701
26. **Koivu J, Myllyla R** 1987 Interchain disulfide bond formation in types I and II procollagen. Evidence for a protein disulfide isomerase catalyzing bond formation. *J Biol Chem* 262:6159-64
27. **Bachinger HP** 1987 The influence of peptidyl-prolyl cis-trans isomerase on the in vitro folding of type III collagen. *J Biol Chem* 262:17144-8
28. **Galat A, Metcalfe SM** 1995 Peptidylproline cis/trans isomerases. *Prog Biophys Mol Biol* 63:67-118

29. **Kivirikko KI, Myllyharju J** 1998 Prolyl 4-hydroxylases and their protein disulfide isomerase subunit. *Matrix Biol* 16:357-68
30. **Myllyharju J** 2003 Prolyl 4-hydroxylases, the key enzymes of collagen biosynthesis. *Matrix Biol* 22:15-24
31. **Nagata K** 2003 HSP47 as a collagen-specific molecular chaperone: function and expression in normal mouse development. *Semin Cell Dev Biol* 14:275-82
32. **Nagata K** 1998 Expression and function of heat shock protein 47: a collagen-specific molecular chaperone in the endoplasmic reticulum. *Matrix Biol* 16:379-86
33. **Engel J, Prockop DJ** 1991 The zipper-like folding of collagen triple helices and the effects of mutations that disrupt the zipper. *Annu Rev Biophys Biophys Chem* 20:137-52
34. **Kagan HM, Li W** 2003 Lysyl oxidase: properties, specificity, and biological roles inside and outside of the cell. *J Cell Biochem* 88:660-72
35. **Kivirikko KI, Myllyla R** 1985 Post-translational processing of procollagens. *Ann N Y Acad Sci* 460:187-201
36. **Viguet-Carrin S, Garnero P, Delmas PD** 2006 The role of collagen in bone strength. *Osteoporos Int* 17:319-36
37. **Siegel RC** 1979 Lysyl oxidase. *Int Rev Connect Tissue Res* 8:73-118
38. **Yamauchi M, Mechanic, G.L.** 1988 Cross-linking of collagen. CRC Press, Boca Raton, Fla
39. **Eyre DR, Paz MA, Gallop PM** 1984 Cross-linking in collagen and elastin. *Annu Rev Biochem* 53:717-48
40. **Tanzer ML** 1976 Cross-linking. Plenum Press, New York
41. **Reiser K, McCormick RJ, Rucker RB** 1992 Enzymatic and nonenzymatic cross-linking of collagen and elastin. *Faseb J* 6:2439-49
42. **Reiser KM** 1998 Nonenzymatic glycation of collagen in aging and diabetes. *Proc Soc Exp Biol Med* 218:23-37
43. **Cloos PA, Christgau S** 2002 Non-enzymatic covalent modifications of proteins: mechanisms, physiological consequences and clinical applications. *Matrix Biol* 21:39-52
44. **Smit AJ, Lutgers HL** 2004 The clinical relevance of advanced glycation endproducts (AGE) and recent developments in pharmaceuticals to reduce AGE accumulation. *Curr Med Chem* 11:2767-84

45. **Kang AH, Faris B, Franzblau C** 1969 Intramolecular cross-link of chick skin collagen. *Biochem Biophys Res Commun* 36:345-9
46. **Tanzer ML** 1973 Cross-linking of collagen. *Science* 180:561-6
47. **Mechanic GL, Katz EP, Henmi M, Noyes C, Yamauchi M** 1987 Locus of a histidine-based, stable trifunctional, helix to helix collagen cross-link: stereospecific collagen structure of type I skin fibrils. *Biochemistry* 26:3500-9
48. **Yamauchi M, Chandler GS, Tanzawa H, Katz EP** 1996 Cross-linking and the molecular packing of corneal collagen. *Biochem Biophys Res Commun* 219:311-5
49. **Yamauchi M, London RE, Guenat C, Hashimoto F, Mechanic GL** 1987 Structure and formation of a stable histidine-based trifunctional cross-link in skin collagen. *J Biol Chem* 262:11428-34
50. **Pinnell SR, Martin GR** 1968 The cross-linking of collagen and elastin: enzymatic conversion of lysine in peptide linkage to alpha-aminoadipic-delta-semialdehyde (allysine) by an extract from bone. *Proc Natl Acad Sci U S A* 61:708-16
51. **Narayanan AS, Siegel RC, Martin GR** 1974 Stability and purification of lysyl oxidase. *Arch Biochem Biophys* 162:231-7
52. **Stassen FL** 1976 Properties of highly purified lysyl oxidase from embryonic chick cartilage. *Biochim Biophys Acta* 438:49-60
53. **Kagan HM, Sullivan KA, Olsson TA, 3rd, Cronlund AL** 1979 Purification and properties of four species of lysyl oxidase from bovine aorta. *Biochem J* 177:203-14
54. **Cronlund AL, Kagan HM** 1986 Comparison of lysyl oxidase from bovine lung and aorta. *Connect Tissue Res* 15:173-85
55. **Kuivaniemi H, Savolainen ER, Kivirikko KI** 1984 Human placental lysyl oxidase. Purification, partial characterization, and preparation of two specific antisera to the enzyme. *J Biol Chem* 259:6996-7002
56. **Shackleton DR, Hulmes DJ** 1990 Purification of lysyl oxidase from piglet skin by selective interaction with Sephacryl S-200. *Biochem J* 266:917-9
57. **Kagan HM, Vaccaro CA, Bronson RE, Tang SS, Brody JS** 1986 Ultrastructural immunolocalization of lysyl oxidase in vascular connective tissue. *J Cell Biol* 103:1121-8
58. **Hamalainen ER, Jones TA, Sheer D, Taskinen K, Pihlajaniemi T, Kivirikko KI** 1991 Molecular cloning of human lysyl oxidase and assignment of the gene to chromosome 5q23.3-31.2. *Genomics* 11:508-16

59. **Mariani TJ, Trackman PC, Kagan HM, et al.** 1992 The complete derived amino acid sequence of human lysyl oxidase and assignment of the gene to chromosome 5 (extensive sequence homology with the murine ras recision gene). *Matrix* 12:242-8
60. **Boyd CD, Mariani TJ, Kim Y, Csiszar K** 1995 The size heterogeneity of human lysyl oxidase mRNA is due to alternate polyadenylation site and not alternate exon usage. *Mol Biol Rep* 21:95-103
61. **Mock BA, Contente S, Kenyon K, Friedman RM, Kozak CA** 1992 The gene for lysyl oxidase maps to mouse chromosome 18. *Genomics* 14:822-3
62. **Chang YS, Svinarich DM, Yang TP, Krawetz SA** 1993 The mouse lysyl oxidase gene (Lox) resides on chromosome 18. *Cytogenet Cell Genet* 63:47-9
63. **Contente S, Csiszar K, Kenyon K, Friedman RM** 1993 Structure of the mouse lysyl oxidase gene. *Genomics* 16:395-400
64. **Layman DL, Narayanan AS, Martin GR** 1972 The production of lysyl oxidase by human fibroblasts in culture. *Arch Biochem Biophys* 149:97-101
65. **Byers PH, Siegel RC, Holbrook KA, Narayanan AS, Bornstein P, Hall JG** 1980 X-linked cutis laxa: defective cross-link formation in collagen due to decreased lysyl oxidase activity. *N Engl J Med* 303:61-5
66. **Royce PM, Steinmann B** 1990 Markedly reduced activity of lysyl oxidase in skin and aorta from a patient with Menkes' disease showing unusually severe connective tissue manifestations. *Pediatr Res* 28:137-41
67. **Peltonen L, Kuivaniemi H, Palotie A, Horn N, Kaitila I, Kivirikko KI** 1983 Alterations in copper and collagen metabolism in the Menkes syndrome and a new subtype of the Ehlers-Danlos syndrome. *Biochemistry* 22:6156-63
68. **Kuivaniemi H, Ala-Kokko L, Kivirikko KI** 1986 Secretion of lysyl oxidase by cultured human skin fibroblasts and effects of monensin, nigericin, tunicamycin and colchicine. *Biochim Biophys Acta* 883:326-34
69. **Trackman PC, Pratt AM, Wolanski A, et al.** 1990 Cloning of rat aorta lysyl oxidase cDNA: complete codons and predicted amino acid sequence. *Biochemistry* 29:4863-70
70. **Trackman PC, Pratt AM, Wolanski A, et al.** 1991 Cloning of rat aorta lysyl oxidase cDNA: complete codons and predicted amino acid sequence. *Biochemistry* 30:8282
71. **Wakasaki H, Ooshima A** 1990 Synthesis of lysyl oxidase in experimental hepatic fibrosis. *Biochem Biophys Res Commun* 166:1201-4

72. **Trackman PC, Bedell-Hogan D, Tang J, Kagan HM** 1992 Post-translational glycosylation and proteolytic processing of a lysyl oxidase precursor. *J Biol Chem* 267:8666-71
73. **Hong HH, Pischon N, Santana RB, et al.** 2004 A role for lysyl oxidase regulation in the control of normal collagen deposition in differentiating osteoblast cultures. *J Cell Physiol* 200:53-62
74. **Atsawasuwan P, Mochida Y, Parisuthiman D, Yamauchi M** 2005 Expression of lysyl oxidase isoforms in MC3T3-E1 osteoblastic cells. *Biochem Biophys Res Commun* 327:1042-6
75. **Feres-Filho EJ, Choi YJ, Han X, Takala TE, Trackman PC** 1995 Pre- and post-translational regulation of lysyl oxidase by transforming growth factor-beta 1 in osteoblastic MC3T3-E1 cells. *J Biol Chem* 270:30797-803
76. **Gacheru SN, Thomas KM, Murray SA, Csiszar K, Smith-Mungo LI, Kagan HM** 1997 Transcriptional and post-transcriptional control of lysyl oxidase expression in vascular smooth muscle cells: effects of TGF-beta 1 and serum deprivation. *J Cell Biochem* 65:395-407
77. **Rodriguez C, Raposo B, Martinez-Gonzalez J, Casani L, Badimon L** 2002 Low density lipoproteins downregulate lysyl oxidase in vascular endothelial cells and the arterial wall. *Arterioscler Thromb Vasc Biol* 22:1409-14
78. **Palamakumbura AH, Sommer P, Trackman PC** 2003 Autocrine growth factor regulation of lysyl oxidase expression in transformed fibroblasts. *J Biol Chem* 278:30781-7
79. **Pischon N, Darbois LM, Palamakumbura AH, Kessler E, Trackman PC** 2004 Regulation of collagen deposition and lysyl oxidase by tumor necrosis factor-alpha in osteoblasts. *J Biol Chem* 279:30060-5
80. **Williams MA, Kagan HM** 1985 Assessment of lysyl oxidase variants by urea gel electrophoresis: evidence against disulfide isomers as bases of the enzyme heterogeneity. *Anal Biochem* 149:430-7
81. **Cronshaw AD, Fothergill-Gilmore LA, Hulmes DJ** 1995 The proteolytic processing site of the precursor of lysyl oxidase. *Biochem J* 306 ( Pt 1):279-84
82. **Panchenko MV, Stetler-Stevenson WG, Trubetskoy OV, Gacheru SN, Kagan HM** 1996 Metalloproteinase activity secreted by fibrogenic cells in the processing of prolysyl oxidase. Potential role of procollagen C-proteinase. *J Biol Chem* 271:7113-9
83. **Fogelgren B, Polgar N, Szauter KM, et al.** 2005 Cellular fibronectin binds to lysyl oxidase with high affinity and is critical for its proteolytic activation. *J Biol Chem* 280:24690-7

84. **Uzel MI, Scott IC, Babakhanlou-Chase H, et al.** 2001 Multiple bone morphogenetic protein 1-related mammalian metalloproteinases process pro-lysyl oxidase at the correct physiological site and control lysyl oxidase activation in mouse embryo fibroblast cultures. *J Biol Chem* 276:22537-43
85. **Thomassin L, Werneck CC, Broekelmann TJ, et al.** 2005 The Pro-regions of lysyl oxidase and lysyl oxidase-like 1 are required for deposition onto elastic fibers. *J Biol Chem* 280:42848-55
86. **Palamakumbura AH, Jeay S, Guo Y, et al.** 2004 The propeptide domain of lysyl oxidase induces phenotypic reversion of ras-transformed cells. *J Biol Chem* 279:40593-600
87. **Kim Y, Boyd CD, Csiszar K** 1995 A new gene with sequence and structural similarity to the gene encoding human lysyl oxidase. *J Biol Chem* 270:7176-82
88. **Csiszar K** 2001 Lysyl oxidases: a novel multifunctional amine oxidase family. *Prog Nucleic Acid Res Mol Biol* 70:1-32
89. **Iguchi H, Sano S** 1985 Cadmium- or zinc-binding to bone lysyl oxidase and copper replacement. *Connect Tissue Res* 14:129-39
90. **Iguchi H, Kasai R, Okumura H, Yamamuro T, Kagan HM** 1990 Effect of dietary cadmium and/or copper on the bone lysyl oxidase in copper-deficient rats relative to the metabolism of copper in the bone. *Bone Miner* 10:51-9
91. **Harris ED** 1976 Copper-induced activation of aortic lysyl oxidase in vivo. *Proc Natl Acad Sci U S A* 73:371-4
92. **Harris ED, Gonnerman WA, Savage JE, O'Dell BL** 1974 Connective tissue amine oxidase. II. Purification and partial characterization of lysyl oxidase from chick aorta. *Biochim Biophys Acta* 341:332-44
93. **Gacheru SN, Trackman PC, Shah MA, et al.** 1990 Structural and catalytic properties of copper in lysyl oxidase. *J Biol Chem* 265:19022-7
94. **Krebs CJ, Krawetz SA** 1993 Lysyl oxidase copper-talon complex: a model. *Biochim Biophys Acta* 1202:7-12
95. **Kosonen T, Uriu-Hare JY, Clegg MS, Keen CL, Rucker RB** 1997 Incorporation of copper into lysyl oxidase. *Biochem J* 327 ( Pt 1):283-9
96. **Kagan HM, Reddy VB, Panchenko MV, et al.** 1995 Expression of lysyl oxidase from cDNA constructs in mammalian cells: the propeptide region is not essential to the folding and secretion of the functional enzyme. *J Cell Biochem* 59:329-38
97. **Seve S, Decitre M, Gleyzal C, et al.** 2002 Expression analysis of recombinant lysyl oxidase (LOX) in myofibroblastlike cells. *Connect Tissue Res* 43:613-9

98. **Rucker RB, Kosonen T, Clegg MS, et al.** 1998 Copper, lysyl oxidase, and extracellular matrix protein cross-linking. *Am J Clin Nutr* 67:996S-1002S
99. **Levene CI** 1969 The effect of lathyrogens on connective tissue. *Bibl Nutr Dieta* 13:144-6
100. **Williamson PR, Kagan HM** 1986 Reaction pathway of bovine aortic lysyl oxidase. *J Biol Chem* 261:9477-82
101. **Williamson PR, Moog RS, Dooley DM, Kagan HM** 1986 Evidence for pyrroloquinolinequinone as the carbonyl cofactor in lysyl oxidase by absorption and resonance Raman spectroscopy. *J Biol Chem* 261:16302-5
102. **Kagan HM** 1994 Lysyl oxidase: mechanism, regulation and relationship to liver fibrosis. *Pathol Res Pract* 190:910-9
103. **Smith-Mungo LI, Kagan HM** 1998 Lysyl oxidase: properties, regulation and multiple functions in biology. *Matrix Biol* 16:387-98
104. **Lucero HA, Kagan HM** 2006 Lysyl oxidase: an oxidative enzyme and effector of cell function. *Cell Mol Life Sci* 63:2304-16
105. **Wang SX, Mure M, Medzihradszky KF, et al.** 1996 A crosslinked cofactor in lysyl oxidase: redox function for amino acid side chains. *Science* 273:1078-84
106. **Bollinger JA, Brown DE, Dooley DM** 2005 The Formation of lysine tyrosylquinone (LTQ) is a self-processing reaction. Expression and characterization of a Drosophila lysyl oxidase. *Biochemistry* 44:11708-14
107. **Williamson PR, Kagan HM** 1987 Electronegativity of aromatic amines as a basis for the development of ground state inhibitors of lysyl oxidase. *J Biol Chem* 262:14520-4
108. **Williamson PR, Kagan HM** 1987 Alpha-proton abstraction and carbanion formation in the mechanism of action of lysyl oxidase. *J Biol Chem* 262:8196-201
109. **Shah MA, Scaman CH, Palcic MM, Kagan HM** 1993 Kinetics and stereospecificity of the lysyl oxidase reaction. *J Biol Chem* 268:11573-9
110. **Gacheru SN, Trackman PC, Kagan HM** 1988 Evidence for a functional role for histidine in lysyl oxidase catalysis. *J Biol Chem* 263:16704-8
111. **Akagawa M, Suyama K** 2001 Characterization of a model compound for the lysine tyrosylquinone cofactor of lysyl oxidase. *Biochem Biophys Res Commun* 281:193-9
112. **Li W, Nellaiappan K, Strassmaier T, Graham L, Thomas KM, Kagan HM** 1997 Localization and activity of lysyl oxidase within nuclei of fibrogenic cells. *Proc Natl Acad Sci U S A* 94:12817-22

113. **Guo Y, Pischon N, Palamakumbura AH, Trackman PC** 2007 Intracellular distribution of the lysyl oxidase propeptide in osteoblastic cells. *Am J Physiol Cell Physiol* 292:C2095-102
114. **Kagan HM** 1986 Characterization and regulation of lysyl oxidase. Academic Press, Orlando, FL
115. **Mc KG, Lalich JJ, Schilling ED, Strong FM** 1954 A crystalline "lathyrus factor" from *Lathyrus odoratus*. *Arch Biochem* 52:313-22
116. **Narayanan AS, Siegel RC, Martin GR** 1972 On the inhibition of lysyl oxidase by -aminopropionitrile. *Biochem Biophys Res Commun* 46:745-51
117. **Tang SS, Trackman PC, Kagan HM** 1983 Reaction of aortic lysyl oxidase with beta-aminopropionitrile. *J Biol Chem* 258:4331-8
118. **Kagan HM** 2000 Intra- and extracellular enzymes of collagen biosynthesis as biological and chemical targets in the control of fibrosis. *Acta Trop* 77:147-52
119. **Tang SS, Simpson DE, Kagan HM** 1984 Beta-substituted ethylamine derivatives as suicide inhibitors of lysyl oxidase. *J Biol Chem* 259:975-9
120. **Gacheru SN, Trackman PC, Calaman SD, Greenaway FT, Kagan HM** 1989 Vicinal diamines as pyrroloquinoline quinone-directed irreversible inhibitors of lysyl oxidase. *J Biol Chem* 264:12963-9
121. **Gavriel P, Kagan HM** 1988 Inhibition by heparin of the oxidation of lysine in collagen by lysyl oxidase. *Biochemistry* 27:2811-5
122. **Nagan N, Callery PS, Kagan HM** 1998 Aminoalkylaziridines as substrates and inhibitors of lysyl oxidase: specific inactivation of the enzyme by N-(5-aminopentyl)aziridine. *Front Biosci* 3:A23-6
123. **Shah MA, Trackman PC, Gallop PM, Kagan HM** 1993 Reaction of lysyl oxidase with trans-2-phenylcyclopropylamine. *J Biol Chem* 268:11580-5
124. **Liu G, Nellaippan K, Kagan HM** 1997 Irreversible inhibition of lysyl oxidase by homocysteine thiolactone and its selenium and oxygen analogues. Implications for homocystinuria. *J Biol Chem* 272:32370-7
125. **Kuroyanagi M, Shimamura E, Kim M, Arakawa N, Fujiwara Y, Otsuka M** 2002 Effects of L-ascorbic acid on lysyl oxidase in the formation of collagen cross-links. *Biosci Biotechnol Biochem* 66:2077-82
126. **Kagan HM, Williams MA, Williamson PR, Anderson JM** 1984 Influence of sequence and charge on the specificity of lysyl oxidase toward protein and synthetic peptide substrates. *J Biol Chem* 259:11203-7

127. **Trackman PC, Kagan HM** 1979 Nonpeptidyl amine inhibitors are substrates of lysyl oxidase. *J Biol Chem* 254:7831-6
128. **Palamakumbura AH, Trackman PC** 2002 A fluorometric assay for detection of lysyl oxidase enzyme activity in biological samples. *Anal Biochem* 300:245-51
129. **Nagan N, Kagan HM** 1994 Modulation of lysyl oxidase activity toward peptidyl lysine by vicinal dicarboxylic amino acid residues. Implications for collagen cross-linking. *J Biol Chem* 269:22366-71
130. **Siegel RC** 1974 Biosynthesis of collagen crosslinks: increased activity of purified lysyl oxidase with reconstituted collagen fibrils. *Proc Natl Acad Sci U S A* 71:4826-30
131. **Cronlund AL, Smith BD, Kagan HM** 1985 Binding of lysyl oxidase to fibrils of type I collagen. *Connect Tissue Res* 14:109-19
132. **Giampuzzi M, Oleggini R, Di Donato A** 2003 Demonstration of in vitro interaction between tumor suppressor lysyl oxidase and histones H1 and H2: definition of the regions involved. *Biochim Biophys Acta* 1647:245-51
133. **Kagan HM, Williams MA, Calaman SD, Berkowitz EM** 1983 Histone H1 is a substrate for lysyl oxidase and contains endogenous sodium borotritide-reducible residues. *Biochem Biophys Res Commun* 115:186-92
134. **Li W, Nugent MA, Zhao Y, et al.** 2003 Lysyl oxidase oxidizes basic fibroblast growth factor and inactivates its mitogenic potential. *J Cell Biochem* 88:152-64
135. **Erler JT, Bennewith KL, Nicolau M, et al.** 2006 Lysyl oxidase is essential for hypoxia-induced metastasis. *Nature* 440:1222-6
136. **Song YL, Ford JW, Gordon D, Shanley CJ** 2000 Regulation of lysyl oxidase by interferon-gamma in rat aortic smooth muscle cells. *Arterioscler Thromb Vasc Biol* 20:982-8
137. **Trackman PC, Graham RJ, Bittner HK, Carnes DL, Gilles JA, Graves DT** 1998 Inflammation-associated lysyl oxidase protein expression in vivo, and modulation by FGF-2 plus IGF-1. *Histochem Cell Biol* 110:9-14
138. **Boak AM, Roy R, Berk J, et al.** 1994 Regulation of lysyl oxidase expression in lung fibroblasts by transforming growth factor-beta 1 and prostaglandin E2. *Am J Respir Cell Mol Biol* 11:751-5
139. **Roy R, Polgar P, Wang Y, Goldstein RH, Taylor L, Kagan HM** 1996 Regulation of lysyl oxidase and cyclooxygenase expression in human lung fibroblasts: interactions among TGF-beta, IL-1 beta, and prostaglandin E. *J Cell Biochem* 62:411-7

140. **Choung J, Taylor L, Thomas K, et al.** 1998 Role of EP2 receptors and cAMP in prostaglandin E2 regulated expression of type I collagen alpha1, lysyl oxidase, and cyclooxygenase-1 genes in human embryo lung fibroblasts. *J Cell Biochem* 71:254-63
141. **Shibanuma M, Mashimo J, Mita A, Kuroki T, Nose K** 1993 Cloning from a mouse osteoblastic cell line of a set of transforming-growth-factor-beta 1-regulated genes, one of which seems to encode a follistatin-related polypeptide. *Eur J Biochem* 217:13-9
142. **Hong HH, Uzel MI, Duan C, Sheff MC, Trackman PC** 1999 Regulation of lysyl oxidase, collagen, and connective tissue growth factor by TGF-beta1 and detection in human gingiva. *Lab Invest* 79:1655-67
143. **Shanley CJ, Gharaee-Kermani M, Sarkar R, et al.** 1997 Transforming growth factor-beta 1 increases lysyl oxidase enzyme activity and mRNA in rat aortic smooth muscle cells. *J Vasc Surg* 25:446-52
144. **Bose KK, Chakraborty J, Khuder S, Smith-Mensah WH, Robinson J** 2000 Lysyl oxidase activity in the cells of flexor retinaculum of individuals with carpal tunnel syndrome. *J Occup Environ Med* 42:582-7
145. **Goto Y, Uchio-Yamada K, Anan S, Yamamoto Y, Ogura A, Manabe N** 2005 Transforming growth factor-beta1 mediated up-regulation of lysyl oxidase in the kidneys of hereditary nephrotic mouse with chronic renal fibrosis. *Virchows Arch* 447:859-68
146. **Koslowski R, Seidel D, Kuhlisch E, Knoch KP** 2003 Evidence for the involvement of TGF-beta and PDGF in the regulation of prolyl 4-hydroxylase and lysyl oxidase in cultured rat lung fibroblasts. *Exp Toxicol Pathol* 55:257-64
147. **Kaku M, Mochida Y, Atsawasuwan P, Parisuthiman D, Yamauchi M** 2007 Post-translational modifications of collagen upon BMP-induced osteoblast differentiation. *Biochem Biophys Res Commun* 359:463-8
148. **Rodriguez C, Alcudia JF, Martinez-Gonzalez J, Raposo B, Navarro MA, Badimon L** 2007 Lysyl oxidase (LOX) down-regulation by TNFalpha: A new mechanism underlying TNFalpha-induced endothelial dysfunction. *Atherosclerosis*
149. **Li W, Chou IN, Boak A, Kagan HM** 1995 Downregulation of lysyl oxidase in cadmium-resistant fibroblasts. *Am J Respir Cell Mol Biol* 13:418-25
150. **Bronson RE, Calaman SD, Traish AM, Kagan HM** 1987 Stimulation of lysyl oxidase (EC 1.4.3.13) activity by testosterone and characterization of androgen receptors in cultured calf aorta smooth-muscle cells. *Biochem J* 244:317-23
151. **Harlow CR, Rae M, Davidson L, Trackman PC, Hillier SG** 2003 Lysyl oxidase gene expression and enzyme activity in the rat ovary: regulation by follicle-

- stimulating hormone, androgen, and transforming growth factor-beta superfamily members in vitro. *Endocrinology* 144:154-62
152. **Yeowell HN, Marshall MK, Walker LC, Ha V, Pinnell SR** 1994 Regulation of lysyl oxidase mRNA in dermal fibroblasts from normal donors and patients with inherited connective tissue disorders. *Arch Biochem Biophys* 308:299-305
  153. **Di Donato A, Ghiggeri GM, Di Duca M, et al.** 1997 Lysyl oxidase expression and collagen cross-linking during chronic adriamycin nephropathy. *Nephron* 76:192-200
  154. **Ravid K, Smith-Mungo LI, Zhao Z, Thomas KM, Kagan HM** 1999 Upregulation of lysyl oxidase in vascular smooth muscle cells by cAMP: role for adenosine receptor activation. *J Cell Biochem* 75:177-85
  155. **Green RS, Lieb ME, Weintraub AS, et al.** 1995 Identification of lysyl oxidase and other platelet-derived growth factor-inducible genes in vascular smooth muscle cells by differential screening. *Lab Invest* 73:476-82
  156. **Chinoy MR, Zgleszewski SE, Cilley RE, Krummel TM** 2000 Dexamethasone enhances ras-recision gene expression in cultured murine fetal lungs: role in development. *Am J Physiol Lung Cell Mol Physiol* 279:L312-8
  157. **Dimaculangan DD, Chawla A, Boak A, Kagan HM, Lazar MA** 1994 Retinoic acid prevents downregulation of ras recision gene/lysyl oxidase early in adipocyte differentiation. *Differentiation* 58:47-52
  158. **Postovit LM, Abbott DE, Payne SL, et al.** 2007 Hypoxia/reoxygenation: A dynamic regulator of lysyl oxidase-facilitated breast cancer migration. *J Cell Biochem*
  159. **Raposo B, Rodriguez C, Martinez-Gonzalez J, Badimon L** 2004 High levels of homocysteine inhibit lysyl oxidase (LOX) and downregulate LOX expression in vascular endothelial cells. *Atherosclerosis* 177:1-8
  160. **Saito M, Fujii K, Tanaka T, Soshi S** 2004 Effect of low- and high-intensity pulsed ultrasound on collagen post-translational modifications in MC3T3-E1 osteoblasts. *Calcif Tissue Int* 75:384-95
  161. **Cui CT, Uriu-Adams JY, Tchapanian EH, Keen CL, Rucker RB** 2004 Metavanadate causes cellular accumulation of copper and decreased lysyl oxidase activity. *Toxicol Appl Pharmacol* 199:35-43
  162. **Maki JM** 2002 Cloning and characterization of the fourth and the fifth human lysyl oxidase isoenzymes, and the consequences of a targeted inactivation of the first described lysyl oxidase isoenzyme in mice Department of Medical Biochemistry and Molecular Biology, University of Oulu University of Oulu OULU, p 73

163. **Maki JM, Rasanen J, Tikkanen H, et al.** 2002 Inactivation of the lysyl oxidase gene *Lox* leads to aortic aneurysms, cardiovascular dysfunction, and perinatal death in mice. *Circulation* 106:2503-9
164. **Hornstra IK, Birge S, Starcher B, Bailey AJ, Mecham RP, Shapiro SD** 2003 Lysyl oxidase is required for vascular and diaphragmatic development in mice. *J Biol Chem* 278:14387-93
165. **Hunter RL, Merkert, C.L.** 1957 Histochemical demonstration of enzymes separated by zone electrophoresis in starch gels. *Science* 125:1294-1295
166. **Kenyon K, Modi WS, Contente S, Friedman RM** 1993 A novel human cDNA with a predicted protein similar to lysyl oxidase maps to chromosome 15q24-q25. *J Biol Chem* 268:18435-7
167. **Saito H, Papaconstantinou J, Sato H, Goldstein S** 1997 Regulation of a novel gene encoding a lysyl oxidase-related protein in cellular adhesion and senescence. *J Biol Chem* 272:8157-60
168. **Jourdan-Le Saux C, Tronecker H, Bogic L, Bryant-Greenwood GD, Boyd CD, Csiszar K** 1999 The *LOXL2* gene encodes a new lysyl oxidase-like protein and is expressed at high levels in reproductive tissues. *J Biol Chem* 274:12939-44
169. **Jang W, Hua A, Spilson SV, Miller W, Roe BA, Meisler MH** 1999 Comparative sequence of human and mouse BAC clones from the *mnd2* region of chromosome 2p13. *Genome Res* 9:53-61
170. **Huang Y, Dai J, Tang R, et al.** 2001 Cloning and characterization of a human lysyl oxidase-like 3 gene (*hLOXL3*). *Matrix Biol* 20:153-7
171. **Jourdan-Le Saux C, Tomsche A, Ujfalusi A, Jia L, Csiszar K** 2001 Central nervous system, uterus, heart, and leukocyte expression of the *LOXL3* gene, encoding a novel lysyl oxidase-like protein. *Genomics* 74:211-8
172. **Maki JM, Kivirikko KI** 2001 Cloning and characterization of a fourth human lysyl oxidase isoenzyme. *Biochem J* 355:381-7
173. **Maki JM, Tikkanen H, Kivirikko KI** 2001 Cloning and characterization of a fifth human lysyl oxidase isoenzyme: the third member of the lysyl oxidase-related subfamily with four scavenger receptor cysteine-rich domains. *Matrix Biol* 20:493-6
174. **Ito H, Akiyama H, Iguchi H, et al.** 2001 Molecular cloning and biological activity of a novel lysyl oxidase-related gene expressed in cartilage. *J Biol Chem* 276:24023-9

175. **Asuncion L, Fogelgren B, Fong KS, Fong SF, Kim Y, Csiszar K** 2001 A novel human lysyl oxidase-like gene (LOXL4) on chromosome 10q24 has an altered scavenger receptor cysteine rich domain. *Matrix Biol* 20:487-91
176. **Borel A, Eichenberger D, Farjanel J, et al.** 2001 Lysyl oxidase-like protein from bovine aorta. Isolation and maturation to an active form by bone morphogenetic protein-1. *J Biol Chem* 276:48944-9
177. **Vadasz Z, Kessler O, Akiri G, et al.** 2005 Abnormal deposition of collagen around hepatocytes in Wilson's disease is associated with hepatocyte specific expression of lysyl oxidase and lysyl oxidase like protein-2. *J Hepatol* 43:499-507
178. **Lee JE, Kim Y** 2006 A tissue-specific variant of the human lysyl oxidase-like protein 3 (LOXL3) functions as an amine oxidase with substrate specificity. *J Biol Chem* 281:37282-90
179. **Szabo Z, Light E, Boyd CD, Csiszar K** 1997 The human lysyl oxidase-like gene maps between STS markers D15S215 and GHLC.GCT7C09 on chromosome 15. *Hum Genet* 101:198-200
180. **Tchernev VT, Yang TP, Kingsmore SF** 1997 Genetic mapping of lysyl oxidase-2 (Loxl) on mouse chromosome 9. *Mamm Genome* 8:621-2
181. **Wydner KS, Kim Y, Csiszar K, Boyd CD, Passmore HC** 1997 An intron capture strategy used to identify and map a lysyl oxidase-like gene on chromosome 9 in the mouse. *Genomics* 40:342-5
182. **Decitre M, Gleyzal C, Raccurt M, et al.** 1998 Lysyl oxidase-like protein localizes to sites of de novo fibrinogenesis in fibrosis and in the early stromal reaction of ductal breast carcinomas. *Lab Invest* 78:143-51
183. **Kim Y, Peyrol S, So CK, Boyd CD, Csiszar K** 1999 Coexpression of the lysyl oxidase-like gene (LOXL) and the gene encoding type III procollagen in induced liver fibrosis. *J Cell Biochem* 72:181-8
184. **Liu X, Zhao Y, Gao J, et al.** 2004 Elastic fiber homeostasis requires lysyl oxidase-like 1 protein. *Nat Genet* 36:178-82
185. **Jourdan-Le Saux C, Le Saux O, Donlon T, Boyd CD, Csiszar K** 1998 The human lysyl oxidase-related gene (LOXL2) maps between markers D8S280 and D8S278 on chromosome 8p21.2-p21.3. *Genomics* 51:305-7
186. **Jourdan-Le Saux C, Le Saux O, Gleyzal C, Sommer P, Csiszar K** 2000 The mouse lysyl oxidase-like 2 gene (mLOXL2) maps to chromosome 14 and is highly expressed in skin, lung and thymus. *Matrix Biol* 19:179-83
187. **Hein S, Yamamoto SY, Okazaki K, Jourdan-LeSaux C, Csiszar K, Bryant-Greenwood GD** 2001 Lysyl oxidases: expression in the fetal membranes and placenta. *Placenta* 22:49-57

188. **Casey ML, MacDonald PC** 1997 Lysyl oxidase (ras recision gene) expression in human amnion: ontogeny and cellular localization. *J Clin Endocrinol Metab* 82:167-72
189. **Jansen MK, Csiszar K** 2007 Intracellular localization of the matrix enzyme lysyl oxidase in polarized epithelial cells. *Matrix Biol* 26:136-9
190. **Contente S, Kenyon K, Rimoldi D, Friedman RM** 1990 Expression of gene rrg is associated with reversion of NIH 3T3 transformed by LTR-c-H-ras. *Science* 249:796-8
191. **Kenyon K, Contente S, Trackman PC, Tang J, Kagan HM, Friedman RM** 1991 Lysyl oxidase and rrg messenger RNA. *Science* 253:802
192. **Kuivaniemi H, Korhonen RM, Vaheri A, Kivirikko KI** 1986 Deficient production of lysyl oxidase in cultures of malignantly transformed human cells. *FEBS Lett* 195:261-4
193. **Hajnal A, Klemenz R, Schafer R** 1993 Up-regulation of lysyl oxidase in spontaneous revertants of H-ras-transformed rat fibroblasts. *Cancer Res* 53:4670-5
194. **Oberhuber H, Seliger B, Schafer R** 1995 Partial restoration of pre-transformation levels of lysyl oxidase and transin mRNAs in phenotypic ras revertants. *Mol Carcinog* 12:198-204
195. **Giampuzzi M, Botti G, Cilli M, et al.** 2001 Down-regulation of lysyl oxidase-induced tumorigenic transformation in NRK-49F cells characterized by constitutive activation of ras proto-oncogene. *J Biol Chem* 276:29226-32
196. **Hamalainen ER, Kempainen R, Kuivaniemi H, et al.** 1995 Quantitative polymerase chain reaction of lysyl oxidase mRNA in malignantly transformed human cell lines demonstrates that their low lysyl oxidase activity is due to low quantities of its mRNA and low levels of transcription of the respective gene. *J Biol Chem* 270:21590-3
197. **Tan RS, Taniguchi T, Harada H** 1996 Identification of the lysyl oxidase gene as target of the antioncogenic transcription factor, IRF-1, and its possible role in tumor suppression. *Cancer Res* 56:2417-21
198. **Peyrol S, Raccurt M, Gerard F, Gleyzal C, Grimaud JA, Sommer P** 1997 Lysyl oxidase gene expression in the stromal reaction to in situ and invasive ductal breast carcinoma. *Am J Pathol* 150:497-507
199. **Ren C, Yang G, Timme TL, Wheeler TM, Thompson TC** 1998 Reduced lysyl oxidase messenger RNA levels in experimental and human prostate cancer. *Cancer Res* 58:1285-90

200. **Peyrol S, Galateau-Salle F, Raccurt M, Gleyzal C, Sommer P** 2000 Selective expression of lysyl oxidase (LOX) in the stromal reactions of broncho-pulmonary carcinomas. *Histol Histopathol* 15:1127-35
201. **Csiszar K, Fong SF, Ujfalusi A, et al.** 2002 Somatic mutations of the lysyl oxidase gene on chromosome 5q23.1 in colorectal tumors. *Int J Cancer* 97:636-42
202. **Tamura K, Ishiguro S, Munakata A, Yoshida Y, Nakaji S, Sugawara K** 1996 Annual changes in colorectal carcinoma incidence in Japan. Analysis of survey data on incidence in Aomori Prefecture. *Cancer* 78:1187-94
203. **Jeay S, Pianetti S, Kagan HM, Sonenshein GE** 2003 Lysyl oxidase inhibits ras-mediated transformation by preventing activation of NF-kappa B. *Mol Cell Biol* 23:2251-63
204. **Hurtado PA, Vora S, Sume SS, et al.** 2008 Lysyl oxidase propeptide inhibits smooth muscle cell signaling and proliferation. *Biochem Biophys Res Commun* 366:156-61
205. **Wu M, Min C, Wang X, et al.** 2007 Repression of BCL2 by the tumor suppressor activity of the lysyl oxidase propeptide inhibits transformed phenotype of lung and pancreatic cancer cells. *Cancer Res* 67:6278-85
206. **Nelson JM, Diegelmann RF, Cohen IK** 1988 Effect of beta-aminopropionitrile and ascorbate on fibroblast migration. *Proc Soc Exp Biol Med* 188:346-52
207. **Lazarus HM, Cruikshank WW, Narasimhan N, Kagan HM, Center DM** 1995 Induction of human monocyte motility by lysyl oxidase. *Matrix Biol* 14:727-31
208. **Li W, Liu G, Chou IN, Kagan HM** 2000 Hydrogen peroxide-mediated, lysyl oxidase-dependent chemotaxis of vascular smooth muscle cells. *J Cell Biochem* 78:550-7
209. **Kirschmann DA, Seftor EA, Fong SF, et al.** 2002 A molecular role for lysyl oxidase in breast cancer invasion. *Cancer Res* 62:4478-83
210. **Payne SL, Fogelgren B, Hess AR, et al.** 2005 Lysyl oxidase regulates breast cancer cell migration and adhesion through a hydrogen peroxide-mediated mechanism. *Cancer Res* 65:11429-36
211. **Payne SL, Hendrix MJ, Kirschmann DA** 2006 Lysyl oxidase regulates actin filament formation through the p130(Cas)/Crk/DOCK180 signaling complex. *J Cell Biochem* 98:827-37
212. **Akiri G, Sabo E, Dafni H, et al.** 2003 Lysyl oxidase-related protein-1 promotes tumor fibrosis and tumor progression in vivo. *Cancer Res* 63:1657-66

213. **Polgar N, Fogelgren B, Shipley JM, Csiszar K** 2007 Lysyl oxidase interacts with hormone placental lactogen and synergistically promotes breast epithelial cell proliferation and migration. *J Biol Chem* 282:3262-72
214. **Laczko R, Szauter KM, Jansen MK, et al.** 2007 Active lysyl oxidase (LOX) correlates with focal adhesion kinase (FAK)/paxillin activation and migration in invasive astrocytes. *Neuropathol Appl Neurobiol*
215. **Wakasaki H, Ooshima A** 1990 Immunohistochemical localization of lysyl oxidase with monoclonal antibodies. *Lab Invest* 63:377-84
216. **Di Donato A, Lacal JC, Di Duca M, Giampuzzi M, Ghiggeri G, Gusmano R** 1997 Micro-injection of recombinant lysyl oxidase blocks oncogenic p21-Ha-Ras and progesterone effects on *Xenopus laevis* oocyte maturation. *FEBS Lett* 419:63-8
217. **Nellaiappan K, Risitano A, Liu G, Nicklas G, Kagan HM** 2000 Fully processed lysyl oxidase catalyst translocates from the extracellular space into nuclei of aortic smooth-muscle cells. *J Cell Biochem* 79:576-82
218. **Giampuzzi M, Botti G, Di Duca M, et al.** 2000 Lysyl oxidase activates the transcription activity of human collagen III promoter. Possible involvement of Ku antigen. *J Biol Chem* 275:36341-9
219. **Oleggini R, Gastaldo N, Di Donato A** 2007 Regulation of elastin promoter by lysyl oxidase and growth factors: cross control of lysyl oxidase on TGF-beta1 effects. *Matrix Biol* 26:494-505
220. **Mello ML, Contente S, Vidal BC, Planding W, Schenck U** 1995 Modulation of ras transformation affecting chromatin supraorganization as assessed by image analysis. *Exp Cell Res* 220:374-82
221. **Domenicucci C, Goldberg HA, Sodek J** 1997 Identification of lysyl oxidase and TRAMP as the major proteins in dissociative extracts of the demineralized collagen matrix of porcine dentine. *Connect Tissue Res* 36:151-63
222. **Gerstenfeld LC, Riva A, Hodgens K, Eyre DR, Landis WJ** 1993 Post-translational control of collagen fibrillogenesis in mineralizing cultures of chick osteoblasts. *J Bone Miner Res* 8:1031-43
223. **Wong M, Siegrist M, Gaschen V, Park Y, Graber W, Studer D** 2002 Collagen fibrillogenesis by chondrocytes in alginate. *Tissue Eng* 8:979-87
224. **Uzel MI, Shih SD, Gross H, Kessler E, Gerstenfeld LC, Trackman PC** 2000 Molecular events that contribute to lysyl oxidase enzyme activity and insoluble collagen accumulation in osteosarcoma cell clones. *J Bone Miner Res* 15:1189-97

225. **Pischon N, Babakhanlou-Chase H, Darbois L, et al.** 2005 A procollagen C-proteinase inhibitor diminishes collagen and lysyl oxidase processing but not collagen cross-linking in osteoblastic cultures. *J Cell Physiol* 203:111-7
226. **Feres-Filho EJ, Menassa GB, Trackman PC** 1996 Regulation of lysyl oxidase by basic fibroblast growth factor in osteoblastic MC3T3-E1 cells. *J Biol Chem* 271:6411-6
227. **Wilmarth KR, Froines JR** 1992 In vitro and in vivo inhibition of lysyl oxidase by aminopropionitriles. *J Toxicol Environ Health* 37:411-23
228. **Dawson DA, Rinaldi AC, Poch G** 2002 Biochemical and toxicological evaluation of agent-cofactor reactivity as a mechanism of action for osteolathyrism. *Toxicology* 177:267-84
229. **Haque A, Hossain M, Wouters G, Lambein F** 1996 Epidemiological study of lathyrism in northwestern districts of Bangladesh. *Neuroepidemiology* 15:83-91
230. **Haque A, Hossain M, Lambein F, Bell EA** 1997 Evidence of osteolathyrism among patients suffering from neurolathyrism in Bangladesh. *Nat Toxins* 5:43-6
231. **Steinmann B, Otten A, Gitzelmann R** 1979 Skin and bone lesions (dermato-osteolathyrism), possible side effects of D-penicillamine treatment, in a boy with cystinuria. *Helv Paediatr Acta* 34:281-91
232. **Lees S, Eyre DR, Barnard SM** 1990 BAPN dose dependence of mature crosslinking in bone matrix collagen of rabbit compact bone: corresponding variation of sonic velocity and equatorial diffraction spacing. *Connect Tissue Res* 24:95-105
233. **Yeager VL, Buranarugsa MW, Arunatut O** 1985 Lathyrism: mini-review and a comment on the lack of effect of protease inhibitors on osteolathyrism. *J Exp Pathol* 2:1-11
234. **Hamre CJ, Yeager VL** 1957 Influence of muscle section on exostoses of lathyric rats. *AMA Arch Pathol* 64:426-33
235. **Baden E, Bouissou H** 1987 Experimental lathyrism: exostoses and aneurysmal-like bone cysts of the mandible in the rat. *Ann Pathol* 7:297-303
236. **Soni NN, Nayar AK, Thomas GP** 1986 Quantitative triple fluorochrome labeling study of lathyritic-rat mandible. *Growth* 50:537-46
237. **Storey E, Varasdi G** 1958 Fracture repair in the rat during aminoacetonitrile administration and following its withdrawal. *Br J Exp Pathol* 39:376-85
238. **Wiancko KB, Kowalewski K** 1961 Strength of callus in fractured humerus of rat treated with anti-anabolic and anabolic compounds. *Acta Endocrinol (Copenh)* 36:310-8

239. **Ekholm EC, Ravanti L, Kahari V, Paavolainen P, Penttinen RP** 2000 Expression of extracellular matrix genes: transforming growth factor (TGF)-beta1 and ras in tibial fracture healing of lathyrict rats. *Bone* 27:551-7
240. **Massague J** 1998 TGF-beta signal transduction. *Annu Rev Biochem* 67:753-91
241. **Shi Y, Massague J** 2003 Mechanisms of TGF-beta signaling from cell membrane to the nucleus. *Cell* 113:685-700
242. **Verrecchia F, Mauviel A** 2002 Transforming growth factor-beta signaling through the Smad pathway: role in extracellular matrix gene expression and regulation. *J Invest Dermatol* 118:211-5
243. **Gressner AM, Weiskirchen R** 2006 Modern pathogenetic concepts of liver fibrosis suggest stellate cells and TGF-beta as major players and therapeutic targets. *J Cell Mol Med* 10:76-99
244. **Kahai S, Vary CP, Gao Y, Seth A** 2004 Collagen, type V, alpha1 (COL5A1) is regulated by TGF-beta in osteoblasts. *Matrix Biol* 23:445-55
245. **Harris SE, Bonewald LF, Harris MA, et al.** 1994 Effects of transforming growth factor beta on bone nodule formation and expression of bone morphogenetic protein 2, osteocalcin, osteopontin, alkaline phosphatase, and type I collagen mRNA in long-term cultures of fetal rat calvarial osteoblasts. *J Bone Miner Res* 9:855-63
246. **ten Dijke P, Hill CS** 2004 New insights into TGF-beta-Smad signalling. *Trends Biochem Sci* 29:265-73
247. **Seyedin SM, Thomas TC, Thompson AY, Rosen DM, Piez KA** 1985 Purification and characterization of two cartilage-inducing factors from bovine demineralized bone. *Proc Natl Acad Sci U S A* 82:2267-71
248. **Pfeilschifter J, Diel I, Scheppach B, et al.** 1998 Concentration of transforming growth factor beta in human bone tissue: relationship to age, menopause, bone turnover, and bone volume. *J Bone Miner Res* 13:716-30
249. **Hering S, Isken E, Knabbe C, et al.** 2001 TGFbeta1 and TGFbeta2 mRNA and protein expression in human bone samples. *Exp Clin Endocrinol Diabetes* 109:217-26
250. **Fromigue O, Modrowski D, Marie PJ** 2004 Growth factors and bone formation in osteoporosis: roles for fibroblast growth factor and transforming growth factor beta. *Curr Pharm Des* 10:2593-603
251. **Balooch G, Balooch M, Nalla RK, et al.** 2005 TGF-beta regulates the mechanical properties and composition of bone matrix. *Proc Natl Acad Sci U S A* 102:18813-8

252. **Janssens K, ten Dijke P, Janssens S, Van Hul W** 2005 Transforming growth factor-beta1 to the bone. *Endocr Rev* 26:743-74
253. **Pfeilschifter J, Wolf O, Naumann A, Minne HW, Mundy GR, Ziegler R** 1990 Chemotactic response of osteoblastlike cells to transforming growth factor beta. *J Bone Miner Res* 5:825-30
254. **Machwate M, Jullienne A, Moukhtar M, Lomri A, Marie PJ** 1995 c-fos protooncogene is involved in the mitogenic effect of transforming growth factor-beta in osteoblastic cells. *Mol Endocrinol* 9:187-98
255. **Bonewald L** 2002 Transforming growth factor beta. Academic Press
256. **Alliston T, Choy L, Ducy P, Karsenty G, Derynck R** 2001 TGF-beta-induced repression of CBFA1 by Smad3 decreases cbfa1 and osteocalcin expression and inhibits osteoblast differentiation. *Embo J* 20:2254-72
257. **Maeda S, Hayashi M, Komiya S, Imamura T, Miyazono K** 2004 Endogenous TGF-beta signaling suppresses maturation of osteoblastic mesenchymal cells. *Embo J* 23:552-63
258. **Fox SW, Lovibond AC** 2005 Current insights into the role of transforming growth factor-beta in bone resorption. *Mol Cell Endocrinol* 243:19-26
259. **Zellin G, Beck S, Hardwick R, Linde A** 1998 Opposite effects of recombinant human transforming growth factor-beta 1 on bone regeneration in vivo: effects of exclusion of periosteal cells by microporous membrane. *Bone* 22:613-20
260. **Bi Y, Stuelten, CH., Kilt, T.** 2005 Extracellular matrix proteoglycans control the fate of bone marrow stromal cells. *J Biol Chem* 26:30481-9
261. **Kim KK, Ji C, Chang W, et al.** 2006 Repetitive exposure to TGF-beta suppresses TGF-beta type I receptor expression by differentiated osteoblasts. *Gene* 379:175-84
262. **Pircher R, Jullien P, Lawrence DA** 1986 Beta-transforming growth factor is stored in human blood platelets as a latent high molecular weight complex. *Biochem Biophys Res Commun* 136:30-7
263. **Annes JP, Munger JS, Rifkin DB** 2003 Making sense of latent TGFbeta activation. *J Cell Sci* 116:217-24
264. **Ramshaw JA, Mitrangas K, Bateman JF** 1991 Heterogeneity in dermatosparaxis is shown by contraction of collagen gels. *Connect Tissue Res* 25:295-300
265. **Young GD, Murphy-Ullrich JE** 2004 Molecular interactions that confer latency to transforming growth factor-beta. *J Biol Chem* 279:38032-9

266. **Qian SW, Burmester JK, Tsang ML, et al.** 1996 Binding affinity of transforming growth factor-beta for its type II receptor is determined by the C-terminal region of the molecule. *J Biol Chem* 271:30656-62
267. **De Crescenzo G, Hinck CS, Shu Z, et al.** 2006 Three key residues underlie the differential affinity of the TGFbeta isoforms for the TGFbeta type II receptor. *J Mol Biol* 355:47-62
268. **Mazzieri R, Jurukovski V, Obata H, et al.** 2005 Expression of truncated latent TGF-beta-binding protein modulates TGF-beta signaling. *J Cell Sci* 118:2177-87
269. **Dallas SL, Rosser JL, Mundy GR, Bonewald LF** 2002 Proteolysis of latent transforming growth factor-beta (TGF-beta )-binding protein-1 by osteoclasts. A cellular mechanism for release of TGF-beta from bone matrix. *J Biol Chem* 277:21352-60
270. **Bonewald LF, Wakefield L, Oreffo RO, Escobedo A, Twardzik DR, Mundy GR** 1991 Latent forms of transforming growth factor-beta (TGF beta) derived from bone cultures: identification of a naturally occurring 100-kDa complex with similarity to recombinant latent TGF beta. *Mol Endocrinol* 5:741-51
271. **Pedrozo HA, Schwartz Z, Robinson M, et al.** 1999 Potential mechanisms for the plasmin-mediated release and activation of latent transforming growth factor-beta1 from the extracellular matrix of growth plate chondrocytes. *Endocrinology* 140:5806-16
272. **Dallas SL, Miyazono K, Skerry TM, Mundy GR, Bonewald LF** 1995 Dual role for the latent transforming growth factor-beta binding protein in storage of latent TGF-beta in the extracellular matrix and as a structural matrix protein. *J Cell Biol* 131:539-49
273. **Dallas SL, Park-Snyder S, Miyazono K, Twardzik D, Mundy GR, Bonewald LF** 1994 Characterization and autoregulation of latent transforming growth factor beta (TGF beta) complexes in osteoblast-like cell lines. Production of a latent complex lacking the latent TGF beta-binding protein. *J Biol Chem* 269:6815-21
274. **Bonewald LF, Dallas SL** 1994 Role of active and latent transforming growth factor beta in bone formation. *J Cell Biochem* 55:350-7
275. **Hildebrand A, Romaris M, Rasmussen LM, et al.** 1994 Interaction of the small interstitial proteoglycans biglycan, decorin and fibromodulin with transforming growth factor beta. *Biochem J* 302 ( Pt 2):527-34
276. **Kresse H, Schonherr E** 2001 Proteoglycans of the extracellular matrix and growth control. *J Cell Physiol* 189:266-74
277. **Droguett R, Cabello-Verrugio C, Riquelme C, Brandan E** 2006 Extracellular proteoglycans modify TGF-beta bio-availability attenuating its signaling during skeletal muscle differentiation. *Matrix Biol* 25:332-41

278. **Masse PG, Rimnac CM, Yamauchi M, et al.** 1996 Pyridoxine deficiency affects biomechanical properties of chick tibial bone. *Bone* 18:567-74
279. **Knott L, Bailey AJ** 1998 Collagen cross-links in mineralizing tissues: a review of their chemistry, function, and clinical relevance. *Bone* 22:181-7
280. **Wang D, Christensen K, Chawla K, Xiao G, Krebsbach PH, Franceschi RT** 1999 Isolation and characterization of MC3T3-E1 preosteoblast subclones with distinct in vitro and in vivo differentiation/mineralization potential. *J Bone Miner Res* 14:893-903
281. **Yamauchi M, Katz EP, Mechanic GL** 1986 Intermolecular cross-linking and stereospecific molecular packing in type I collagen fibrils of the periodontal ligament. *Biochemistry* 25:4907-13
282. **Yamauchi M, Shiiba M** 2002 Lysine hydroxylation and crosslinking of collagen. *Methods Mol Biol* 194:277-90
283. **Yamauchi M, Katz EP** 1993 The post-translational chemistry and molecular packing of mineralizing tendon collagens. *Connect Tissue Res* 29:81-98
284. **Stanford CM, Jacobson PA, Eanes ED, Lembke LA, Midura RJ** 1995 Rapidly forming apatitic mineral in an osteoblastic cell line (UMR 106-01 BSP). *J Biol Chem* 270:9420-8
285. **Parisuthiman D, Mochida Y, Duarte WR, Yamauchi M** 2005 Biglycan modulates osteoblast differentiation and matrix mineralization. *J Bone Miner Res* 20:1878-86
286. **Townsend PR, Miegel RE, Rose RM** 1976 Structure and function of the human patella: the role of cancellous bone. *J Biomed Mater Res* 10:605-11
287. **Ottani V, Raspanti M, Ruggeri A** 2001 Collagen structure and functional implications. *Micron* 32:251-60
288. **Weiner S, Traub W** 1986 Organization of hydroxyapatite crystals within collagen fibrils. *FEBS Lett* 206:262-6
289. **Landis WJ, Song MJ, Leith A, McEwen L, McEwen BF** 1993 Mineral and organic matrix interaction in normally calcifying tendon visualized in three dimensions by high-voltage electron microscopic tomography and graphic image reconstruction. *J Struct Biol* 110:39-54
290. **Yamauchi M, Katz EP, Otsubo K, Teraoka K, Mechanic GL** 1989 Cross-linking and stereospecific structure of collagen in mineralized and nonmineralized skeletal tissues. *Connect Tissue Res* 21:159-67; discussion 168-9

291. **Otsubo K, Katz EP, Mechanic GL, Yamauchi M** 1992 Cross-linking connectivity in bone collagen fibrils: the COOH-terminal locus of free aldehyde. *Biochemistry* 31:396-402
292. **Wassen MH, Lammens J, Tekoppele JM, et al.** 2000 Collagen structure regulates fibril mineralization in osteogenesis as revealed by cross-link patterns in calcifying callus. *J Bone Miner Res* 15:1776-85
293. **Pornprasertsuk S, Duarte WR, Mochida Y, Yamauchi M** 2005 Overexpression of lysyl hydroxylase-2b leads to defective collagen fibrillogenesis and matrix mineralization. *J Bone Miner Res* 20:81-7
294. **Mochida Y, Duarte WR, Tanzawa H, Paschalis EP, Yamauchi M** 2003 Decorin modulates matrix mineralization in vitro. *Biochem Biophys Res Commun* 305:6-9
295. **Pornprasertsuk S, Duarte WR, Mochida Y, Yamauchi M** 2004 Lysyl hydroxylase-2b directs collagen cross-linking pathways in MC3T3-E1 cells. *J Bone Miner Res* 19:1349-55
296. **Kuboki Y, Kudo A, Mizuno M, Kawamura M** 1992 Time-dependent changes of collagen cross-links and their precursors in the culture of osteogenic cells. *Calcif Tissue Int* 50:473-80
297. **Beekman B, Verzijl N, Bank RA, von der Mark K, TeKoppele JM** 1997 Synthesis of collagen by bovine chondrocytes cultured in alginate; posttranslational modifications and cell-matrix interaction. *Exp Cell Res* 237:135-41
298. **Levene ClaGJ** 1959 Alterations in state of molecular aggregation of collagen induced in chick embryos by beta-aminopropionitrile (lathyrus factor). *J Exp Med* 110:771-790
299. **Erler JT, Giaccia AJ** 2006 Lysyl oxidase mediates hypoxic control of metastasis. *Cancer Res* 66:10238-41
300. **Hock JM, Centrella M, Canalis E** 1988 Insulin-like growth factor I has independent effects on bone matrix formation and cell replication. *Endocrinology* 122:254-60
301. **Schmid C, Ernst, M., Binz, K., Zapf, J., Froesch, ER** 1991 The endocrine/paracrine actions of IGFs in bone. . Elsevier, New York
302. **Minuto F, Palermo C, Arvigo M, Barreca AM** 2005 The IGF system and bone. *J Endocrinol Invest* 28:8-10
303. **Canalis E, Lian JB** 1988 Effects of bone associated growth factors on DNA, collagen and osteocalcin synthesis in cultured fetal rat calvariae. *Bone* 9:243-6

304. **Tanaka H, Wakisaka A, Ogasa H, Kawai S, Liang CT** 2002 Effect of IGF-I and PDGF administered in vivo on the expression of osteoblast-related genes in old rats. *J Endocrinol* 174:63-70
305. **Verrecchia F, Mauviel A** 2004 TGF-beta and TNF-alpha: antagonistic cytokines controlling type I collagen gene expression. *Cell Signal* 16:873-80
306. **Mauviel A, Daireaux M, Redini F, Galera P, Loyau G, Pujol JP** 1988 Tumor necrosis factor inhibits collagen and fibronectin synthesis in human dermal fibroblasts. *FEBS Lett* 236:47-52
307. **Mauviel A, Lapiere JC, Halcin C, Evans CH, Uitto J** 1994 Differential cytokine regulation of type I and type VII collagen gene expression in cultured human dermal fibroblasts. *J Biol Chem* 269:25-8
308. **Hurley MM, Abreu C, Harrison JR, Lichtler AC, Raisz LG, Kream BE** 1993 Basic fibroblast growth factor inhibits type I collagen gene expression in osteoblastic MC3T3-E1 cells. *J Biol Chem* 268:5588-93
309. **Chaudhary LR, Avioli LV** 2000 Extracellular-signal regulated kinase signaling pathway mediates downregulation of type I procollagen gene expression by FGF-2, PDGF-BB, and okadaic acid in osteoblastic cells. *J Cell Biochem* 76:354-9
310. **Xie J, Bian H, Qi S, et al.** 2008 Effects of basic fibroblast growth factor on the expression of extracellular matrix and matrix metalloproteinase-1 in wound healing. *Clin Exp Dermatol* 33:176-82
311. **Nakoman C, Resmi H, Ay O, Acikel U, Atabey N, Guner G** 2005 Effects of basic fibroblast factor (bFGF) on MMP-2, TIMP-2, and type-I collagen levels in human lung carcinoma fibroblasts. *Biochimie* 87:343-51
312. **Yamane K, Suzuki H, Ihn H, Kato M, Yoshikawa H, Tamaki K** 2005 Cell type-specific regulation of the TGF-beta-responsive alpha2(I) collagen gene by CpG methylation. *J Cell Physiol* 202:822-30
313. **Luppen CA, Leclerc N, Noh T, et al.** 2003 Brief bone morphogenetic protein 2 treatment of glucocorticoid-inhibited MC3T3-E1 osteoblasts rescues commitment-associated cell cycle and mineralization without alteration of Runx2. *J Biol Chem* 278:44995-5003
314. **Takuwa Y, Ohse C, Wang EA, Wozney JM, Yamashita K** 1991 Bone morphogenetic protein-2 stimulates alkaline phosphatase activity and collagen synthesis in cultured osteoblastic cells, MC3T3-E1. *Biochem Biophys Res Commun* 174:96-101
315. **Pfeilschifter J, Pignat W, Leighton J, Marki F, Vosbeck K, Alkan S** 1990 Transforming growth factor beta 2 differentially modulates interleukin-1 beta- and tumour-necrosis-factor-alpha-stimulated phospholipase A2 and prostaglandin E2 synthesis in rat renal mesangial cells. *Biochem J* 270:269-71

316. **Bonewald LF** 2002 Osteocytes: a proposed multifunctional bone cell. *J Musculoskelet Neuronal Interact* 2:239-41
317. **Li PA, He Q, Cao T, et al.** 2004 Up-regulation and altered distribution of lysyl oxidase in the central nervous system of mutant SOD1 transgenic mouse model of amyotrophic lateral sclerosis. *Brain Res Mol Brain Res* 120:115-22
318. **Mochida Y, Parisuthiman D, Yamauchi M** 2006 Biglycan is a positive modulator of BMP-2 induced osteoblast differentiation. *Adv Exp Med Biol* 585:101-13
319. **Termine JD, Belcourt AB, Conn KM, Kleinman HK** 1981 Mineral and collagen-binding proteins of fetal calf bone. *J Biol Chem* 256:10403-8
320. **Cheng H, Caterson B, Yamauchi M** 1999 Identification and immunolocalization of chondroitin sulfate proteoglycans in tooth cementum. *Connect Tissue Res* 40:37-47
321. **Inman GJ, Nicolas FJ, Callahan JF, et al.** 2002 SB-431542 is a potent and specific inhibitor of transforming growth factor-beta superfamily type I activin receptor-like kinase (ALK) receptors ALK4, ALK5, and ALK7. *Mol Pharmacol* 62:65-74
322. **Bonewald LF, Kester MB, Schwartz Z, et al.** 1992 Effects of combining transforming growth factor beta and 1,25-dihydroxyvitamin D3 on differentiation of a human osteosarcoma (MG-63). *J Biol Chem* 267:8943-9
323. **Alliston T** 2006 TGF-beta regulation of osteoblast differentiation and bone matrix properties. *J Musculoskelet Neuronal Interact* 6:349-50
324. **Iglesias-De La Cruz MC, Ruiz-Torres P, Alcami J, et al.** 2001 Hydrogen peroxide increases extracellular matrix mRNA through TGF-beta in human mesangial cells. *Kidney Int* 59:87-95
325. **Frippiat C, Chen QM, Zdanov S, Magalhaes JP, Remacle J, Toussaint O** 2001 Subcytotoxic H<sub>2</sub>O<sub>2</sub> stress triggers a release of transforming growth factor-beta 1, which induces biomarkers of cellular senescence of human diploid fibroblasts. *J Biol Chem* 276:2531-7
326. **Xiao YQ, Freire-de-Lima CG, Janssen WJ, et al.** 2006 Oxidants selectively reverse TGF-beta suppression of proinflammatory mediator production. *J Immunol* 176:1209-17
327. **Li WQ, Qureshi HY, Liacini A, Dehnade F, Zafarullah M** 2004 Transforming growth factor Beta1 induction of tissue inhibitor of metalloproteinases 3 in articular chondrocytes is mediated by reactive oxygen species. *Free Radic Biol Med* 37:196-207

- 328. **Gooch JL, Gorin Y, Zhang BX, Abboud HE** 2004 Involvement of calcineurin in transforming growth factor-beta-mediated regulation of extracellular matrix accumulation. *J Biol Chem* 279:15561-70
- 329. **Shibanuma M, Kuroki T, Nose K** 1992 Cell-cycle dependent phosphorylation of HSP28 by TGF beta 1 and H<sub>2</sub>O<sub>2</sub> in normal mouse osteoblastic cells (MC3T3-E1), but not in their ras-transformants. *Biochem Biophys Res Commun* 187:1418-25
- 330. **Jiang Z, Seo JY, Ha H, et al.** 2003 Reactive oxygen species mediate TGF-beta1-induced plasminogen activator inhibitor-1 upregulation in mesangial cells. *Biochem Biophys Res Commun* 309:961-6
- 331. **Murphy-Ullrich JE, Schultz-Cherry S, Hook M** 1992 Transforming growth factor-beta complexes with thrombospondin. *Mol Biol Cell* 3:181-8